

# Multimodal Transport Networks\*

Simon Fuchs

Atlanta Fed

Woan Foong Wong

University of Oregon & CEPR

February 2024  
Preliminary

## Abstract

Movement of goods involves multiple modes of transportation. This paper studies multimodal transport networks, and their economic and environmental implications for infrastructure investments. We develop a tractable quantitative spatial equilibrium model incorporating multimodal routing, despite increased dimensionality of the underlying network, and congestion at intermodal terminals, where mode-switching takes place. Using vessel-positioning data, we estimate the strength of intermodal port congestion by investigating ship dwell times and their responsiveness to port traffic. Using highway and rail data, we estimate a modal diversion elasticity with respect to infrastructure improvements. With these estimates, we calibrate the model to US domestic freight flows using road, rail, and port traffic and geography data. Evaluating the welfare effects of US terminal investments, we identify important bottlenecks in the center of the US—a 1% reduction of transportation cost in the most important terminals generates welfare gains equivalent to 200-300 million USD of additional GDP (in 2012 USD). Modal diversion from truck to rail traffic further result in decreases in greenhouse gas emissions.

**JEL Code:** F11, R12, R42

**Keywords:** Multimodal transport, Transport network, Spatial equilibrium, Infrastructure investments

---

\*Contact: simon.fuchs@atl.frb.org and wfwong@uoregon.edu. We are grateful to the NBER, DOT, and NSF for project support under the “Economics of Transportation in the 21st Century” Initiative. We thank Adina Ardelean, Mark Colas, Yuhei Miyachi, Andrii Parkhomenko, as well as seminar and conference participants at Berkeley Haas, UCLA Trade Mini-Conference, University of Rochester Ron Jones Workshop, BFI Junior Spatial conference, 2022 German Economists Abroad meeting, AEA/ASSA 2023, SAET, and SEA for helpful comments. Benjamin Delgado and Philip Economides provided excellent research assistance. The views in this paper are solely the responsibility of the authors and should not necessarily be interpreted as reflecting the views of the Board of Governors of the Federal Reserve System or of any other person associated with the Federal Reserve System. All errors are our own.

# 1 Introduction

Firms, workers, and locations are intrinsically linked via transport, trade, and production networks. Improvements or disruptions within these networks can have large impacts on economic activity and welfare. Much of the focus on transport networks has been on one mode, like roads or ocean shipping. However, transportation takes place multimodally, driven by geography and containerization, with intermodal terminals—which allow for the switching between modes—playing an important role in integrating the entire network. On top of this, congestion effects at intermodal terminals, like ports, can exacerbate the disruption effects on the entire multimodal transport network or mitigate the positive returns from improvements. These welfare impacts can further generate vastly different environmental consequences: transport modes emit differing levels of emissions (trucks emit 8 times more CO<sub>2</sub> per ton-mile than rail, [CBO \(2022\)](#)).

We study multimodal transport networks and their impact on the economic and environmental returns to infrastructure investments and disruptions. In particular, we focus on how these outcomes will depend on the geography of the multimodal transportation network, the location and congestion levels of intermodal terminals that allow for switches between modes of transportation, as well as the relative cost of transportation across modes. By incorporating these features we provide a framework that allows us to realistically evaluate disruptions and infrastructure policies taking the complete domestic transportation network into account. We highlight that changes within the multimodal transport network can generate direct and indirect effects across modes. Improving the highway network, for example, will directly decrease truck transport costs. Indirectly, there can be two additional effects. First, better road access will improve the general market access of locations via a decrease in overall transport costs, increasing their overall demand for transportation across all modes—a *modal complementarity* effect. At the same time, this improvement increases the relative costs of other transport modes, and the transport use for other modes will decline relative to road—a *modal diversion* effect. This also allows us, for the first time, to evaluate the environmental impact of infrastructure investments that stems from modal complementarity and diversion.

We first develop a quantitative spatial equilibrium model that incorporates transportation across multiple transport modes. Drawing on recent innovations in transportation modeling we characterize the optimal route and sourcing choice of an agent making nested choices along the network in a recursive manner. This modeling choice has two distinct advantages: First, by relying on a recursive characterization we can characterize the optimal routing problem and

the associated (*ad valorem*) transportation cost without explicitly enumerating all multi-modal paths. Second, the nesting structure is driven by the topology of the network and naturally allows for overlapping nests, thus allowing for the relaxation of the IIA assumption. We also incorporate congestion at intermodal terminals as well as the road network.

In order to calibrate our model, we estimate two central parameters. First, we examine the impact of congestion at intermodal terminals. Using vessel positioning data down to the minute interval, we investigate the time ships take to load and unload at ports which are important intermodal terminals. We then estimate an elasticity of port congestion by investigating how responsive the ship's dwell times are to overall port traffic at the time of the ship's arrival. Since ship dwell times can be endogenous to conditions at port, we develop a shift-share instrument in order to identify the impact of overall port traffic on ship dwell times. We find that a 1 percent increase in port traffic increases ship dwell times by 0.2-0.3 percent.

Second, we estimate a modal diversion elasticity with respect to infrastructure improvements by building on the seminal work by [Duranton and Turner \(2011\)](#) which finds that a 1 percent increase in interstate highways lead to more truck traffic use in cities by about 1.7-2.1 percent. Matching confidential waybill rail data to cities, we show that this improvement in road access has a positive but imprecise impact on rail traffic use, due to opposing forces from modal complementarity and diversion, that is 4-7 times smaller in magnitude (0.3-0.4). Taking the ratio of rail to truck traffic use, we show that the modal diversion effect dominates—the increase in rail traffic use is less than the truck increase, a 1 percent increase in interstate highways result in a decrease in rail to truck traffic use by 0.9-1.2 percent.

Next, we calibrate the model to fit and reproduce salient features of the US domestic transportation network. We first build a graph representation of the US multimodal transportation system drawing on high-resolution GIS data on road, rail and maritime linkages, as well as the location of intermodal switching facilities. In combination with detailed road traffic and railroad data the model can then be applied to evaluate infrastructure investments, taking the multimodal nature of the US domestic transport system into account. We employ the model to evaluate and compare the welfare impact of investing in different terminals across the country, thus improving the intermodal integration of the primary and secondary transportation network. The analysis points towards substantial and highly heterogeneous welfare gains across space. We find that terminals that generate the largest gains are in the center of US like Minneapolis and Chicago, highlighting the role of multimodal network transporting goods from coastal regions to the interior. Investments that would lower transportation costs in the most important

nodes by only 1 percent would generate an aggregate welfare gain equivalent to 200-300 million USD of additional GDP (in 2012 USD). These investments generate interesting modal diversion effects, shifting traffic use from road to rail. Since trucks generate more greenhouse gases relative to trains, these modal diversion effects have environmental consequences for infrastructure investment in terminals.

Our paper is related to a number of different strands of research. First, this paper contributes to a rapidly expanding literature incorporating realistic transportation network into quantitative spatial equilibrium models (see [Redding \(2020\)](#) for a recent survey). Within that literature, there have been multiple efforts to merge the dis-aggregated network structure of transportation infrastructure with a general equilibrium economic geography model. ([Fajgelbaum and Schaal, 2017](#); [Allen and Arkolakis, 2022](#)). In particular, [Allen and Arkolakis \(2022\)](#) proposed a tractable way of incorporating the optimal routing choice into an spatial equilibrium model, allowing the authors to examine the general equilibrium implications of transportation improvements. While much theoretical progress has been made, the literature has often focused on one mode of transportation, approximating transport costs with either road, maritime, or rail transportation costs ([Coşar and Demir, 2018](#); [Brancaccio, Kalouptsidi and Papageorgiou, 2020](#); [Heiland et al., 2019](#); [Ganapati, Wong and Ziv, 2021](#); [Wong, 2022](#); [Degiovanni and Yang, 2023](#)). A more recent literature has focused on the contributions of highways and domestic roads to transport costs and port access ([Fan, Lu and Luo, 2019](#); [Fan and Luo, 2020](#); [Bonadio, 2021](#); [Jaworski, Kitchens and Nigai, 2023](#)).<sup>1</sup> Our project adds to this literature by studying the general equilibrium analysis of the US multi-modal transportation system—highways, rail, and barges—as well as intermodal switching terminals which allows for transshipments.

Second, our paper is related to a long-standing literature in transportation studies that examines route and mode choice both empirically and theoretically ([McFadden, Winston and Boersch-Supan, 1986](#); [Rich, Kveiborg and Hansen, 2011](#); [Beuthe, Jourquin and Urbain, 2014](#); [Winston, 1981](#)). The state-of-the-art in transportation studies solves high-dimensional traffic assignment problems algorithmically accounting for both dis-aggregated heterogeneity in modal and route choice.<sup>2</sup> We employ similar tools to those recently developed in transportation studies. Specif-

---

<sup>1</sup>[Fan, Lu and Luo \(2019\)](#) and [Jaworski, Kitchens and Nigai \(2023\)](#) focus on domestic road and highways while [Bonadio \(2021\)](#) focuses on roads and road access to ports. [Fan and Luo \(2020\)](#) is a note which characterizes bilateral transport costs and their elasticities with respect to transshipment costs.

<sup>2</sup>For a recent theoretical contribution compare [Kitthamkesorn, Chen and Xu \(2015\)](#) which solves for the traffic assignment problem allowing for both endogenous route and mode choice. A recent applied quantitative contribution in this literature ([Li, Xie and Bao, 2022](#)) models the multimodal linkages between the US and China with endogenous route choice and congestion at port locations.

ically, we employ what the transportation literature calls a *stochastic user equilibrium* where routes and modes are chosen subject to a stochastic perception error. However, we go beyond the transportation literature, by fully embedding the stochastic user equilibrium into a spatial general equilibrium framework, where input and output markets across space clear and factor and output prices are endogenously determined.

Third, our paper is related to the recent literature on the environmental impacts of transportation. Most of this literature focuses on the link between international trade and greenhouse gas emissions via transportation, and changes to this relationship in response to environmental regulations (Shapiro, 2016; Mundaca, Strand and Young, 2021; Lugovskyy, Skiba and Terner, 2022) or trade policies (Cristea et al., 2013). We instead highlight how infrastructure investments can have environmental consequences via the multimodal transportation network. While some of these papers have found compositional shifts in transport mode use due to regulation and trade policy changes,<sup>3</sup> our quantitative general equilibrium framework allows us to distinguish between the two modal complementarity and diversion effects. Additionally, our empirical framework allows us to investigate the strength of both of these effects with respect to infrastructure improvements.

The remainder of the draft is structured as follows. Section 2 describes the US multimodal transport network and our data. We then detail the multimodal routing model in Section 3 and describe how we estimate our congestion and modal substitution elasticities in Section 4. We incorporate our elasticities and apply our model to evaluate the welfare impact of terminal investments in Section 5 and conclude in Section 6.

## 2 US Domestic Freight Transportation and Data

In this section, we provide an overview of the US domestic transportation system and introduce our data sources.

### 2.1 US Domestic Freight Transportation

As mentioned above, the movement of goods from origin to destination takes place over multiple modes of transportation. While trucks are mostly used to move US freight over shorter distances

---

<sup>3</sup>Cristea et al. (2013) finds that trade liberalization between countries will increase trade from more distant partner countries, resulting in a proportional increase in air transport use and greenhouse gas emission. Lugovskyy, Skiba and Terner (2022) finds that environmental regulations capping CO<sub>2</sub> emissions from maritime shipping will substitute demand towards air transport, increasing total transport-related CO<sub>2</sub> emissions.

domestically, freight share by railroads and multiple modes increases steadily over longer distances. For freight moved over longer distances of 1000 miles or more, rail and multiple modes of transport account for one-third of freight by value (Figure 1) and more than half by weight (Figure A.1). For freight moved over more than 2000 miles, more than half of freight value is transported via rail and multiple modes. For context, the road distance between Los Angeles and Chicago is roughly 2000 miles. The geography of the US multimodal transport network includes rail, road, and waterways with intermodal switching terminals playing a major role in facilitating the movement of goods between the transport modes (Figure 2). Additionally, the dense road network plays an important role in facilitating transportation at the start and end of the movement of goods. This is commonly known as the first and last mile in freight transportation (Rodrigue, 2020; Ranieri et al., 2018).

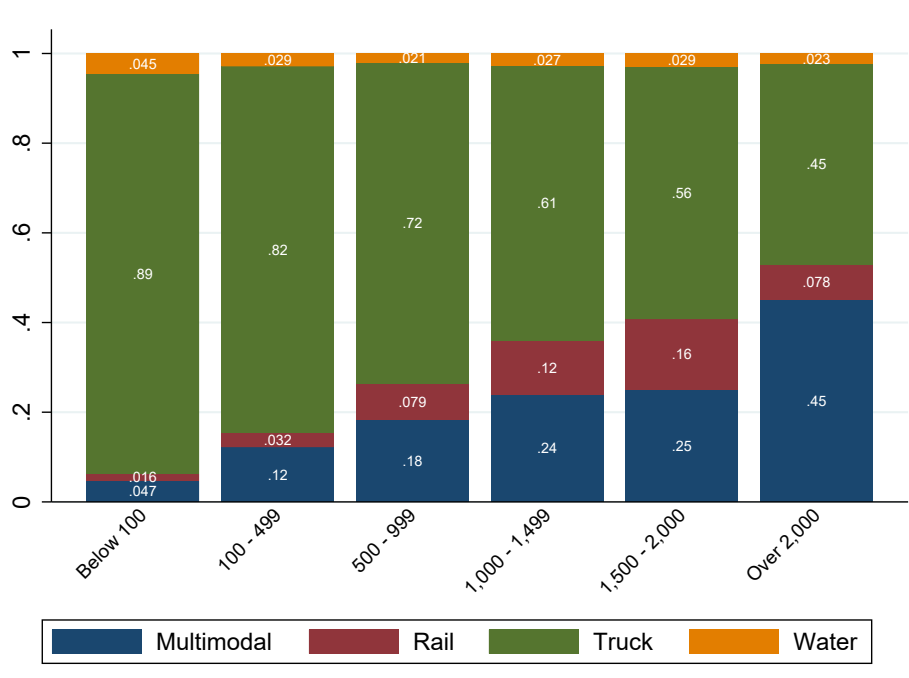
Furthermore, the US domestic freight landscape has been changing rapidly. In the 1980s, the top three modes of transporting freight in the United states are truck, railroads, and coast-wise ocean shipping (Figure A.2). However, by 2017, ocean shipping shares have drastically declined while the other two mode shares have increased. Trucking and rail both have been increasing their overall shares by about 10 percentage points by 2017. In 1980, trucking and rail accounted for 41 percent and 30 percent respectively. By 2017, trucking shares have increased to almost 50 percent while rail has increased to about 40 percent. On the other hand, ocean shipping has been declining. Ocean shipping accounted for about 20 percent of US freight in 1980 but this has declined to 4.2 percent by 2017. Inland waterway shipping shares started at 9.3 percent and declined slightly to 7.4 percent. Since air freight shares are small throughout this period (0.15 percent in 1980 to 0.34 percent by 2017), we abstract away from this mode of transport in our analysis.

With rail offering a cost- and energy-efficient alternative to trucking, it is widely expected that rail continues to increase in importance. Since the rail network is not sufficiently dense to directly reach final consumers, nevertheless trucking will remain as one of the only feasible solutions to the last mile problem. This situation emphasizes the importance of understanding the multimodal capacity of the US freight network, the key aim of this paper.

## 2.2 Data

This subsection introduces the different data sources that we use for our motivating empirical analysis in this section, as well as for our structural analysis in Section 5.

**Figure 1.** US Transport Mode Value Shares by Distance, 2018



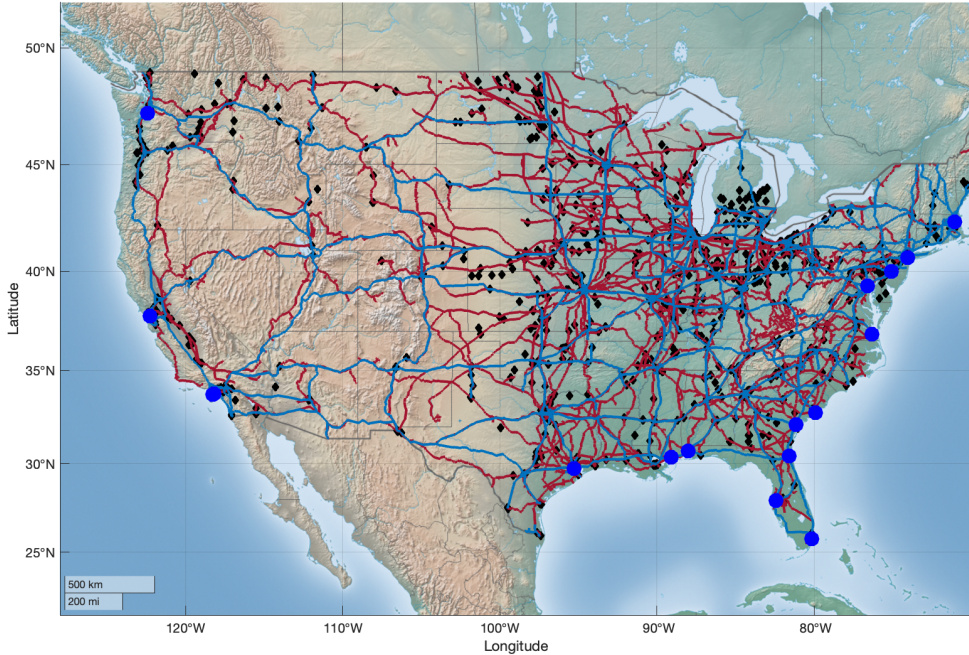
**Notes:** This figure plots the observed value share of cargo transported by different modes across various distances. Multimodal indicates cargo movement that involves more than one mode. Source: Freight Analysis Framework, US Department of Transportation, and authors' calculations.

### 2.2.1 AIS Vessel Traffic Data

We utilize automatic identification system (AIS) vessel traffic data from Marine Cadastre, a joint initiative between the Bureau of Ocean Energy Management and the National Oceanic and Atmospheric Administration. This data captures vessel location in US waters at 1-minute intervals using 200 land-based receiving stations. We observe the vessel's identifying information, its longitude and latitude location down to the minute, speed, and navigation status. The vessel's identifying information includes its International Maritime Organization Vessel number (IMO). The vessel's navigation status captures whether the vessel is being propelled (under way using engine), or moored—held in position at a pier.<sup>4</sup> Using information on the ship's speed and navigation status, we define a ship's dwell time to be the time it spends being moored at a pier and has zero speed. This is a conservative measure of ship dwell time at ports because (1) a ship

<sup>4</sup>There are additional AIS navigational statuses than the ones described here, for example being propelled via sail (under way sailing) or at anchor (held in position by an anchor but not at a dock). Future work will consider utilizing additional statuses.

**Figure 2.** US Multimodal Transportation Network



**Notes:** This figure shows the combined US multimodal freight network. We obtain the original GIS information from the U.S. Census Bureau's Topologically Integrated Geographic Encoding and Referencing (TIGER) Database. The red lines indicate the Class I multimodal railroad network. The blue lines indicate the interstate highway system (IHS). Black diamonds indicate freight terminals that are owned by Class I operators allow for road-to-rail or rail-to-road intermodal movements. The blue circles indicate the top 18 ports.

will spend time navigating within the port area as it prepares to moor at a pier and (2) a ship can also end up waiting outside of the port area at anchor before navigating to the port ([New York Times, 2021](#)). In future work we plan on investigating additional measures of dwell times, including the entire time a ship spends within the port areas (not just when they are moored), as well as the time a ship spends at anchor within or just outside of port areas.

In order to match these ships to the ports they are located at, we next require geographical information of the ports. We use the Port Statistical Area shapefiles from the US Army Corps of Engineers and match these ships to the top 30 container ports in the US. These port polygon areas also allows us to calculate the total amount of time a ship spends within the port region on top of the time it spends moored at a dock. Additionally, in order to identify the cargo capacity of these ships and their containership status, we match these ships to the Port Entrance and Clearance dataset from the US Army Corps of Engineers using their identifying information and when they are at these ports. The ship cargo capacity measures the volume of the ship that can be used for loading cargo (also known as net tonnage of a ship). This cargo capacity measure

for each ship will contribute to our port traffic measure at each port every day.

We highlight two examples to show how we capture these ships and the time they spend at a port. Panel (A) Figure 3 shows the path of containership CMA CGM Christophe Colomb as it enters the Port of Los Angeles (LA) on May 2, 2022. It is a containership with a cargo capacity of 86,100 tons (13,800 twenty-foot equivalent unit containers (TEUs)) and is operated by container shipping company CMA CGM. Panel (B) Figure 3 shows the path of containership Guthorm Maersk entering and leaving the Port of Newark. Guthorm Maersk is a containership with a cargo capacity of 57,000 tons (11,000 TEUs) and is operated by container shipping company Maersk. The ship path entering the port is highlighted in the figure and the redder color indicates slower speed. The darker region of both figures indicate the port polygon for both ports as defined by the US Army Corps of Engineers.

**Port Traffic** Our measure of port traffic is defined as the sum of the net tonnage of each ship moored at the port each day, multiplied by the percent of the day they spend at the port—crucially including ships that arrived prior to that day but still remained moored at port. To be more specific, if a ship remained moored at port all day without exiting, their contribution to port traffic would be 100% of their net tonnage (100% of the time they spent at the port). If a ship left at any point during that day, their net tonnage contribution would be less than 100% and instead determined by the amount of time they spent moored at port that day.

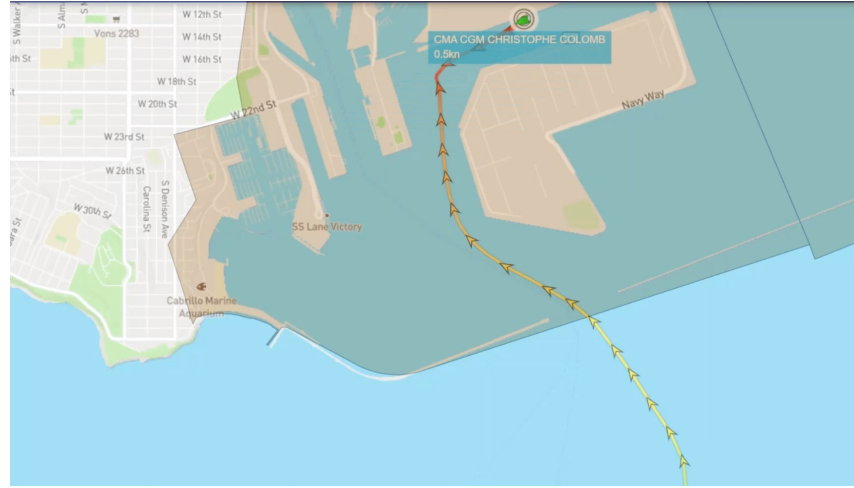
With this daily port traffic measure, we calculate moving averages of the port-level traffic for varying amounts of time. We have done this for 3, 7, 14, 21, and 28 days. We present the 28-day moving average results and have included the rest in the appendix.<sup>5</sup>

**Summary Statistics** Our matched dataset from 2015 to 2021 has 3,755 unique vessels with 1,444 containerships. The top 30 ports in our dataset account for around 95% of all US container trade annually. Figure 4 plots the average of containership dwell times at the top 30 US ports from June 2015 to December 2021. The average dwell time over this period is around 33.3 hours per ship with a standard deviation of 5 hours. However, as seen in Figure 4, there is a significant increase in the ship dwell times post 2021. The average ship dwell time after 2021 is 42.8 hours.

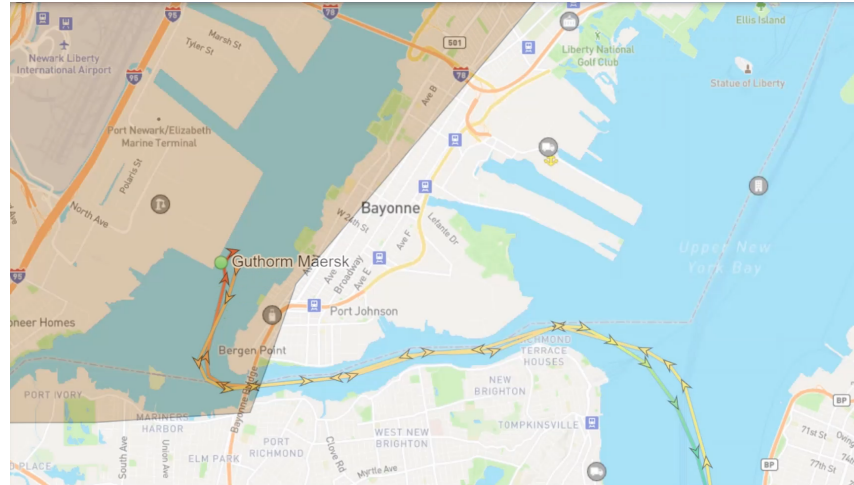
---

<sup>5</sup>It is acknowledged here that this measure could be interpreted as an upper bound measure of the amount of traffic at each port since using the net tonnage measure of a ship assumes that it is filled to capacity. Future work will incorporate the draft information we observe for these ships which will allow us to infer net capacity change. Additionally, an alternative lower bound measure of port traffic is a count of ships currently at the port (since smaller ships would have equal weight as large ships).

**Figure 3.** Illustration of AIS Mooring Paths



(a) Port of Los Angeles



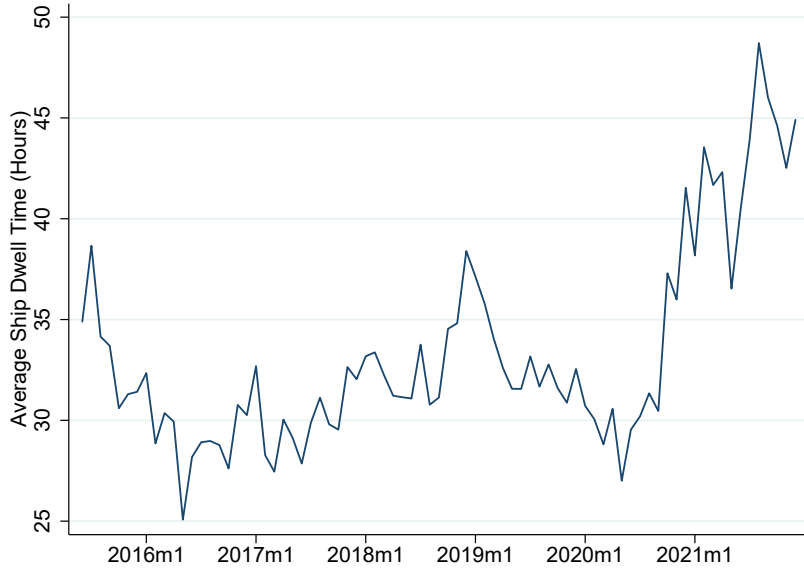
(b) Port of Newark

**Notes:** Panel (a) shows the containership CMA CGM Christophe Colomb at the Port of Los Angeles while Panel (b) shows the containership Guthorm Maersk at the Port of Newark. The path of each ship to and from the port shows its exact travel path. The darker regions at each port shows the port polygons as defined by the US Army Corps of Engineers.

### 2.2.2 Rail Dwell Times Data

We obtain weekly rail station dwell times from the Surface Transportation Board (STB). Railroads provide the STB with the average time a railcar resides at a station, measured in hours, for their 10 largest stations in terms of railcars processed. This dwell time measure excludes cars on through trains—trains that travels without stops en route. Since this dataset only captures a subset of all rail stations (albeit the largest ones), we match the ports in the previous section to their local rail stations. We do this by expanding the port polygon areas in 50km intervals. The rail stations that are captured in the buffer areas of their closest port is be considered a rail station in the vicinity of this port and is likely to service traffic to and from the port. Due

**Figure 4.** Containership Dwell Times at Port



**Notes:** This figure plots the average of containership dwell times at the top 30 US ports from June 2015 to December 2021. Weighted by ship net tonnage.

to their proximity, The ports of Los Angeles and Long Beach are combined into one port for this exercise. We use a buffer area of 150km which captures 7 ports and 12 rail stations. We test the robustness of this buffer area by increasing the interval in our analysis to 200km where we capture 8 ports and 14 rail stations. Further increases to this interval result in more muted responses of rail station dwell times to port traffic, as these rail stations are much further away.

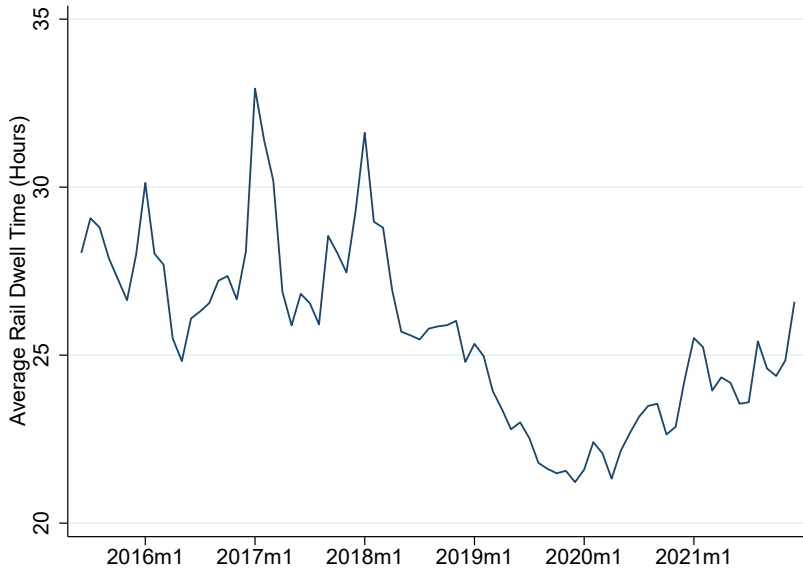
Additionally, the rail dwell times dataset is reported at the weekly level. In order to match this to our daily port traffic measure for analysis, we aggregate our port traffic measure up to the weekly level. We start our week on a Monday since we observe in our data that most ships tend to enter a port on Mondays.

**Summary Statistics** Figure 7 plots the average of rail station dwell times from June 2015 to December 2021. The average dwell time over this period is around 25.5 hours per station with a standard deviation of 2.5 hours. However, there is also a large decrease in dwell times around the start of the pandemic followed up a steep increase afterwards.

### 2.2.3 Rail Traffic Data

We have obtained access to confidential US rail traffic data from the Surface Transportation Board. This is a stratified sample of carload waybills for all U.S. rail traffic submitted by those rail carriers terminating 4,500 or more revenue carloads annually, covering 48 states (except Alaska

**Figure 5.** Rail Station Dwell Times



**Notes:** This figure plots the average time a railcar spends at a rail station from June 2015 to July 2022.

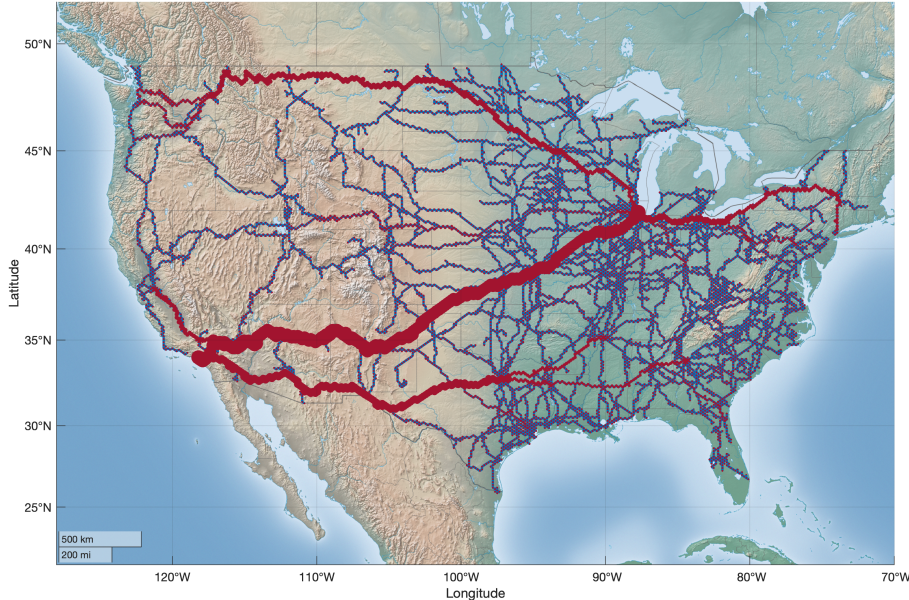
and Hawaii). The carload waybills report the origin location, origin rail station, interchange stations, terminating station, and destination location of the freight commodities. The rich geographical information in this confidential data set allows us to study the routing of these commodities through the railroad network over this time period. Additionally, this data set also contains commodity-specific information including number of car loads, weight, freight charges, whether it is a domestic or international shipment, and its inter-modality—if the movement of this commodity included other transport modes. Overall, the data covers 48 states (except Alaska and Hawaii) and 39 STCC 2 digit commodities. Work is currently ongoing to merge both the rail traffic data to the AIS vessel traffic data at ports.

### 3 Economic Geography Model with Multimodal Routing

In this section, we embed a recursive formulation of the multimodal routing problem into an otherwise standard economic geography model with domestic trade between a discrete number of locations and freely mobile labor reallocation across locations as in [Allen and Arkolakis \(2014\)](#), [Redding \(2016\)](#), and [Allen and Arkolakis \(2022\)](#).

We assume perfect competition in our freight transport companies. While this is a simplifying assumption since the focus of this paper is on the multimodal network transport structure, the transportation literature has also established that multimodal container transport is generally

**Figure 6.** Rail Traffic Flows



**Notes:** This figure plots the average time a railcar spends at a rail station from June 2015 to July 2022.

more competitive relative to unimodal transport ([Zgonc, Tekavčič and Jakšić, 2019](#)), and within rail transport relative to non-containerized shipments ([Surface Transportation Board, 2009](#)).<sup>6</sup> The main reason for this is that container transport services can be provided by different modes of transportation, including trucks which have long been established to be perfectly competitive (NEED CITE).

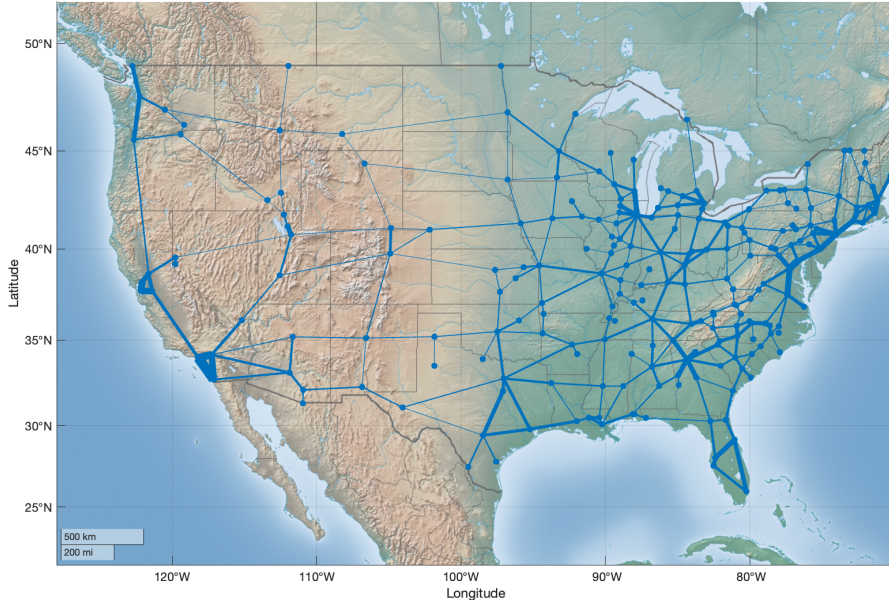
### 3.1 Geography and Transportation

Let  $\mathcal{G} \equiv (\mathcal{N}, \mathcal{L})$  be a multigraph representing a (multi-)modal transportation network where  $\mathcal{N}$  and  $\mathcal{L}$  are the set of nodes and links respectively. We define the set of successor nodes  $\mathcal{F}(i)$  and the set of predecessor nodes  $\mathcal{B}(i)$  for each node  $i \in \mathcal{N}$ . Furthermore, let  $\mathcal{G}_m \equiv (\mathcal{N}_m, \mathcal{L}_m)$  be the subgraph representing the transportation network for mode  $m$ , where  $\mathcal{N}_m \subseteq \mathcal{N}$  and  $\mathcal{L}_m \subseteq \mathcal{L}$  are the mode-specific nodes and links respectively. We also define the mode-specific successor and predecessor nodes  $\mathcal{F}_m(i)$  and  $\mathcal{B}_m(i)$ . Each link  $ij \in \mathcal{L}_m$  is associated with a generalized link

---

<sup>6</sup>[Zgonc, Tekavčič and Jakšić \(2019\)](#) studies the impact of distance on multimodal road-rail transport compared to unimodal road transport and finds that multimodal transport can be competitive relative to unimodal transport even over relatively short distances. In a study on the US freight rail industry, ([Surface Transportation Board, 2009](#)) reports that multimodal rail shipments have lower markups than other shipments, and that rail rates are lower for locations that are closer to alternative transport modes. With data on door-to-door container shipments, one would be able to study the issue of market power in container freight transport in more detail. However, to the best of our knowledge, this data is not available in a comprehensive manner.

**Figure 7.** Rail Traffic Flows



**Notes:** This figure plots the average time a railcar spends at a rail station from June 2015 to July 2022.

travel cost  $t_{ij,m}$  which can be flow dependent. The set of OD pairs is defined as  $\mathcal{W}$ .

Moving goods from origin  $i$  to destination  $j$  along route  $r$ , which involves a series of links index from 0 to  $K$ , is indicated by vector  $r \equiv \{i = r_0, r_1, \dots, r_K = j\}$ . We define a primary modal network,  $m = 0$ , that represents the dense road network on which all cities and road intersections are located. All other modes ( $m \neq 0$ ) are secondary transport networks (i.e. rail, barges etc.). A subset of nodes on the primary and secondary networks are intermodal terminals which allow for switches between modal networks.

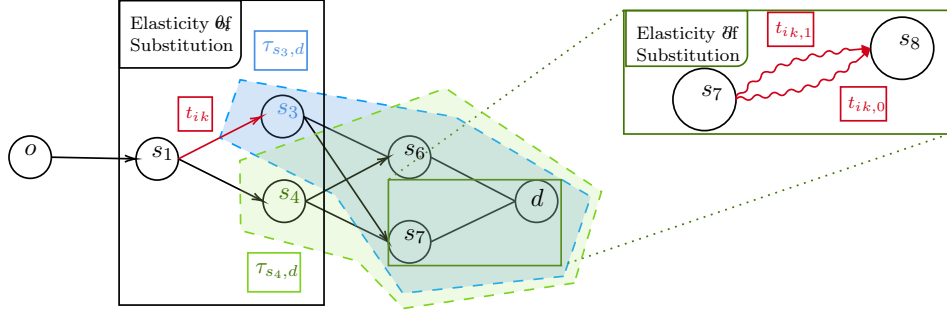
### 3.2 Consumption and Production

A representative agent lives in location  $j$ , supplies her unit endowment of labor inelastically, earns a wage rate  $w_j$ , and purchases quantities of a continuum of consumption goods,  $\nu \in [0, 1]$ . She is endowed with constant elasticity of substitution (CES) preferences where the elasticity of substitution is given by  $\sigma \geq 0$ . Her preferences are given by,

$$U_j = \left( \sum_{\nu} q_{ij}^{\frac{\sigma-1}{\sigma}} (\nu) \right)^{\frac{\sigma}{\sigma-1}}$$

where  $U_j$  aggregates the quantities produced from all other locations  $i$ . Furthermore, we define

**Figure 8.** Multimodal Transportation Network



**Notes:** The figure illustrates a simplified multimodal transport network. Nodes without primes are located on the primary road network, while nodes with primes are located on the secondary multimodal network. Each link is associated with an (iceberg) transport cost. The mode-specific transport cost of each link on either the primary or secondary network is given by  $t$ . The existence of links between nodes on both networks allows for switching between the networks—intermodal terminals (e.g.  $k$  and  $k'$  on the primary and secondary network respectively). The switching cost of going through these intermodal terminals is  $s$ .

aggregate income as  $Y^W$ , the total labor endowment as  $\bar{L}$ , and average per capita income as the numeraire, i.e.  $Y^W/\bar{L} = 1$ .

Each location  $i$  produces each good  $\nu \in [0, 1]$  subject to a constant returns to scale technology and transports it to each destination  $j$  along each of the feasible routes  $r \in \mathcal{R}_{ij}^1 \cup \mathcal{R}_{ij}^{1,2}$ . The set of feasible routes combines unimodal and multimodal routes that connect locations on the primary network. We assume perfect competition which implies that the price of good  $\nu$  in destination  $j$  from origin  $i$  along route  $r$  is given by

$$p_{ij,r} = \frac{w_i \left( \prod_{k=1}^K t_{r_{k-1}, r_k} \right)}{A_i}$$

where the marginal cost of production in  $i$  is  $\frac{w_i}{A_i}$ , local wages are  $w_i$ , and each worker can produce  $A_i$  units of goods. Trade cost is route-specific and multiplicative over all links along route  $r$ . In this context, it is assumed that individuals choose the good with the lowest price, i.e. they choose the cheapest location-route combination.

### 3.3 Recursive Routing and Trade

We follow recent innovations in route choice modeling (Oyama, Hara and Akamatsu, 2022; Papola and Marzano, 2013; Daly and Bierlaire, 2006) and characterize the individuals' routing and sourcing choice as a joint choice of elemental links of the route in an ordered sequence from the

residential location  $o$  toward the sourcing destination  $d$ , which [Papola and Marzano \(2013\)](#) call an ordered joint choice context. Such a joint choice can be modeled as a recursive choice subject to extreme value preference shocks without discounting. The individual then makes routing choices along the network by choosing the cost-minimizing link  $ij$  conditional on the previously chosen node  $i$ . At each node the individual therefore chooses between links that imply recursively defined source-route specific prices, i.e.

$$p_{id} = \mathbb{E} \left[ \min_{j \in \mathcal{F}(i)} \{t_{ij} p_{jd} \varepsilon_{ij}\} \right] = \left( \sum_{j \in \mathcal{F}(i)} (t_{ij} p_{jd})^{-\theta_i} \right)^{-\frac{1}{\theta_i}}$$

We make two distinct assumptions: One is that the extreme value shocks are recursively defined following ([Daly and Bierlaire, 2006](#)). The other is that there is a nested choice: Conditional on the previously chosen node  $i$ , the individual first chooses between modes than between links within modal networks at each node. We model this by introducing an extreme value shock that is multiplicatively separable between a mode specific shock and a link specific shock.

In this context, it is assumed that individuals choose the good with the lowest price, i.e. they choose the cheapest location-route combination. Following [Eaton and Kortum \(2002\)](#), we assume that  $\varepsilon_{ij,r}(\nu)$  is iid Fréchet distributed across routes and goods with scale parameter  $1/A_i$ , where  $A_i$  captures origin-specific efficiency (the same  $A_i$  as earlier) and shape parameter  $\theta$  regulates the inverse of shock dispersion. Given the preference shocks, the probability that  $j$  purchases a good from  $i$  using route  $r$  is given by,<sup>7</sup>

$$\pi_{ij,d} = \frac{(w_d)^{-\theta} (t_{ij} \tau_{jd})^{-\theta}}{\sum_{d \in \mathcal{N}} (w_d)^{-\theta} \sum_{j' \in \mathcal{F}(i)} (t_{ij'} \tau_{j'd})^{-\theta}}$$

### 3.3.1 Recursive Equilibrium

### 3.3.2 Multimodal Routing and transport cost

$$\tau_{id} = \mathbb{E} \left[ \min_{j \in \mathcal{F}(i)} \left\{ \mathbb{E} \left[ \min_{m \in \mathcal{M}(i)} \{t_{ijm} \varepsilon_m\} \right] \tau_{jd} \varepsilon_{ij} \right\} \right]$$

---

<sup>7</sup>See detailed derivations in Appendix [B.1](#).

### 3.4 Traffic flows and congestion

We proceed by deriving the implied traffic flow along different parts of the network. In this subsection we will re-iterate the derivation of the traffic on the primary network as in [Allen and Arkolakis \(2022\)](#) before then turning towards novel results, i.e. the traffic on the secondary network and the traffic at terminal stations. The purpose of deriving these objects is to introduce traffic and congestion in the equilibrium conditions (12) and (13). Specifically, we will be interested in introducing switching costs that depend on the throughput at any given terminal, thus creating bottlenecks in the multimodal transportation system.

**Traffic on the Aggregate Network.** We begin by characterizing the traffic on the aggregate network across any mode.<sup>8</sup> We utilize our recursive framework to characterize the number of times a link  $(k, l)$  is used in trade between  $(i, j)$ ,  $\pi_{ij}^{kl}$ , which - analogously to AA2022 - we refer to as link intensity. To obtain the link intensity we construct the probability that a route  $i$  to  $j$  is used and the likelihood that a particular link  $(k, l)$  is chosen, i.e.

$$\pi_{ij}^{kl} = \left( \frac{\tau_{ij}}{\tau_{ik} t_{kl} \tau_{ij}} \right)^\theta \quad (1)$$

In the appendix we show how the formula follows directly from our recursive routing choice.

We can then use these derivations to characterize traffic on the primary network,

$$\Xi_{kl} = \sum_{i \in \mathcal{N}} \sum_{j \in \mathcal{N}} \pi_{ij,kl} E_j = \sum_{i \in \mathcal{N}} \sum_{j \in \mathcal{N}} \pi_{ij}^{kl} X_{ij} \quad (2)$$

Combining the market access and the link intensity expression (1) allows us to derive the expression for equilibrium traffic,

$$\Xi_{kl}^1 = t_{kl}^{-\theta} \times P_k^{-\theta} \times \Pi_l^{-\theta} \quad (3)$$

Equation (3) is a gravity equation for traffic on the primary network. The expression connects traffic flows to inward,  $P_k^{-\theta}$  and outward market access measures,  $\Pi_l^{-\theta}$ . Both market access measures depend on the transportation cost across the multimodal transport network.

**Traffic on the Modal Networks.** We proceed by characterizing the traffic on the secondary transport network. We define  $\pi_{ij}^{k'l'}$  as the link intensity of a link  $k'l'$  on the secondary transporta-

---

<sup>8</sup>Detailed derivations for traffic on the primary and secondary network as well as traffic at terminal stations is given in Appendix [B.4](#).

tion network, which is given by,

$$\pi_{ij}^{k'l'} \equiv \sum_{r \in \mathcal{R}_{ij}^{1,2}} \left( \frac{\pi_{ij,r}}{\sum_{r' \in \mathcal{R}_{ij}^1 \cup \mathcal{R}_{ij}^{1,2}} \pi_{ij,r'}} \right) n_r^{k'l'} \quad (4)$$

which can be written using matrix algebra as,

$$\pi_{ij}^{kl,m} = \left( \frac{\tau_{ij}}{\tau_{ik} t_{kl} \tau_{ij}} \right)^\theta \left( \frac{t_{ki}}{t_{ki,m}} \right)^\eta \quad (5)$$

The difference between (1) compared to (5) consists in tracing out the importance of linkages along the secondary network relative to the overall average transport cost between  $i$  and  $j$ . It is important to note that this not only depends on the transportation cost along the secondary network between  $k'$  and  $l'$ , but also on the switching cost to the secondary network at node  $k$  and  $l$ . Using this expression for link intensity we can characterize traffic on the secondary transport infrastructure, i.e.

$$\Xi_{k'l'} \equiv \sum_{i \in \mathcal{N}} \sum_{j \in \mathcal{N}} \sum_{r \in \mathcal{R}_{ij}^{1,2}} \pi_{ij,r} n_r^{k'l'} E_j = \sum_{i \in \mathcal{N}} \sum_{j \in \mathcal{N}} \pi_{ij}^{k'l'} X_{ij},$$

Combining the market access and the link intensity expressions (5) allows us to derive the expression for equilibrium traffic on the secondary transportation network,

$$\Xi_{kl}^2 = s_{kk'}^{-\theta} \tau_{k'l'}^{-\theta} s_{l'l}^{-\theta} \times P_k^{-\theta} \times \Pi_l^{-\theta}, \quad (6)$$

Equation (6) is the natural counterpart to equation (3) for the secondary network. It also reflects a gravity equation and connects traffic flows to market access measures. Crucially, bilateral traffic here depends on the transportation cost on the secondary network and the switching costs incurred when transitioning from the primary to the secondary network.

**Traffic at Terminals.** Finally, we turn towards characterizing traffic at terminals where switches between the primary and secondary network occur. Since a terminal is represented by a link on the partitioned graph, we can simply follow the same steps as before. For the link intensity between a node on the primary network  $k$  and a node on the secondary network  $k'$ ,  $\pi_{ij}^{kk'}$ , is as follows:

$$\pi_{ij}^{kk'} \equiv \sum_{r \in \mathcal{R}_{ij}^{1,2}} \left( \frac{\pi_{ij,r}}{\sum_{r' \in \mathcal{R}_{ij}^1 \cup \mathcal{R}_{ij}^{1,2}} \pi_{ij,r'}} \right) n_r^{kk'}$$

With some matrix calculus we obtain,

$$\pi_{ij}^{kk'} = \left( \frac{\tau_{ij}}{\tau_{ik} s_{kk'} \tau_{k'j}} \right)^\theta \quad (7)$$

We can characterize equilibrium flows,

$$\Xi_{kk'} \equiv \sum_{i \in \mathcal{N}} \sum_{j \in \mathcal{N}} \sum_{r \in \mathcal{R}_{ij}^{1;2}} \pi_{ij,r} n_r^{kk'} E_j = \sum_{i \in \mathcal{N}} \sum_{j \in \mathcal{N}} \pi_{ij}^{kk'} X_{ij}, \quad (8)$$

Combining with the market access gravity equation, we obtain,

$$\Xi_{kk'} = (s_{kk'})^{-\theta} \times P_k^{-\theta} \times \sum_l \tau_{k'l'}^{-\theta} s_{l'l}^{-\theta} \Pi_l^{-\theta}, \quad (9)$$

$$\Xi_{k'k} = (s_{k'k})^{-\theta} \times \Pi_k^{-\theta} \times \sum_l \tau_{k'l'}^{-\theta} s_{l'l}^{-\theta} P_k^{-\theta}, \quad (10)$$

Equations (9) and (10) differ slightly to the previous traffic equations in that they feature an additional summation term. This summation term is a higher order market access term that reflects the fact that in- and outgoing traffic at a terminal depends on the sum of traffic that is generated by nodes that can be reached via that terminal along the secondary network. This higher order market access term is also a natural measure of the centrality of the terminals in terms of connecting primary and secondary network and thus - in a sense - their capacity to become a bottleneck to the overall transportation network.

Taking stock, equations (3) and (6) characterize traffic on the primary and secondary network, while (9) and (10) characterize equilibrium traffic at terminals.

### 3.5 Equilibrium with Traffic

In this section, we exploit the recursive routing formulation to express the equilibrium in terms of edge-specific - and possibly flow-dependent - transport costs.

In a first step, we restate the equilibrium conditions given the model fundamentals and iceberg transport cost  $\{\bar{A}_i, \bar{u}_i, \tau_{ij}\}$  as in AA2022. We follow their derivations, by imposing market clearing and balanced trade and we impose welfare equalization, i.e.  $W_j = \frac{w_j}{P_j} u_j$  (Allen and Arkolakis, 2014) and assume localized productivity ( $A_i$ ) and amenity spillovers ( $u_i$ ) that

depend on the density of workers in a locality, i.e.

$$A_i = \bar{A}_i L_i^\alpha, \quad u_i = \bar{u}_i L_i^\beta \quad (11)$$

where  $\bar{A}_i$  is exogenous component of productivity at location  $i$  and  $\alpha$  determines the extent to which productivity is affected by the local population  $L_i$  (productivity spillovers),  $\bar{u}_i$  is the exogenous utility derived from living in location  $i$  and  $\beta$  governs the extent to which amenities are affected by the location population (amenity spillovers). Given iceberg transport cost the equilibrium conditions are unchanged and are restated for convenience,

$$\bar{A}_i^{-\theta} y_i^{1+\theta} l_i^{-\theta(1+\alpha)} = \chi \sum_{j=1}^N (\tau_{ij})^{-\theta} \bar{u}_j^\theta y_j^{1+\theta} l_j^{\theta(\beta-1)} \quad (12)$$

$$\bar{u}_i^{-\theta} y_i^{-\theta} l_i^{\theta(1-\beta)} = \chi \sum_{j=1}^N (\tau_{ij}^1)^{-\theta} \bar{A}_j^\theta y_j^{-\theta} l_j^{\theta(\alpha+1)} \quad (13)$$

where we have written the equilibrium condition in terms of shares of world income in location  $i$ ,  $y_i \equiv \frac{Y_i}{YW}$ , and shares of total labor in location  $i$ ,  $l_i \equiv \frac{L_i}{LW}$ . Furthermore,  $\chi \equiv \left(\frac{L(\alpha+\beta)}{W}\right)^\theta$  is an endogenous scalar that is inversely related to the global welfare of the spatial economy.<sup>9</sup> The equilibrium system is identical to the one in [Allen and Arkolakis \(2022\)](#), but distinguishes between trade on the primary and secondary transportation system. Specifically, given the fundamentals  $\{\bar{A}_i, \bar{u}_i, \tau_{ij}\}$ , the system of  $2N$  equations can be solved for the  $2N$  endogenous equilibrium values,  $\{y_i, l_i\}$ . Transportation cost is endogenous and depends on the agent's routing choice which itself depends on the underlying multimodal transportation network.

In a final step, we re-consider the equilibrium equations (12) and (13) which pin down income, welfare and labor densities as a function of the transportation cost. Our framework determines transportation cost endogenously as a function of the routing (and therefore mode choice) of the agent, subject to congestion forces along the primary network and at terminal stations.

In this section we combine the equilibrium condition with the expression for the endogenous transportation cost and perform a matrix inversion to obtain the equilibrium in terms of primary

---

<sup>9</sup>See Online Appendix D.1 for detailed derivations.

and secondary traffic. This matrix inversion gives the following equations.<sup>10</sup>

$$y_i^{\frac{1+\theta\lambda_1+\theta}{1+\theta\lambda_1} l_i^{\frac{-\theta(1+\alpha+\theta\lambda_1(\alpha+\beta))}{1+\theta\lambda_1}}} = \chi \bar{A}_i^\theta \bar{u}_i^\theta y_i^{\frac{1+\theta\lambda_1+\theta}{1+\theta\lambda_1} l_i^{\frac{\theta(\beta-1)}{1+\theta\lambda_1}}} \\ + \chi^{\frac{\theta\lambda_1}{1+\theta\lambda_1}} \sum_j (\bar{t}_{ij} \bar{L}^{\lambda_1})^{-\frac{\theta}{1+\theta\lambda_1}} \bar{A}_i^\theta \bar{u}_i^{\theta \frac{\theta\lambda_1}{1+\theta\lambda_1}} \bar{A}_j^{-\frac{\theta}{1+\theta\lambda_1}} y_j^{\frac{1+\theta}{1+\theta\lambda_1} l_j^{-\frac{\theta(1+\alpha)}{1+\theta\lambda_1}}} \\ + \sum_j s_{ii'}^{-\theta} \tau_{i'j'}^{-\theta} s_{j'j}^{-\theta} \bar{A}_j^{-\theta} y_j^{1+\theta} l_j^{-\theta(1+\alpha)} \bar{A}_i^\theta l_i^{-\theta(\beta-1) \frac{\theta\lambda_1}{1+\theta\lambda_1}} y_i^{-\theta \frac{\theta\lambda_1}{1+\theta\lambda_1}} \quad (14)$$

$$y_i^{-\frac{\theta(1-\lambda_1)}{1+\theta\lambda_1} l_i^{\frac{\theta(1-\beta-\theta\lambda_1(\alpha+\beta))}{1+\theta\lambda_1}}} = \chi \bar{A}_i^\theta \bar{u}_i^\theta y_i^{-\frac{\theta(1-\lambda_1)}{1+\theta\lambda_1} l_i^{\frac{\theta(\alpha+1)}{1+\theta\lambda_1}}} \\ + \chi^{\frac{\theta\lambda_1}{1+\theta\lambda_1}} \sum_j (\bar{t}_{ji} \bar{L}^{\lambda_1})^{-\frac{\theta}{1+\theta\lambda_1}} \bar{A}_i^{\theta \frac{\theta\lambda_1}{1+\theta\lambda_1}} \bar{u}_i^\theta \bar{u}_j^{-\frac{\theta}{1+\theta\lambda_1}} l_j^{\frac{\theta(1-\beta)}{1+\theta\lambda_1}} y_j^{-\frac{\theta}{1+\theta\lambda_1}} \\ + \sum_j s_{jj'}^{-\theta} \tau_{j'i'}^{-\theta} s_{i'i}^{-\theta} \bar{u}_j^{-\theta} y_j^{-\theta} l_j^{\theta(1-\beta)} \bar{u}_i^\theta l_i^{-\theta(1+\alpha) \frac{\theta\lambda_1}{1+\theta\lambda_1}} y_i^{\frac{\theta\lambda_1(1+\theta)}{1+\theta\lambda_1}} \quad (15)$$

Equations (14) and (15) describe the equilibrium distribution of economic activity as function of the underlying  $\{y_i, l_i\}$  as a function of the model parameters,  $\{\alpha, \beta, \theta, \lambda\}$ , geography and underlying  $\{\bar{A}_i, \bar{u}_i\}$ , as well as the fundamental transportation infrastructure, i.e. the primary transport network,  $\bar{\mathbf{T}} \equiv [\bar{t}_{kl}]$ , the terminal transport network connecting primary and secondary network,  $\bar{\mathbf{S}} \equiv [\bar{S}_{kk'}]$ , as well as the secondary transport network  $\bar{\mathbf{T}} \equiv [\bar{t}_{kl}]$ .

While the introduction of multimodal transportation on a segmented transportation system introduced added conceptual complexity to the problem, the equilibrium system remains *as tractable* as the system presented in Allen and Arkolakis (2022). Specifically, the convenience of the additive separability of the inverse of a partitioned matrix allows us to derive a similar equilibrium system as the original one, with the only alteration being an added summation term in each equation that traces out the spatial variation in access to the secondary transport system. The spatial distribution of economic activity is then jointly determined by the topography of the primary and secondary transport system.

### 3.6 Counterfactuals

To evaluate the welfare impact of infrastructure investments along either the primary, secondary network or terminal locations in a setting where agents make complicated routing and mode choices while also allowing for a rich characterization of congestion across the multimodal trans-

---

<sup>10</sup>For simplicity we do not yet substitute at this point for how switching costs depend on traffic at terminal locations as mirrored by equations (10) and (9). We will do so in the next step when deriving the counterfactual equilibrium.

port system. To do so we first adjust the equilibrium conditions, (14) and (15), to reflect the congestion forces outlined above. We then follow Dekle, Eaton and Kortum (2008) and employ 'Hat Algebra' to express the equilibrium in terms of changes of the endogenous variables. In the following we denote with hats changes in variables,  $\hat{\gamma}_i \equiv \frac{\gamma'_i}{\gamma_i}$ .<sup>11</sup> The proposition below describes the resulting system of equations that determines the counterfactual equilibrium.

**Proposition 1 (Counterfactual Equilibrium)** *Consider an economy in equilibrium with primary transport network,  $\bar{\mathbf{T}} \equiv [\bar{t}_{kl}]$ , and a terminal transport network connecting primary and secondary network,  $\bar{\mathbf{S}} \equiv [\bar{S}_{kk'}]$ , as well as the secondary transport network  $\bar{\mathbf{T}} \equiv [\bar{t}_{kl}]$ . Consider any change either in the underlying infrastructure network denoted by  $\hat{t}_{kl}$ , or any change in the switching cost,  $\hat{s}_{kk'}$ . Given observed traffic flows  $(\Xi_{ij}^1, \Xi_{i'j'}^2)$ , economic activity in the geography  $(Y_i, E_j)$ , and parameters  $\{\alpha, \beta, \theta, \lambda_1, \lambda_2, \nu\}$ , the equilibrium change in economic outcomes  $(\hat{y}_i, \hat{l}_i, \hat{\chi})$  is the solution of the following system of equations:*

$$\begin{aligned} \hat{l}_i^{-\frac{\theta(1+\alpha+\theta\lambda_1(\alpha+\beta))}{1+\theta\lambda_1}} \hat{y}_i^{-\frac{\theta(1-\lambda_1)}{1+\theta\lambda_1}} &= \hat{\chi} \left( \frac{E_i}{E_i + \sum_j \Xi_{ij}^1 + \sum_j \Xi_{ij}^2} \right) \hat{y}_i^{\frac{1+\theta\lambda_1+\theta}{1+\theta\lambda_1}} \hat{l}_i^{\frac{\theta(\beta-1)}{1+\theta\lambda_1}} \\ &+ \hat{\chi}^{\frac{\theta\lambda_1}{1+\theta\lambda_1}} \sum_j \left( \frac{\Xi_{ij}^1}{E_i + \sum_j \Xi_{ij}^1 + \sum_j \Xi_{ij}^2} \right) \hat{t}_{ij}^{-\frac{\theta}{1+\theta\lambda_1}} \hat{l}_j^{\frac{-\theta(\alpha+1)}{1+\theta\lambda_1}} \hat{y}_j^{\frac{\theta+1}{1+\theta\lambda_1}} \\ &+ \hat{\chi}^{\frac{2\theta\lambda_2}{1+\theta\lambda_2}} \left( \hat{y}_i \hat{l}_i^{\beta-1} \right)^{\frac{\theta^2(\lambda_1-\lambda_2)}{(1+\theta\lambda_1)(1+\theta\lambda_2)}} \sum_j \left( \frac{\Xi_{ij}^2}{E_i + \sum_j \Xi_{ij}^1 + \sum_j \Xi_{ij}^2} \right) \hat{s}_{ii'}^{-\frac{\theta}{1+\theta\lambda_2}} \hat{\tau}_{i'j'}^{-\theta} \hat{s}_{j'j}^{-\frac{\theta}{1+\theta\lambda_2}} \hat{l}_j^{\frac{-\theta(\alpha+1)}{1+\theta\lambda_2}} \hat{y}_j^{\frac{\theta+1}{1+\theta\lambda_2}} \\ &\times \left( \sum_l \frac{\Xi_{i'l'}^2}{\sum_l \Xi_{i'l'}^2} \hat{\tau}_{i'l'}^{-\theta} \hat{s}_{l'l}^{-\theta} \left( \hat{l}_l^{\alpha+1} \hat{y}_l^{-\frac{\theta+1}{\theta}} \right)^{-\theta} \right)^{-\frac{\theta\lambda_2}{1+\theta\lambda_2}} \left( \sum_l \frac{\Xi_{j'l'}^2}{\sum_l \Xi_{j'l'}^2} \hat{\tau}_{j'l'}^{-\theta} \hat{s}_{l'l}^{-\theta} \left( \hat{y}_l \hat{l}_l^{\beta-1} \right)^{-\theta} \right)^{-\frac{\theta\lambda_2}{1+\theta\lambda_2}} \\ \hat{l}_i^{-\frac{\theta(1+\alpha+\theta\lambda_1(\alpha+\beta))}{1+\theta\lambda_1}} \hat{y}_i^{-\frac{\theta(1-\lambda_1)}{1+\theta\lambda_1}} &= \hat{\chi} \left( \frac{Y_i}{Y_i + \sum_j \Xi_{ji}^1 + \sum_j \Xi_{ji}^2} \right) \hat{y}_i^{\frac{-\theta(1-\lambda_1)}{1+\theta\lambda_1}} \hat{l}_i^{\frac{\theta(\alpha+1)}{1+\theta\lambda_1}} \\ &+ \hat{\chi}^{\frac{\theta\lambda_1}{1+\theta\lambda_1}} \sum_j \left( \frac{\Xi_{ij}^1}{Y_i + \sum_j \Xi_{ji}^1 + \sum_j \Xi_{ji}^2} \right) \hat{t}_{ji}^{-\frac{\theta}{1+\theta\lambda_1}} \hat{l}_j^{\frac{\theta(1-\beta)}{1+\theta\lambda_1}} \hat{y}_j^{\frac{-\theta}{1+\theta\lambda_1}} \\ &+ \hat{\chi}^{\frac{2\theta\lambda_2}{1+\theta\lambda_2}} \left( \hat{l}_i^{\alpha+1} \hat{y}_i^{-\frac{\theta+1}{\theta}} \right)^{\frac{\theta^2(\lambda_1-\lambda_2)}{(1+\theta\lambda_1)(1+\theta\lambda_2)}} \sum_j \left( \frac{\Xi_{ij}^2}{Y_i + \sum_j \Xi_{ji}^1 + \sum_j \Xi_{ji}^2} \right) \hat{s}_{jj'}^{-\frac{\theta}{1+\theta\lambda_2}} \hat{\tau}_{j'i'}^{-\theta} \hat{s}_{i'i}^{-\frac{\theta}{1+\theta\lambda_2}} \hat{l}_j^{\frac{\theta(1-\beta)}{1+\theta\lambda_2}} \hat{y}_j^{\frac{-\theta}{1+\theta\lambda_2}} \\ &\times \left( \sum_l \frac{\Xi_{i'l'}^2}{\sum_l \Xi_{i'l'}^2} \hat{\tau}_{i'l'}^{-\theta} \hat{s}_{l'l}^{-\theta} \left( \hat{y}_l \hat{l}_l^{\beta-1} \right)^{-\theta} \right)^{-\frac{\theta\lambda_2}{1+\theta\lambda_2}} \left( \sum_l \frac{\Xi_{j'l'}^2}{\sum_l \Xi_{j'l'}^2} \hat{\tau}_{j'l'}^{-\theta} \hat{s}_{l'l}^{-\theta} \left( \hat{l}_l^{\alpha+1} \hat{y}_l^{-\frac{\theta+1}{\theta}} \right)^{-\theta} \right)^{-\frac{\theta\lambda_2}{1+\theta\lambda_2}} \end{aligned}$$

Proposition (1) indicates that given observed traffic flows on the primary network, bilateral flows on the secondary network<sup>12</sup>,  $(\Xi_{ij}^1, \Xi_{i'j'}^2)$  as well as knowledge of the model parameters,

<sup>11</sup>Detailed derivations are provided in Online Appendix E.1

<sup>12</sup>Notice the slight abuse of notation here. While  $\Xi_{ij}^1$  refers to the edge-specific traffic along the primary network,

$\{\alpha, \beta, \theta, \lambda_1, \lambda_2, \nu\}$ , we can employ the model to evaluate infrastructure improvements along the primary network or at terminal stations, thus improving the connectedness of the primary and secondary transport network. The proposition provides a straightforward extension of equation (28) and (29) in AA2022. The only difference is the presence of the additional summation term at the end of each equation, which mirrors the presence and importance of the secondary transportation system. This adjustments adds a novel channel towards evaluation infrastructure improvements. In this setting, the impact of improving transportation infrastructure has the same direct and general equilibrium effect as in AA2022 where route choice is impacted, congestion can be alleviated, input and output markets can adjust and where all this adds up to welfare gains. In our setting, additionally, we also feature a direct interplay between the primary and secondary network. Mode-specific infrastructure investments can lead to modal diversion and thus alleviate congestion on the alternative transport network. The extent to which this might occur depends on the cross-sectional variation in the access to the secondary transportation system, which is reflected by variations in the weights on the final term across space.

As a corollary we can also characterize the change in the equilibrium traffic flows along the primary and secondary transport system.

**Corollary 1** *Given the equilibrium change in economic outcomes  $(\hat{y}_i, \hat{l}_i, \hat{\chi})$ , observed traffic flows  $(\Xi_{ij}^1, \Xi_{i'j'}^2)$ , economic activity in the geography  $(Y_i, E_j)$ , and parameters  $\{\alpha, \beta, \theta, \lambda_1, \lambda_2, \nu\}$ , the resulting change in the traffic flows can be computed using the following formulae:*

$$\widehat{\Xi}_{kl}^1 = \hat{\chi}^{-\frac{1}{1+\theta\lambda_1}} \left( \hat{t}_{kl} \right)^{\frac{\theta}{1+\theta\lambda_1}} \times \left( \hat{y}_k \hat{l}_k^{\beta-1} \right)^{-\frac{\theta}{1+\theta\lambda_1}} \times \left( \hat{l}_l^{\alpha+1} \hat{y}_l^{-\frac{\theta+1}{\theta}} \right)^{-\frac{\theta}{1+\theta\lambda_1}} \quad (16)$$

$$\widehat{\Xi}_{kl}^2 = \hat{s}_{kk'}^{-\frac{\theta}{1+\theta\lambda}} \hat{s}_{l'l}^{-\frac{\theta}{1+\theta\lambda}} \hat{P}_k^{-\frac{\theta}{1+\theta\lambda_2}} \hat{\Pi}_l^{-\frac{\theta}{1+\theta\lambda_2}} \hat{\tau}_{k'l'}^{-\theta} \left( \sum_l \frac{\Xi_{k'l'}^2}{\sum_{l'} \Xi_{k'l'}^2} \hat{\tau}_{k'l'}^{-\theta} \hat{s}_{l'l}^{-\theta} \hat{\Pi}_l^{-\theta} \right)^{-\frac{\theta\lambda}{1+\theta\lambda}} \left( \sum_l \frac{\Xi_{k'l'}^2}{\sum_{l'} \Xi_{k'l'}^2} \hat{\tau}_{k'l'}^{-\theta} \hat{s}_{l'l}^{-\theta} \hat{P}_l^{-\theta} \right)^{-\frac{\theta\lambda}{1+\theta\lambda}} \quad (17)$$

Corollary 1 allows us to account for the changes in the observed traffic flows. This can be a convenient tool to analyse the implied environmental impact of infrastructure investments.

---

$\Xi_{i'j'}^2$  instead refers to rail flows between  $i'$  and  $j'$  along the secondary network and is therefore not edge-specific. However,  $\Xi_{i'j'}^2$  summarizes railroad traffic in the sense that it refers to any flows between  $i'$  and  $j'$  no matter their origin or destination on the primary network. This is convenient - as we will argue below - since this is the data moment that is directly observed in the rail traffic data.

## 4 From Theory to Data

In order to quantify our model, we require two key elasticities. As in Proposition 1, the counterfactual equilibrium crucially depends on the model parameters, in particular the strength of the congestion forces on the primary network and at terminals  $(\lambda_1, \lambda_2)$ . While our calibration broadly follows [Allen and Arkolakis \(2022\)](#) who provide an estimate for the strength of congestion on the primary network, we have introduced a new parameter that pins down congestion at intermodal terminals,  $\lambda_2$ . In this section we present how the relationship between dwell times at intermodal facilities and throughput can be used to estimate the strength of congestion and the magnitude of this parameter. Next, to motivate the key mode choice channels in our model, we require an elasticity of substitution between transport modes. In order to estimate this elasticity, we revisit and build upon the seminal work by [Duranton and Turner \(2011\)](#) within the context of multimodal transportation.

### 4.1 Estimation of Port Congestion

In this subsection, we measure port congestion by estimating the elasticity of ship dwell time with respect to port traffic. We estimate the following regression (Column (3), Table 1):

$$\ln \text{Ship Dwell Time}_{spdmy} = \beta_1 \ln \text{Port Traffic}_{pdmy} + \delta_{dmy} + \alpha_{spy} + \epsilon_{spdmy} \quad (18)$$

where  $\text{Ship Dwell Time}_{spdmy}$  is the number of hours ship  $s$  spent at port  $p$  on day of the week  $d$  month  $m$  and year  $y$ ,  $\text{Port Traffic}_{pdmy}$  is the 28-day moving average amount of port traffic at port  $p$  ending on day  $d$  month  $m$  and year  $y$ ,  $\delta_{dmy}$  is day-month-year fixed effects, and  $\alpha_{spy}$  is ship-port-year fixed effects. The key parameter of interest,  $\beta_1$ , captures the elasticity of ship dwell times with respect to port traffic. Standard errors are two-way clustered at the ship and port level.

The ship-port-year fixed effects control for fixed and time-varying characteristics at the ship-port level. Fixed ship-port characteristics include time-invariant comparative advantage differences for different ports that result in larger ships being received at these ports which mechanically take longer time to unload, for example ports with deeper natural harbors. It also includes fixed ship characteristics like ship sizes and fixed port characteristics like its geography. Time-varying ship-port characteristics account for potential technology changes over time that ports can undertake that might affect ship dwell times, for example technology upgrades at ports over time to accommodate larger ships. Additionally, the day-month-year fixed effects control for

aggregate events that impacts all ships.

We find that a one percent increase in port traffic is correlated with a statistically significant increase in ship dwell times by 0.1 percent (Column (3), Table 1). This elasticity is robust to specifications with ship fixed effects and port-year fixed effects separately (Column (1), Table 1) as well as with ship-port fixed effects and port-year fixed effects separately (Column (2), Table 1).

In order to account for the extraordinary pandemic period, we include an indicator for the pandemic period (post March 2020) in order to estimate separate elasticities for port congestion. We find that our pre-March 2020 estimate is within one standard error of the baseline results (Column (4), Table 1). As expected, our estimate post-March 2020 is slightly higher in magnitude compared to the pre-period elasticity. Additionally, the West Coast ports have a history of port strikes and slowdowns. They also have naturally deeper harbors which allow for larger ships, and service large volumes of US-Asia trade—LA and Long Beach are the top two US ports. These factors can result in longer dwell times for ships that are servicing these busy ports. We show that the elasticity for West Coast ports is much larger in magnitude by limiting our samples to just West Coast ports (Column (5), Table 1).

The baseline results use a 28-day moving average of total daily net tonnage at the port. Using a shorter period of the moving average calculation, we find that the elasticity of port traffic with respect to ship dwell times decreases in magnitude. With a shorter period of moving average calculation, the ship dwell times respond less to changes to the average tonnage at the port. Column (1) reproduces our baseline results using the 28-day moving average from Table 1, Column (2) presents the 21-day moving average, Column (3) presents the 14-day moving average, and Column (4) presents the 7-day moving average.

In order to establish the causal impact of port traffic on ship dwell times, we require demand shifter for port traffic that is uncorrelated with unobserved ship dwell times determinants  $\epsilon_{spdmy}$ . Our IV strategy uses aggregate compositional changes for imports at the region- and product-level into the top 30 US ports to predict demand for traffic at each port:

$$\text{Port Trade Exposure}_{pm} \equiv \sum_O \sum_N X_{on \setminus p, my} \times \omega_{onp, 2011}$$

where the lagged weighted sum of top 30 US ports imports from region  $o$  and product  $n$  excluding port  $p$  at month  $m$  and year  $y$ , and the weights are region- and product-level shares from at least 5 years ago (2011). This trade data is available from the Census Bureau at the monthly level

**Table 1.** OLS Elasticity of Port Traffic with respect to Ship Dwell Times

	(1)	(2)	(3)	(4)	(5)
Port Traffic	0.0955** (0.0374)	0.100** (0.0399)	0.103** (0.0394)		0.241*** (0.0534)
Port Traffic $\times$ Before Mar 2020				0.0955** (0.0408)	
Port Traffic $\times$ After Mar 2020				0.122*** (0.0389)	
Day-Month-Year FE	✓	✓	✓	✓	✓
Ship-Port-Year FE			✓	✓	✓
Port-Year FE	✓	✓			
Ship-Port FE		✓			
Ship FE	✓				
West Coast Ports					✓
Observations	86094	86094	86094	86094	21205
$R^2$	0.70	0.78	0.83	0.83	0.87
F	6.53	6.29	6.85	5.60	20.35

**Notes:** Robust standard errors in parentheses are clustered by port. All variables are in logs. Port traffic is the 28-day moving average of total daily net tonnage at the port. Weighted by ship net tonnage.

and by both value (dollars) and weight (kg).

For this IV strategy to be valid, the port trade exposure measure has to be generally uncorrelated with unobserved ship dwell times determinants controlling for fixed characteristics at the ship-port level, time varying characteristics at the port-level, and aggregate time-varying events that impact all ships.

## 4.2 Modal Complementarity and Diversion

Infrastructure improvements on one transport mode will have both direct and indirect effects within the general equilibrium multimodal framework. We illustrate these effects using the example of an improvement in road infrastructure. Directly, truck transport costs will go down which will increase road traffic use as established in our theory model (Equation (3)). Indirectly, we find two important effects. First, an improvement in road access would generally decrease trade costs in and out of these cities and improve their general market access. This is in line with our general market access measures outlined in Equation (6), where destination-level road infrastructure improvement would impact the inward market access measure  $P_k$  and origin-level improvement would impact the outward market access measure  $\Pi_l$ . Second, however, this road

**Table. 2.** OLS Elasticity by Time Aggregations

	(1)	(2)	(3)	(4)
Port Traffic	0.103** (0.0394)	0.0848*** (0.0297)	0.0527** (0.0203)	0.0266** (0.0113)
Day-Month-Year FE	✓	✓	✓	✓
Ship-Port-Year FE	✓	✓	✓	✓
Moving Average (Days)	28	21	14	7
Observations	86094	86094	86092	86058
$R^2$	0.83	0.83	0.83	0.83
F	6.85	8.17	6.74	5.59

**Notes:** Robust standard errors in parentheses are clustered by port. All variables are in logs. Column (1) estimates the elasticity using the 28-day moving average of total daily net tonnage at the port and is replicated from the baseline results in Column (3) Table 1. Column (2) presents the 21-day moving average, Column (3) presents the 14-day moving average, and Column (4) presents the 7-day moving average. Weighted by ship net tonnage.

**Table. 3.** Congestion Elasticity of Port Traffic with respect to Ship Dwell Times

	(1) OLS	(2) OLS	(3) First-Stage	(4) IV	(5) First-Stage	(6) IV
Port Traffic	0.0926** (0.0392)	0.0995** (0.0418)		0.264** (0.122)		0.236** (0.109)
Port Trade Exposure by Weight			0.229*** (0.0536)		0.228*** (0.0535)	
Day-Month-Year FE	✓	✓	✓	✓	✓	✓
Port-Year FE						
Ship-Port FE	✓	✓	✓	✓	✓	✓
Ship FE		✓			✓	✓
Observations	90516	90516	90516	90516	90516	90516
F				18.27		18.19

Standard errors in parentheses

\*  $p < 0.10$ , \*\*  $p < 0.05$ , \*\*\*  $p < 0.01$

**Notes:** Robust standard errors in parentheses are clustered by port. All variables are in logs. Port traffic is the 28-day moving average of total daily net tonnage at the port. Weighted by ship net tonnage.

access improvement would also have a modal diversion or substitution effect—rail transport costs are now relatively more expensive and this will decrease overall rail traffic use. The indirect impact of a mode-specific infrastructure improvement on the traffic use of alternate modes is ultimately an empirical question. We estimate these indirect effects by building on the seminal work by Duranton and Turner (2011).

**Table 4.** Value IV for robustness

	(1) OLS	(2) OLS	(3) First-Stage	(4) IV	(5) First-Stage	(6) IV
Port Traffic	0.0926** (0.0392)	0.0995** (0.0418)		0.253 (0.280)		0.186 (0.310)
Port Trade Exposure by Value			0.112*** (0.0385)		0.111*** (0.0381)	
Day-Month-Year FE	✓	✓	✓	✓	✓	✓
Port-Year FE						
Ship-Port FE	✓	✓	✓	✓	✓	✓
Ship FE		✓			✓	✓
Observations	90516	90516	90516	90516	90516	90516
F				8.53		8.51

Standard errors in parentheses

\*  $p < 0.10$ , \*\*  $p < 0.05$ , \*\*\*  $p < 0.01$

**Notes:** Robust standard errors in parentheses are two-way clustered by ship and port. All variables are in logs. Port traffic is the 28-day moving average of total daily net tonnage at the port. Weighted by ship net tonnage.

[Duranton and Turner \(2011\)](#) find that building more roads, as measured by lane kilometers of interstate highways, increases the vehicle-kilometers traveled (VKT) in US metropolitan cities. In order to overcome the potential endogeneity between the demand for VKT and changes to the stock of roads at the metropolitan statistical areas (MSAs) level, they utilize three instruments: kilometers of preliminary interstate highway in each MSA as part of the 1947 highway plan ([Baum-Snow, 2007](#); [Michaels, 2008](#)), kilometers of 1898 railroads in each MSA, and exploration routes between 1528-1850.<sup>13</sup> In particular, they find that commercial truck traffic plays an important role in this VKT increase. By aggregating our waybill rail data to the MSA level and matching it to their data, we find empirical evidence of modal diversion dominating with respect to infrastructure investments: when road infrastructure improves, the ratio of rail to road traffic use decreases.<sup>14</sup>

<sup>13</sup>Using the same three instruments, [Duranton and Turner \(2012\)](#) estimates the impact of interstate highways on urban growth between 1983 and 2003 and finds that a 10% increase in a city's stock of interstate highways increases its employment by about 1.5%. With the same instruments, [Duranton, Morrow and Turner \(2014\)](#) estimates the impact of highways on the trade composition of US cities and finds that more highways result in cities specializing in exporting goods with higher weight-to-value ratios.

<sup>14</sup>We have 221 MSAs due to the matching process between MSAs and our rail traffic data which is 7 less compared to [Duranton and Turner \(2011\)](#) (see Section C.1.5 for more information). We first show that we are able to replicate the [Duranton and Turner \(2011\)](#) results in Table 5. Our fixed effects and IV estimates have the same sign and are within one standard deviation of the results from [Duranton and Turner \(2011\)](#) (Columns (6) to (10), Table 9, [Duranton and Turner \(2011\)](#)).

**OLS specification with fixed effects** We first consider the following OLS specification with fixed effects from Duranton and Turner (2011):

$$\ln Y_{cy} = \alpha \ln \text{Interstate Highway Lanes}_{cy} + \psi C_{cy} + \zeta_c + \iota_y + \varepsilon_{cy} \quad (19)$$

where  $\ln Y_{cy}$  is the log traffic use outcomes for MSA  $c$  in year  $y$ ,  $\ln \text{Interstate Highway Lanes}_{cy}$  is the log number of interstate highway lanes going through MSA  $c$  which proxies for the road infrastructure for that MSA in year  $y$ .  $C_{jt}$  are city-specific time-varying controls including population, physical geography, census divisions, and socioeconomic characteristics that are taken from Duranton and Turner (2011).  $\zeta_c$  is a MSA city-level fixed effect, and  $\iota_y$  is a year fixed effect.

To measure road traffic use, we employ the truck VKT from Duranton and Turner (2011). To construct a rail traffic use variable that is commensurate with truck VKT that is measured in vehicle-kilometers traveled, we calculate rail traffic in railcar-kilometers-traveled for each city. Our more detailed data allows us to calculate the rail VKT by destination—the amount of incoming rail traffic use—and by origin—outgoing rail traffic use. We also observe the amount of weight in these rail cars, and can construct an alternative measure of rail traffic use by weight in weight-kilometers-traveled. In order to measure modal diversion for US cities in response to road infrastructure improvements, we take the ratio of rail traffic use (measured in railcar-km or weight-km) to road traffic (measured in truck vehicle-km) for city  $c$  in year  $t$  ( $\frac{\text{Rail Traffic Use}_{cy}}{\text{Road Traffic Use}_{cy}}$ ).

As previously mentioned and established in our theory model (Equation (3)), Duranton and Turner (2011) finds that commercial truck traffic has a positive relationship with road infrastructure improvements as measured by inter-state highways. We replicate these results using our matched dataset (Columns (1) and (2), Table 5). Our OLS estimates with fixed effects have the same sign and are within one standard deviation of the results from Duranton and Turner (2011) (Columns (6) and (7), Table 9, Duranton and Turner (2011)).

Using railcar-kilometers traveled as our rail traffic use measure in Equation (19), we find that rail traffic use has a negative relationship with road infrastructure improvement in US cities as proxied by inter-state highways (Columns (1) and (2), Table 6). These relationships are imprecisely estimated due to two opposing forces. First, an improvement in road access would generally decrease trade cost in and out of these cities and improve their general market access. This is inline with our general market access measures predicted in Equation (6), where destination-level road infrastructure improvement would impact the inward market access measure  $P_k$  and origin-level improvement would impact the outward market access measure  $\Pi_l$ . Second, however, this

**Table 5.** Elasticity of Truck VKT with respect to Interstate Highway Lane Kilometers

	(1)	(2)	(3)	(4)	(5)
	OLS	OLS	IV	IV	IV
Inter-State Highway Lane KM	1.606*** (0.328)	1.616*** (0.338)	1.746*** (0.427)	2.083*** (0.483)	2.099*** (0.530)
Population		0.967* (0.550)	-0.278 (0.303)	-0.615 (0.376)	-0.484 (0.393)
Geography				✓	✓
Census Divisions				✓	✓
Socioeconomic Characteristics		✓			✓
MSA FE	✓	✓			
Year FE	✓	✓	✓	✓	✓
Observations	663	663	663	663	663
R-squared	0.77	0.78	-	-	-
KP F-stat			13.48	10.08	10.02

*Notes:* \*  $p < 0.1$ , \*\*  $p < 0.05$ , \*\*\*  $p < 0.01$ . Robust standard errors clustered by MSAs in parentheses. All variables are in logs. Instruments are 1835 exploration routes, 1898 railroad route kilometers, and 1947 planned interstate highways. 663 observations corresponding to 221 MSAs for each regression. See Table A.2 for first-stage regressions.

road access improvement would also have a modal substitution or diversion effect—rail transport costs are now relatively more expensive and this will decrease overall rail traffic use. We find similar results using rail traffic measured in weight-kilometers (Columns (1) and (2), Table A.9).

Next, we compare these changes in rail and road traffic use by estimating Equation (19) using the ratio of rail traffic use to road traffic use. In Columns (1) and (2) of Table 7, we find that the ratio of rail to truck traffic use has a negative and significant relationship with road infrastructure improvement in US cities. This result is robust to the inclusion of city-level fixed effects and year-level fixed effects, as well including time-varying city-level controls like socioeconomic characteristics and population. We note that this result, a regression coefficient of around -1.4, is not entirely driven by the inverse of truck traffic use result: our estimates are lower in absolute terms and beyond one standard error from the replicated truck VKT estimates of positive 1.6 from Table 5 (Columns (1) and (2)). This suggests that while rail traffic use has a positive relationship with road infrastructure improvement, as we have shown in Table 6, this rail increase is less than the road traffic use increase. This negative relationship is robust to measuring rail traffic use in terms of rail weight as well (Columns (1) and (2), Table A.20).

**IV specification** Since transport infrastructure and traffic use may be simultaneously determined, we required an instrumental variable approach in order to identify the causal effects

**Table. 6.** Elasticity of Rail Car Traffic-Kilometers with respect to Interstate Highway Lane Kilometers

	(1)	(2)	(3)	(4)	(5)
	OLS	OLS	IV	IV	IV
Interstate Highway Lane KM	-0.103 (0.173)	-0.0993 (0.175)	0.434 (0.314)	0.254 (0.337)	0.401 (0.315)
Population		0.346 (0.299)	0.695*** (0.245)	0.878*** (0.286)	0.757*** (0.273)
Geography				✓	✓
Census Divisions				✓	✓
Socioeconomic Characteristics		✓			✓
MSA FE	✓	✓			
Year FE	✓	✓	✓	✓	✓
Observations	663	663	663	663	663
R-squared	0.94	0.94	-	-	-
KP F-stat			13.48	10.08	10.02

**Notes:** \*  $p < 0.1$ , \*\*  $p < 0.05$ , \*\*\*  $p < 0.01$ . Robust standard errors clustered by MSAs in parentheses. All variables are in logs. Instruments are 1835 exploration routes, 1898 railroad route kilometers, and 1947 planned interstate highways. 663 observations corresponding to 221 MSAs for each regression. See Table A.6 for first stage regressions.

**Table. 7.** Elasticity of Rail to Truck Traffic Use with respect to Road Infrastructure Improvements

	(1)	(2)	(3)	(4)	(5)
	OLS	OLS	IV	IV	IV
Interstate Highway Lane KM	-1.432*** (0.195)	-1.432*** (0.196)	-0.867** (0.376)	-1.249*** (0.388)	-1.099*** (0.364)
Population		-0.150 (0.337)	0.699** (0.289)	1.092*** (0.328)	0.891*** (0.306)
Geography				✓	✓
Census Divisions				✓	✓
Socioeconomic Characteristics		✓			✓
MSA FE	✓	✓			
Year FE	✓	✓	✓	✓	✓
Observations	658	658	658	658	658
R-squared	0.88	0.88	-	-	-
KP F-stat			14.48	10.76	10.04

**Notes:** \*  $p < 0.1$ , \*\*  $p < 0.05$ , \*\*\*  $p < 0.01$ . Robust standard errors clustered by MSAs in parentheses. All variables are in logs. Rail traffic use, measured in railcar-kilometers, is constructed using confidential rail waybill data. Truck traffic use (in vehicle-kilometers) and other variables are from Duranton and Turner (2011). Instruments are 1835 exploration routes, 1898 railroad route kilometers, and 1947 planned interstate highways. 663 observations corresponding to 221 MSAs for each regression. See Table A.15 for first stage regressions.

of road infrastructure on rail traffic use and modal substitution. We employ the three instruments by Duranton and Turner (2011) to predict the stock of roads in US cities: kilometers of preliminary interstate highway in each MSA as part of the 1947 highway plan (Baum-Snow,

2007; Michaels, 2008), kilometers of 1898 railroads in each MSA, and exploration routes between 1528-1850. We estimate the following two-stage least squares IV regression:

$$\begin{aligned} \ln \text{Interstate Highway Lanes}_{cy} &= \eta_1 \ln \text{Instruments}_c + \kappa C_{cy} + \iota_y + \nu_{cy} \\ \ln Y_{cy} &= \eta_2 \ln \text{Interstate Highway Lanes}_{cy} + \phi C_{cy} + \iota_y + \mu_{cy} \end{aligned} \quad (20)$$

where  $\ln Y_{cy}$  is the log traffic use outcomes for MSA  $c$  in year  $y$ ,  $\ln \text{Instruments}_c$  is the set of three instruments discussed earlier,  $\ln \text{Interstate Highway Lanes}_{cy}$  is the log number of interstate highway lanes going through each city  $c$  which proxies for the road infrastructure for that city in year  $y$ .  $C_{jt}$  are city-specific time-varying controls including population, physical geography, census divisions, and socioeconomic characteristics that are taken from Duranton and Turner (2011), and  $\iota_y$  is year fixed effects.

The validity of the IV strategy here requires that the instrument be uncorrelated with unobserved changes in road and rail traffic use conditional on the control variables and fixed effects in Equation (20). We first show that we can replicate the IV results in Duranton and Turner (2011): our IV estimates in Columns (3) and (4) (Table 5) have the same sign and are within one standard error of the results from Duranton and Turner (2011) (Columns (9) and (10), Table 9, Duranton and Turner (2011)). Similar to them, we find that the IV estimates are slightly higher than the OLS estimates. Our results are also robust to including socioeconomic characteristics (Column (5), Table 5). We then show that road infrastructure has a positive and noisy impact on rail traffic (Columns (3) to (5), Table 6). Using rail traffic measured in weight-kilometers, we again find similar positive but noisy effects (Columns (3) to (5), Table A.9).

Comparing these increases in rail and road traffic use, we find that road infrastructure improvements result in a larger increase in road traffic use relative to the rail increase—resulting in a decrease in the ratio of rail traffic use to road traffic use. A 1 percent increase in interstate highways causes a 0.9-1.2 percent decrease in rail to road traffic use (Columns (3) to (5), Table 7). It is important to note that this result is not driven by the inverse of truck traffic use result: our estimates are lower in absolute terms and beyond one standard error from the replicated truck VKT estimates where a 1 percent increase in interstate highways causes a 1.7-2.1 percent increase in truck VKT (Columns (3) to (5), Table 5). These estimates are similar in magnitude when measuring rail traffic by weight (Columns (3) to (5), Table A.20).

**Robustness** Since our rail traffic data is more disaggregated, we are able investigate incoming and outgoing rail traffic use separately. We find that these directional results retain the same

signs and are within one standard error of most of our main results, suggesting that both incoming and outgoing rail traffic use respond similarly to road infrastructure improvements. While both rail traffic use measures are imprecisely estimated, they are similar in magnitude (Tables A.5 and A.7 respectively for incoming and outgoing rail traffic use measured in railcar-km). We find similar results using incoming and outgoing rail traffic measured in weight-kilometers (Tables A.11 and A.13 respectively). Comparing the ratio of directional rail traffic use to road traffic use, we find that a 1 percent increase in interstate highways increases the elasticity of incoming rail traffic use to road traffic use by 1-1.2 percent (Columns (3) to (5), Table A.16) while a 1 percent increase in interstate highways increases the elasticity of outgoing rail traffic use to road traffic use by about 1.2 percent (Columns (3) to (5), Table A.18). These results are slightly higher using rail traffic use measured in weight-kilometers (Tables A.22 and A.24 respectively for incoming and outgoing rail traffic use measured in railcar-km).

## 5 Counterfactuals

We apply our multimodal economic geography framework to evaluate the welfare impact of small improvements in the operation of intermodal terminals, taking into account both the primary and secondary transportation network.

### 5.1 The Welfare Benefit of Multimodal Investments (To be added)

### 5.2 Impact of Railroad strikes (To be added)

### 5.3 Closure of the Panama Canal (To be added)

### 5.4 Repeal of the Jones Act (To be added)

## 6 Conclusion

The movement of goods from origin to destination involves an extensive transport network of multiple modes, including highways, railroads, oceans, and waterways. This network, like production and trade networks, are extensive and can have large and compounding impacts on economic activity and welfare. Additionally, extensive reliance on particular transport modes like highways can result in negative externalities like congestion and pollution. While recognizing that transport is fundamental to the economy and society and attempting to make it more sustainable, the European Commission calls for multimodal transport solutions relying on waterborne and rail modes for long-hauls ([European Commission, 2011](#)).

**Table 8.** Elasticity of Rail Dwell Times with respect to Port Traffic

	(1)	(2)	(3)	(4)	(5)
Total Port Traffic	0.0267 (0.00517)	0.0268 (0.00518)	0.0273 (0.00662)	0.0245 (0.00641)	
Total Port Traffic $\times$ Before Mar 2020					0.0258 (0.00886)
Total Port Traffic $\times$ After Mar 2020					0.0305 (0.0134)
Port Buffer Area	150km	150km	150km	200km	150km
Week-Month-Year FE	✓	✓	✓	✓	✓
Rail Station-Port-Month FE		✓	✓	✓	✓
Port-Month FE	✓				
Rail Station FE	✓				
Without West Coast Ports			✓		
Observations	4087	4087	3361	4813	4087
$R^2$	0.81	0.81	0.81	0.81	0.81
F	26.79	26.87	17.01	14.65	23.10

**Notes:** Robust standard errors in parentheses are clustered by port. All variables are in logs.  
Local railroads are determined by a 150km buffer area around the ports.

We study the multimodal transport network and their impact on the economic and environmental returns to new technology and infrastructure investments. In particular, we focus on how these outcomes will depend on the geography of the multimodal transportation network, the placement of intermodal terminals that allow for switches between modes of transportation, as well as the relative cost of transportation across modes. By incorporating these features we provide a framework that allows us to realistically evaluate infrastructure policies taking the complete domestic transportation network into account.

## References

- Allen, Treb, and Costas Arkolakis.** 2014. “Trade and the Topography of the Spatial Economy.” *The Quarterly Journal of Economics*, 129(3): 1085–1140.
- Allen, Treb, and Costas Arkolakis.** 2022. “The Welfare Effects of Transportation Infrastructure Improvements.” *The Review of Economic Studies*.
- Baum-Snow, Nathaniel.** 2007. “Did highways cause suburbanization?” *The quarterly journal of economics*, 122(2): 775–805.
- Beuthe, Michel, Bart Jourquin, and Natalie Urbain.** 2014. “Estimating Freight Transport Price Elasticity in Multi-mode Studies: A Review and Additional Results from a Multimodal Network Model.” *Transport Reviews*, 34(5): 626–644.
- Board, Transportation Research, Engineering National Academies of Sciences, and Medicine.** 2017. *Guide for Conducting Benefit-Cost Analyses of Multimodal, Multijurisdictional Freight Corridor Investments*. Washington, DC: The National Academies Press.
- Bonadio, Barthélémy.** 2021. “Ports vs. Roads: Infrastructure, Market Access and Regional Outcomes.” Working Paper.
- Brancaccio, Giulia, Myrto Kalouptsidi, and Theodore Papageorgiou.** 2020. “Geography, transportation, and endogenous trade costs.” *Econometrica*, 88(2): 657–691.
- Congressional Budget Office (CBO).** 2022. “Emissions of Carbon Dioxide in the Transportation Sector.” CBO Publication 58566.
- Coşar, A Kerem, and Banu Demir.** 2018. “Shipping inside the box: Containerization and trade.” *Journal of International Economics*, 114: 331–345.
- Cristea, Anca, David Hummels, Laura Puzzello, and Misak Avetisyan.** 2013. “Trade and the greenhouse gas emissions from international freight transport.” *Journal of environmental economics and management*, 65(1): 153–173.
- Daly, Andrew, and Michel Bierlaire.** 2006. “A general and operational representation of Generalised Extreme Value models.” *Trans. Res. Part B: Methodol.*, 40(4): 285–305.
- Degiovanni, Pedro, and Ron Yang Yang.** 2023. “Economies of Scale and Scope in Railroad-ing.” Working Paper.
- Dekle, Robert, Jonathan Eaton, and Samuel Kortum.** 2008. “Global Rebalancing with Gravity: Measuring the Burden of Adjustment.” National Bureau of Economic Research, Inc NBER Working Papers 13846.
- Duranton, Gilles, and Matthew A Turner.** 2011. “The fundamental law of road congestion: Evidence from US cities.” *American Economic Review*, 101(6): 2616–52.
- Duranton, Gilles, and Matthew A Turner.** 2012. “Urban growth and transportation.” *Review of Economic Studies*, 79(4): 1407–1440.

- Duranton, Gilles, Peter M Morrow, and Matthew A Turner.** 2014. "Roads and Trade: Evidence from the US." *Review of Economic Studies*, 81(2): 681–724.
- Eaton, Jonathan, and Samuel Kortum.** 2002. "Technology, Geography, and Trade." *Econometrica*, 70(5): 1741–1779.
- European Commission.** 2011. "Roadmap to a Single European Transport Area-Towards a competitive and resource efficient transport system." *White Paper*, 144.
- Fajgelbaum, Pablo D, and Edouard Schaal.** 2017. "Optimal Transport Networks in Spatial Equilibrium." National Bureau of Economic Research Working Paper 23200.
- Fan, Jingting, and Wenlan Luo.** 2020. "A Tractable Model of Transshipment." Working Paper.
- Fan, Jingting, Yi Lu, and Wenlan Luo.** 2019. "Valuing domestic transport infrastructure: a view from the route choice of exporters." *The Review of Economics and Statistics*, 1–46.
- Ganapati, Sharat, Woan Foong Wong, and Oren Ziv.** 2021. "Entrepot: Hubs, scale, and trade costs." National Bureau of Economic Research Working Paper 29015.
- Heiland, Inga, Andreas Moxnes, Karen-Helene Ulltveit-Moe, and Yuan Zi.** 2019. "Trade From Space: Shipping Networks and The Global Implications of Local Shocks." C.E.P.R. Discussion Papers CEPR Discussion Papers 14193.
- Horn, Roger A, and Charles R Johnson.** 2012. *Matrix analysis*. Cambridge university press.
- Jaworski, Taylor, Carl Kitchens, and Sergey Nigai.** 2023. "Highways and globalization." *International Economic Review*, 64(4): 1615–1648.
- Kitthamkesorn, Songyot, Anthony Chen, and Xiangdong Xu.** 2015. "Elastic demand with weibit stochastic user equilibrium flows and application in a motorised and non-motorised network." *Transportmetrica A: Transport Science*, 11(2): 158–185.
- Li, Xinyan, Chi Xie, and Zhaoyao Bao.** 2022. "A multimodal multicommodity network equilibrium model with service capacity and bottleneck congestion for China-Europe containerized freight flows." *Transportation Research Part E: Logistics and Transportation Review*, 164: 102786.
- Lugovskyy, Volodymyr, Alexandre Skiba, and David Terner.** 2022. "Unintended Consequences of Environmental Regulation of Maritime Shipping: Carbon Leakage to Air Shipping." Working Paper.
- McFadden, Daniel, Clifford Winston, and Axel Boersch-Supan.** 1986. "Joint estimation of freight transportation decisions under nonrandom sampling." *Analytical Studies in Transport Economics*, , ed. Andrew F. Daughety, 137–158. Cambridge University Press.
- Michaels, Guy.** 2008. "The effect of trade on the demand for skill: Evidence from the interstate highway system." *The Review of Economics and Statistics*, 90(4): 683–701.

- Mundaca, Gabriela, Jon Strand, and Ian R Young.** 2021. “Carbon pricing of international transport fuels: Impacts on carbon emissions and trade activity.” *Journal of Environmental Economics and Management*, 110: 102517.
- Oyama, Yuki, Yusuke Hara, and Takashi Akamatsu.** 2022. “Markovian traffic equilibrium assignment based on network generalized extreme value model.” *Trans. Res. Part B: Methodol.*, 135–159.
- Papola, Andrea, and Vittorio Marzano.** 2013. “A Network Generalized Extreme Value Model for Route Choice Allowing Implicit Route Enumeration.” *Comput.-aided civ. infrastruct. eng.*, 28(8): 560–580.
- Ranieri, Luigi, Salvatore Digiesi, Bartolomeo Silvestri, and Michele Roccotelli.** 2018. “A review of last mile logistics innovations in an externalities cost reduction vision.” *Sustainability*, 10(3): 782.
- Redding, Stephen J.** 2016. “Goods trade, factor mobility and welfare.” *Journal of International Economics*, 101: 148–167.
- Redding, Stephen J.** 2020. “Trade and Geography.” NBER Working Paper 27821.
- Rich, J., O. Kveiborg, and C.O. Hansen.** 2011. “On structural inelasticity of modal substitution in freight transport.” *Journal of Transport Geography*, 19(1): 134–146.
- Rodrigue, Jean-Paul.** 2020. *The geography of transport systems*. Routledge.
- Shapiro, Joseph S.** 2016. “Trade Costs, CO<sub>2</sub>, and the Environment.” *American Economic Journal: Economic Policy*, 8(4): 220–54.
- Surface Transportation Board.** 2009. “A Study of Competition in the US Freight Railroad Industry and Analysis of Proposals that might Enhance Competition.” Report prepared by Laurits R. Christensen Associates.
- Winston, Clifford.** 1981. “A Disaggregate Model of the Demand for Intercity Freight Transportation.” *Econometrica*, 49(4): 981–1006.
- Wong, Woan Foong.** 2022. “The round trip effect: Endogenous transport costs and international trade.” *American Economic Journal: Applied Economics*, 14(4): 127–66.
- Zgonc, Borut, Metka Tekavčič, and Marko Jakšić.** 2019. “The impact of distance on mode choice in freight transport.” *European Transport Research Review*, 11(1): 1–18.

# Part

# Appendix

## Table of Contents

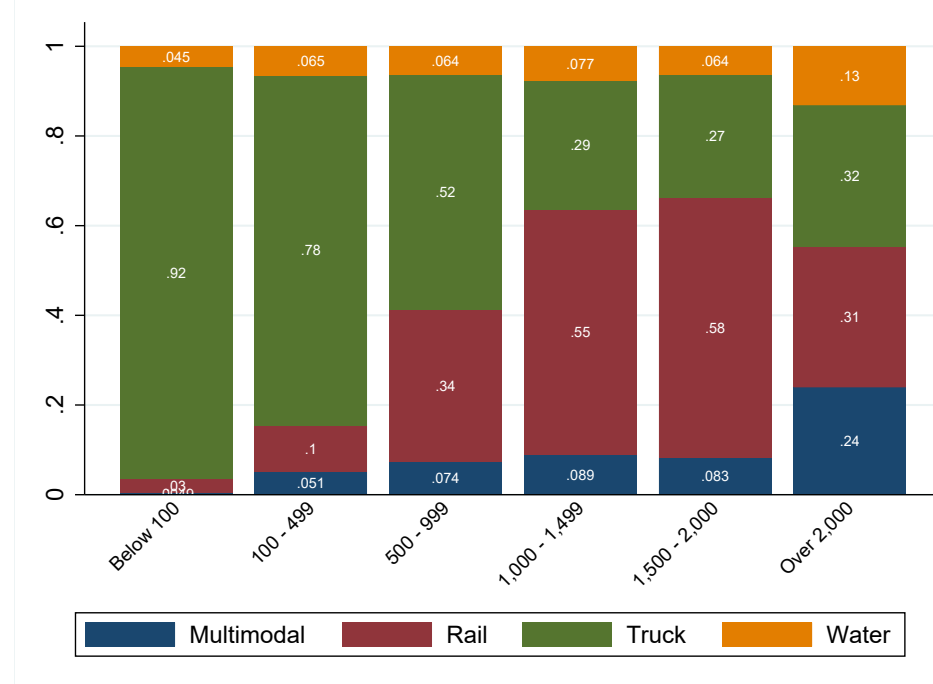
---

<b>A Additional Tables and Figures</b>	<b>A2</b>
<b>B Theoretical Derivations</b>	<b>A3</b>
B.1 Section 3.1: Recursive choice probabilities and transport costs . . . . .	A3
B.2 Section 3.3.1: Multimodal Routing and Transportation Cost . . . . .	A6
B.3 Isomorphism with Allen and Arkolakis (2022) . . . . .	A7
B.4 Section 3.3.2: Modal Traffic Flows . . . . .	A10
<b>C Data and Additional Results</b>	<b>A16</b>
C.1 Data Appendix . . . . .	A16
C.2 Modal Diversion: Additional Results . . . . .	A16
C.3 Railroad Infrastructure Improvement: Heartland Corridor . . . . .	A18
<b>D Additional Derivations</b>	<b>A25</b>
D.1 Section 3.3: Equilibrium for Economic Geography Model with Multimodal Routing . . . . .	A25
D.2 Regression design for modal diversion . . . . .	A32
D.3 Comparison with Fan and Luo (2020) . . . . .	A35
<b>E Proofs</b>	<b>A37</b>
E.1 Proof of Proposition 1: Counterfactual Equilibrium . . . . .	A37

---

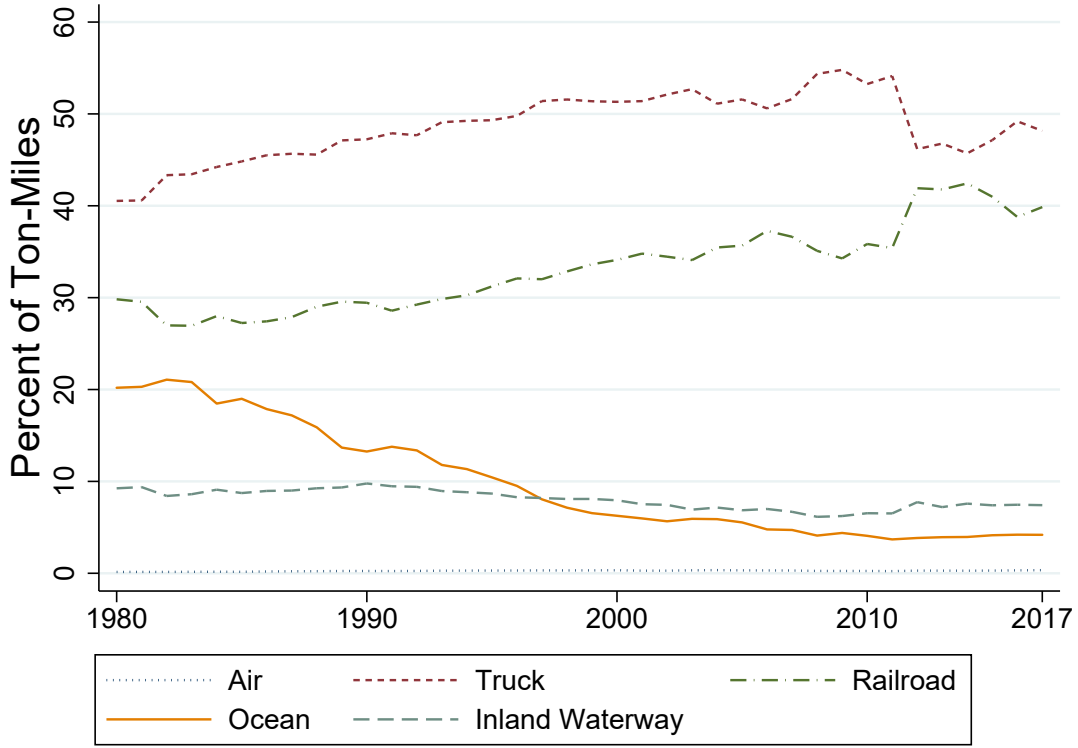
## A Additional Tables and Figures

**Figure A.1.** US Transport Mode Weight Shares by Distance, 2018



**Notes:** This figure plots the observed weight share of cargo transported by different modes across various distances. Multimodal indicates cargo movement that involves more than one mode. Source: Freight Analysis Framework, US Department of Transportation, and authors' calculations.

**Figure A.2.** US Modal Freight Shares



**Notes:** This figure shows the US modal freight shares going back to 1980. Source: Bureau of Transportation Statistics

## B Theoretical Derivations

This appendix presents derivations for the results in Section 3. Additional derivations are presented in Online Appendix E.1.3.

### B.1 Section 3.1: Recursive choice probabilities and transport costs

A consumer resides in location  $j$  and makes a route-sourcing choice comparing prices across all sourcing locations  $i$  and transportation costs across multiple routes  $r$ . Our aim is to characterize the choice probability that

We make the assumption that transport cost are multiplicative and that they are furthermore the product of edge-specific transport costs along the route  $r$ , i.e.  $\tau_{ij,r}^{-\theta} = \left( \prod_{l=1}^K t_{r_{t-1},r_l}^{-\theta} \right)$ . Finally, we assume that the consumer makes a recursive route-sourcing choice, beginning at the origin location  $j$  comparing the sourcing prices across neighboring nodes  $k \in \mathcal{F}(j)$  and net the transportation cost of traversing via the neighboring nodes,  $t_{jk}$ . Below we will furthermore define the edge-specific transportation cost  $t_{jk}$  as arising as the expected minimum cost of traversing to the neighboring node along a multimodal transport network. For now - without loss of generality - we simply assume that the consumer faces a routing problem along a single-layered graph. In summary, the consumer at location  $j$  faces the following set of (recursively defined) prices:

$$p_{ij,k}(\nu) = \frac{t_{jk}\tau_{ki}w_i}{\varepsilon_{ij,k}(\nu)}$$

where  $\varepsilon_{ij,k}(\nu)$  is a random variable drawn from a Frechet distribution with cumulative distribution

Variable Name	Variable
Multi-layered graph	$\mathcal{G} \equiv (\mathcal{N}, \mathcal{L})$
Successor nodes	$\mathcal{B}(i)$
Predecessor nodes	$\mathcal{F}(i)$
Route of length K	$r \equiv \{i = r_0, r_1, \dots, r_K = j\}$
Elasticity of substitution (goods)	$\sigma$
Dispersion parameter (route)	$\theta$
Dispersion parameter (mode)	$\eta$
Expected minimal transport cost between $i$ and $j$	$\tau_{ij}$
(Expected minimal) Edge-specific transport cost between $i$ and $k$	$t_{ik}$
Mode-specific transport cost between $i$ and $k$ for mode $m$	$\tilde{t}_{ik,m}$
Link intensity	$\pi_{ij}^{kl}$
Link-sourcing probability	$\pi_{ij,k}$
Link choice probability conditional on sourcing from $i$ to $j$	$\pi_{ij}^k$
Mode choice probability conditional on link $ik$	$\pi_{ij,k}^m$
Mode-link-sourcing probability	$\pi_{ij,k,m}$

**Table. A.1.** Overview of notation

given by,

$$F_{ijk}(\epsilon) = e^{-T_{ijk}\epsilon^{-\theta}}$$

The consumer in location  $j$  is presented with a set of route-source specific prices across sourcing locations  $i$  and choosing a route by traversing towards neighboring node  $k$ , i.e.

$$\begin{aligned} G_{ijk}(p) &= \Pr(P_{ijk} \leq p) = 1 - F_{ijk} \left( \frac{t_{jk}\tau_{ki}w_i}{p} \right) \\ &= 1 - e^{-T_{ijk}(t_{jk}\tau_{ki}w_i)^{-\theta}p^\theta} \end{aligned}$$

We can use this distribution to characterize the lowest route-source specific price that consumer in location  $j$  faces. To do so, fix an arbitrary threshold price  $p$ . The lowest price will be less than  $p$ , unless each route-source specific price is greater than  $p$ . We therefore seek to characterize,  $G_{ijk}(p) = \Pr(P_{ijk} \leq p)$ , which is given by,

$$\begin{aligned} G_j(p) &= 1 - \prod_{i,k} (1 - G_{ijk}(p)) \\ &= 1 - \prod_{i,k} e^{-T_{ijk}(t_{jk}\tau_{ki}w_i)^{-\theta}p^\theta} \\ &= 1 - e^{-\Phi_j p^\theta} \end{aligned}$$

where,

$$\Phi_j = \sum_{ik} T_{ijk} (t_{jk}\tau_{ki}w_i)^{-\theta}$$

If  $p_{ij,k}(\nu) = p$  then the probability that  $ijk$  is the cost minimizing route-source choice is given by,

$$\begin{aligned}\prod_{i' \neq i, k' \neq k} \Pr [P_{ijrm} \geq p] &= \prod_{i' \neq i, k' \neq k} [1 - G_{i'jk'}] \\ &= \prod_{i' \neq i, k' \neq k} e^{-T_{ijk}(t_{jk}\tau_{ki}w_i)^{-\theta} p^\theta} \\ &= e^{-(\sum_{i,k} T_{ijr}(t_{jk}\tau_{ki}w_i)^{-\theta}) p^\theta}\end{aligned}$$

Integrating over all possible equilibrium prices  $p$  we can characterize the probability that country  $i$  and node  $k$  are the cost minimizing route-source choices:

$$\begin{aligned}\pi_{ij,k} &= \int_0^\infty \prod_{i' \neq i, k' \neq k} [1 - G_{i'jk'}] dG_{ijk}(p) \\ &= \int_0^\infty \prod_{i' \neq i, k' \neq k} e^{-T_{i'jk'}(t_{jk'}\tau_{j'i'}w_{i'})^{-\theta} p^\theta} dG_{ijk}(p)\end{aligned}$$

Replacing with  $dG_{ijk}(p) = [T_{ijk}(t_{jk}\tau_{ji}w_i)^{-\theta} \theta p^{\theta-1}] e^{-T_{ijk}(t_{jk}\tau_{ji}w_i)^{-\theta} p^\theta} dp$ , we obtain,

$$\begin{aligned}\pi_{ij,k} &= \int_0^\infty \prod_{i' \neq i, k' \neq k} e^{-T_{i'jk'}(t_{jk'}\tau_{j'i'}w_{i'})^{-\theta} p^\theta} dG_{ijk}(p) \\ &= \int_0^\infty \prod_{i' \neq i, k' \neq k} e^{-T_{i'jk'}(t_{jk'}\tau_{j'i'}w_{i'})^{-\theta} p^\theta} [T_{ijk}(t_{jk}\tau_{ji}w_i)^{-\theta} \theta p^{\theta-1}] e^{-T_{ijk}(t_{jk}\tau_{ji}w_i)^{-\theta} p^\theta} dp \\ &= T_{ijk}(t_{jk}\tau_{ji}w_i)^{-\theta} \int_0^\infty \prod_{i,k} e^{-T_{ijk}(t_{jk}\tau_{ji}w_i)^{-\theta} p^\theta} [\theta p^{\theta-1}] dp \\ &= T_{ijk}(t_{jk}\tau_{ji}w_i)^{-\theta} \int_0^\infty e^{-(\sum_{i,k} T_{ijk}(t_{jk}\tau_{ji}w_i)^{-\theta}) p^\theta} [\theta p^{\theta-1}] dp \\ &= T_{ijk}(t_{jk}\tau_{ji}w_i)^{-\theta} \int_0^\infty e^{-\Phi_j p^\theta} [\theta p^{\theta-1}] dp \\ &= T_{ijk}(t_{jk}\tau_{ji}w_i)^{-\theta} \left[ \frac{1}{\Phi_j} e^{-\Phi_j p^\theta} \right]_0^\infty \\ &= \frac{T_{ijk}(t_{jk}\tau_{ji}w_i)^{-\theta}}{\Phi_j}\end{aligned}$$

Replacing with  $\Phi_j = \sum_{ik} T_{ijk}(t_{jk}\tau_{ji}w_i)^{-\theta}$ , we obtain,

$$\pi_{ij,k} = \frac{T_{ijk}(t_{jk}\tau_{ji}w_i)^{-\theta}}{\sum_{ik} T_{ijk}(t_{jk}\tau_{ji}w_i)^{-\theta}}$$

replacing  $T_{ijk} \equiv \left(\frac{1}{A_i}\right)^\theta$ , we obtain,

$$\pi_{ij,k} = \frac{(w_i/A_i)^{-\theta} (t_{jk}\tau_{ki})^{-\theta}}{\sum_{i \in \mathcal{N}} (w_i/A_i)^{-\theta} \sum_{k' \in \mathcal{F}(i)} (t_{jk'}\tau_{k'i})^{-\theta}}$$

as stated above. Furthermore, the expected minimal price is given by,

$$\begin{aligned} p_{ij,k} &= \mathbb{E} \left[ \min_{k \in \mathcal{F}(i)} \{t_{jk} \tau_{ki} w_i\} \right] \\ &\propto \sum_{i \in \mathcal{N}} (w_i/A_i)^{-\theta} \sum_{k' \in \mathcal{F}(i)} (t_{jk'} \tau_{k'i})^{-\theta} \\ &= \sum_{i \in \mathcal{N}} (w_i/A_i)^{-\theta} \tau_{ij}^{-\theta} \end{aligned}$$

where in the last line we have used the result that if we consider separately the routing problem this implies an expected transport cost that is in itself recursively defined, i.e.

$$\tau_{id} = \mathbb{E} \left[ \min_{j \in \mathcal{F}(i)} \{t_{ij} \tau_{jd} \varepsilon_{ij}\} \right] = \left( \sum_{j \in \mathcal{F}(i)} (t_{ij} \tau_{jd})^{-\theta} \right)^{-\frac{1}{\theta}}$$

which expressed the transport cost as an index of the continuation values along the different edges of the graph.

## B.2 Section 3.3.1: Multimodal Routing and Transportation Cost

As presented in the previous section, we consider a consumer that resides in location  $j$  and makes a route-sourcing choice by choosing sequentially edges along the graph. This provides a convenient characterization of routing that avoids the curse of dimensionality by expressing the problem as a recursive problem instead of considering the universe of possible routes along a possibly high-dimensional graph. To furthermore accommodate multimodal routing choices, we incorporate a nested modal choice. In that setting, conditional on the neighboring node chosen, the consumer makes a modal choice by choosing the cost minimizing mode out of all modes along the edge, i. to traverse the edge (subject to an extreme value distributed cost shock). To fix ideas, consider a consumer in location  $j$  having chosen to route towards the neighboring node  $k$ . The consumer then compares all the different modes that are available along this edge, i.e.  $m \in \mathcal{M}_{jk}$ , where  $\mathcal{M}_{jk}$  is the set of modes available between nodes  $j$  and  $k$ , and where the edge mode specific transport costs given by,

$$\tilde{t}_{jk,m} = \begin{cases} \tilde{t}_{jk} & \text{if } m = 1 \\ s_{jj,m} \tau_{jk,m} s_{kk,m} & \text{if } m \neq 1 \end{cases}$$

where for the primary mode no switching cost is required, but for any non-primary mode ( $m \neq 1$ ) a switching cost is imposed, while  $\tau_{jk,m}$  refers to the iceberg transport cost of traversing the edge between node  $j$  and  $k$  along mode  $m$ . Notice that this specification is extremely general and allows for geographies where non-primary modes might connect an entirely different set of nodes than primary nodes. The consumer then faces a cost minimizing choice subject to an extreme-value distributed cost shock, i.e.

$$\min_{m \in \mathcal{M}(j,k)} \{t_{jk} \varepsilon_m\}$$

where the properties of the Frechet distribution implies that the expected cost minimizing transport along any mode between nodes  $j$  and  $k$  is given by,

$$t_{ik}^{-\theta} \propto \left( \sum_{m \in \mathcal{M}(i,k)} \tilde{t}_{ik,m}^{-\eta} \right)^{\frac{\theta}{\eta}}$$

Overall, the consumer's route-sourcing choice can be written as a nested minimization problem where we can characterize the overall expected minimal cost, i.e.

$$\begin{aligned}
p_{ij} &= \mathbb{E} \left[ \min_{j \in \mathcal{F}(i)} \left\{ \mathbb{E} \left[ \min_{m \in \mathcal{M}(i,k)} \{ \tilde{t}_{ik,m} \varepsilon_m \} \right] \tau_{jd} w_i \varepsilon_{ij} \right\} \right] \\
&\propto \sum_{i \in \mathcal{N}} (w_i / A_i)^{-\theta} \sum_{k' \in \mathcal{F}(i)} \left( \left( \sum_{m \in \mathcal{M}(i,k)} \tilde{t}_{ik,m}^{-\eta} \right)^{-\frac{1}{\eta}} \tau_{k'i} \right)^{-\theta} \\
&= \sum_{i \in \mathcal{N}} (w_i / A_i)^{-\theta} \tau_{ij}^{-\theta}
\end{aligned}$$

where in the last line we again have used the definition of the transportation cost in terms of the edge-specific costs and associated continuation values along neighboring nodes.

$$\tau_{id} = \mathbb{E} \left[ \min_{j \in \mathcal{F}(i)} \{ t_{ij} \tau_{jd} \varepsilon_{ij} \} \right] = \left( \sum_{j \in \mathcal{F}(i)} \left( \left( \sum_{m \in \mathcal{M}(i,k)} \tilde{t}_{ik,m}^{-\eta} \right)^{-\frac{1}{\eta}} \tau_{jd} \right)^{-\theta} \right)^{-\frac{1}{\theta}}$$

which expressed the transport cost as an index of the continuation values along the different edges of the graph.

where the mode-route-sourcing choice probability is given by,

$$\begin{aligned}
\pi_{ij,k,m} &= \frac{(w_i / A_i)^{-\theta} (t_{ik} \tau_{ki})^{-\theta}}{\sum_{i \in \mathcal{N}} (w_i / A_i)^{-\theta} \sum_{k' \in \mathcal{F}(i)} (t_{ik'} \tau_{k'i})^{-\theta}} \frac{\tilde{t}_{ik,m}^{-\eta}}{t_{ik}} \\
&= \pi_{ij,k} \times \pi_{ij,k}^m
\end{aligned}$$

where we can decompose in the last line the link choice probability and the mode choice probability along the link.

### B.3 Isomorphism with [Allen and Arkolakis \(2022\)](#)

It might be insightful to link the recursive expression in our paper to the approach in AA2022 that instead relies on explicit enumeration of the universe of paths and utilizes matrix algebra to express the expected minimum transport cost in terms of the leontief inverse of the adjacency matrix that captures the underlying infrastructure network. As we will show, the model is isomorphic in the case where there is a simple unimodal transport network. Furthermore, we will also show that for the simplified case where the mode choice elasticity is equal to the route choice elasticity, we can show that their approach can be extended to provide a clean expression of the multimodal transport cost in terms of (leontief inverses) of the infrastructure matrices. First, let us demonstrate the isomorphism for unimodal transport network. Consider the recursive transport cost stated above,

$$\tau_{id} = \mathbb{E} \left[ \min_{j \in \mathcal{F}(i)} \{ t_{ij} \tau_{jd} \varepsilon_{ij} \} \right] = \left( \sum_{j \in \mathcal{F}(i)} (t_{ij} \tau_{jd})^{-\theta} \right)^{-\frac{1}{\theta}}$$

If we assume a finite graph, then we can iteratively substitute and obtain a closed-form expression for the endogenous transport cost, i.e.

$$\begin{aligned}
(\tau_{id})^{-\theta} &= t_{d-1d}^{-\theta} \sum_{j \in F(i)} t_{ij}^{-\theta} \sum_{j' \in F(j)} \dots \sum_{k' \in F(d-1)} t_{k'd-1}^{-\theta} \\
&= \sum_{r \in \mathfrak{R}_{ij}} \left( \prod_{l=1}^K t_{r_{l-1}, r_l}^{-\theta} \right) \\
&= \sum_{K=0}^{\infty} A_{ij}^K \\
&= (\mathbf{I} - \mathbf{A})^{-1} \equiv \mathbf{B}
\end{aligned}$$

where in the second line we recognize that the recursive substitution on a finite graph results in a characterization of all possible routes of any length along the network. The resulting expression is identical to expression for endogenous transport cost in AA2022. In the third and fourth line we then employ the same argument as in their paper to show that the implied transport cost can be expressed as the leontief inverse of the underlying infrastructure matrix, where  $\mathbf{A} \equiv [t_{ij}^{-\theta}]$  is an  $N \times N$  matrix with  $(i, j)$  element  $t_{ij}^{-\theta}$  and  $A_{ij}^K$  is the  $(ij)$  element of the matrix  $A$  to the matrix power  $K$ . This shows that in essence, the two different approaches are isomorphic and capture the same underlying endogenous transport cost, albeit in different ways.

We now turn towards showing that for the special case where the mode choice elasticity is equal to the route choice elasticity, we can furthermore extend the approach in AA2022 to derive a clean decomposition of the multimodal transport cost in terms of a set of underlying mode-specific infrastructure matrices. Let us therefore consider the case where  $\eta = \theta$ . Notice that in this special case, the edge-specific transport cost is given by,

$$t_{ik}^{-\theta} \propto \sum_{m \in \mathcal{M}(i, k)} \tilde{t}_{ik, m}^{-\theta}$$

where  $\tilde{t}_{ik, m}^{-\theta}$  are the mode specific traversal costs between node  $i$  and  $k$ . As above, we can express recursively substitute the expected transport across modes between nodes, and obtain,

$$(\tau_{id})^{-\theta} = t_{d-1d}^{-\theta} \sum_{j \in F(i)} t_{ij}^{-\theta} \sum_{j' \in F(j)} \dots \sum_{k' \in F(d-1)} t_{k'd-1}^{-\theta}$$

by substituting the edge-specific transport cost in terms of the mode-specific cost, we obtain,

$$\begin{aligned}
(\tau_{id})^{-\theta} &= \left( \sum_{m \in \mathcal{M}(d-1, d)} \tilde{t}_{d-1d, m}^{-\theta} \right) \sum_{j \in F(i)} \left( \sum_{m \in \mathcal{M}(i, j)} \tilde{t}_{ij, m}^{-\theta} \right) \sum_{j' \in F(j)} \dots \sum_{k' \in F(d-1)} \left( \sum_{m \in \mathcal{M}(k', d-1)} \tilde{t}_{k'd-1, m}^{-\theta} \right) \\
&= \sum_{r \in \mathfrak{R}_{ij}} \left( \prod_{l=1}^K \sum_{m \in \mathcal{M}(r_{l-1}, r_l)} \tilde{t}_{r_{l-1}, r_l, m}^{-\theta} \right)
\end{aligned}$$

where the second line is a concise way of summarizing all possible uni and multi-modal paths along the multi-layered network. Without loss of generality, let us consider the case of two modes - one primary mode where flows originate and terminate, and a secondary mode that is accessible subject to some switching cost. Define the  $(N_1 + N_2) \times (N_1 + N_2)$  matrix  $\mathbf{A} = [a_{ij} \equiv t_{ij}^{-\theta}]$ . Notice that this

adjacency matrix forms a block partitioned matrix, i.e.

$$\mathbf{A} = \begin{bmatrix} \mathbf{A}_1 & \mathbf{S} \\ \mathbf{S}' & \mathbf{A}_2 \end{bmatrix}$$

where  $\mathbf{A}_1 = [a_{ij}] = [t_{ij}^{-\theta}]$  is the adjacency matrix for the primary transportation network,  $\mathbf{A}_2 = [a_{i'j'}] = [t_{i'j'}^{-\theta}]$  is the adjacency matrix for the secondary transportation network, and  $\mathbf{S} = [s_{ii'}^{-\theta}]$  is the diagonal matrix that represents linkages between the primary and secondary transportation network. We can write  $\tau_{ij}$  from by explicitly summing across all possible routes of all possible lengths. To do so, we sum across all locations that are traveled through all the possible paths as follows:

$$\begin{aligned} \tau_{ij}^{-\theta} &= \sum_{r \in \mathcal{R}_{ij}} \left( \prod_{l=1}^K \sum_{m \in \mathcal{M}(r_{l-1}, r_l)} t_{r_{l-1}, r_l, m}^{-\theta} \right) \\ &= \sum_{K=0}^{\infty} \left( \sum_{k_1=1}^{(N_1+N_2)} \sum_{k_2=1}^{(N_1+N_2)} \dots \sum_{k_{K-1}=1}^{(N_1+N_2)} a_{i,k_1} \times a_{k_1, k_2} \times \dots \times a_{k_{K-2}, k_{K-1}} \times a_{k_{K-1} j} \right) \end{aligned}$$

explicitly recognizing that this sum across all locations through all possible paths can be partitioned into unimodal paths on each transportation network and an arbitrary number of switches between transportation modes, we have,

$$\tau_{ij}^{-\theta} = \sum_{t_1=1}^N \sum_{t_2=1}^N \dots \sum_{t_S=1}^N \left( \left( \sum_{K=0}^{\infty} \mathbf{A}_{1,it_1}^K \right) \times s_{t_1 t_1'}^{-\theta} \times \dots \times s_{t_s' t_s}^{-\theta} \left( \sum_{K=0}^{\infty} \mathbf{A}_{1,T_S j}^K \right) \right)$$

which in matrix notation can be written as,

$$\tau_{ij}^{-\theta} = \sum_{K=0}^{\infty} \left( \left( \sum_{K=0}^{\infty} \mathbf{A}_1^K \right) \left( \mathbf{S} \left( \sum_{K=0}^{\infty} \mathbf{A}_2^K \right) \mathbf{S}' \right) \right)^K \left( \sum_{K=0}^{\infty} \mathbf{A}_1^K \right)$$

To simplify this expression let us first define the Leontief inverse for each infrastructure matrix separately, i.e.

$$\begin{aligned} \sum_{K=0}^{\infty} \mathbf{A}_1^K &= (\mathbf{I} - \mathbf{A}_1)^{-1} \equiv \mathbf{B} \\ \sum_{K=0}^{\infty} \mathbf{A}_2^K &= (\mathbf{I} - \mathbf{A}_2)^{-1} \equiv \mathbf{C} \end{aligned}$$

We also define - for convenience - the sandwich matrix that adjusts the transport cost along the secondary transportation network for switching costs and therefore traces out the option value of having access to the secondary transportation network,

$$\mathbf{S} \left( \sum_{K=0}^{\infty} \mathbf{A}_2^K \right) \mathbf{S}' \equiv \mathbf{D}$$

From matrix calculus we can restate the following result that relates the inverse of the Schur com-

plement of the partitioned infrastructure matrix to the geometric sum of matrix operations, specifically,

$$\sum_{K=0}^{\infty} (\mathbf{B}^{-1}\mathbf{D})^K \mathbf{B}^{-1} = (\mathbf{B} - \mathbf{D})^{-1} \equiv \mathbf{E}$$

applying this result we can write,

$$\begin{aligned} \tau_{ij}^{-\theta} &= \sum_{K=0}^{\infty} ((\mathbf{I} - \mathbf{A}_1)^{-1} (\mathbf{S}(\mathbf{I} - \mathbf{A}_2)^{-1} \mathbf{S}'))^K (\mathbf{I} - \mathbf{A}_1)^{-1} \\ &= [(\mathbf{I} - \mathbf{A}_1) - \mathbf{S}(\mathbf{I} - \mathbf{A}_2)^{-1} \mathbf{S}']_{ij}^{-1} \end{aligned}$$

therefore we can write,

$$\tau_{ij} = e_{ij}^{-\frac{1}{\theta}}$$

Furthermore, the Woodbury matrix identity (see e.g. [Horn and Johnson \(2012\)](#)) states,

$$(\mathbf{A} + \mathbf{U}\mathbf{C}\mathbf{V})^{-1} = \mathbf{A}^{-1} - \mathbf{A}^{-1}\mathbf{U}(\mathbf{C}^{-1} + \mathbf{V}\mathbf{A}^{-1}\mathbf{U})^{-1}\mathbf{V}\mathbf{A}^{-1}$$

which implies

$$\begin{aligned} \tau_{ij}^{-\theta} &= [(\mathbf{I} - \mathbf{A}_1) - \mathbf{S}(\mathbf{I} - \mathbf{A}_2)^{-1} \mathbf{S}']_{ij}^{-1} \\ &= [\mathbf{B} + \mathbf{B}\mathbf{S}(\mathbf{A}/\mathbf{A}_1)^{-1} \mathbf{S}'\mathbf{B}]_{ij} \\ &= [(\mathbf{I} - \mathbf{A}_1)^{-1} + (\mathbf{I} - \mathbf{A}_1)^{-1} \mathbf{S}(\mathbf{A}/\mathbf{A}_1)^{-1} \mathbf{S}' (\mathbf{I} - \mathbf{A}_1)^{-1}]_{ij} \end{aligned}$$

where  $\mathbf{A}/\mathbf{A}_1 := (\mathbf{I} - \mathbf{A}_1)^{-1} - \mathbf{S}(\mathbf{A}/\mathbf{A}_1)^{-1} \mathbf{S}'$  defines the Schur complement of the adjacency matrix  $A$ . The expression corresponds to the expression given in the main text and intuitively decomposes the transport cost into a component that originates from the unimodal paths and another component that originates from the multimodal paths. This result can also directly be obtained by applying to the partitioned matrix  $A$  the formula for the inverse of block-partitioned matrices (see e.g. [Horn and Johnson \(2012\)](#)).

## B.4 Section 3.3.2: Modal Traffic Flows

We characterize equilibrium traffic at different nodes of the transportation network. First, we utilize the recursive routing choice to characterize aggregate traffic between any two nodes across any mode. Second, we characterize mode-specific traffic between nodes. Finally, we characterize traffic at terminal stations.

### B.4.1 Traffic on the aggregate transport network

We start by characterizing the aggregate traffic between any two nodes across any mode. To do so we start by restating the (recursively defined) sourcing and link choice probability which is given by:

$$\pi_{ij,k} = \frac{(w_i/A_i)^{-\theta} (t_{jk}\tau_{ki})^{-\theta}}{\sum_{i \in \mathcal{N}} (w_i/A_i)^{-\theta} \sum_{k' \in \mathcal{F}(i)} (t_{jk'}\tau_{k'i})^{-\theta}}$$

which can be decomposed in the sourcing share and the link choice probability conditional on the

sourcing choice, i.e.

$$\begin{aligned}
\pi_{ij,kl} &= \frac{(t_{ik}\tau_{ki})^{-\theta}}{\sum_{k' \in \mathcal{F}(i)} (t_{ik'}\tau_{k'i})^{-\theta}} \frac{\tau_{ij}^{-\theta} p_i^{-\theta}}{\sum_{i \in \mathcal{N}} \tau_{ij}^{-\theta} p_i^{-\theta}} \\
&= \frac{(t_{ik}\tau_{ki})^{-\theta}}{\tau_{ij}^{-\theta}} \frac{\tau_{ij}^{-\theta} p_i^{-\theta}}{\sum_{i \in \mathcal{N}} \tau_{ij}^{-\theta} p_i^{-\theta}} \\
&= \pi_{ij}^k \times \pi_{ij}
\end{aligned}$$

The previous derivations only characterize the probability of choosing neighboring link  $k$  when routing between  $i$  and  $j$ . Notice that we can construct the probability of using any edge  $kl$  when transporting goods from  $i$  to  $j$  in straightforward way, i.e.

$$\begin{aligned}
\pi_{kj}^{kl} &= \frac{t_{kl}^{-\theta} \tau_{lj}^{-\theta}}{\tau_{kj}^{-\theta}} \\
&= \frac{\tau_{ik}^{-\theta} t_{kl}^{-\theta} \tau_{lj}^{-\theta}}{\tau_{ik}^{-\theta} \tau_{kj}^{-\theta}} \\
&= \frac{\tau_{ik}^{-\theta} t_{kl}^{-\theta} \tau_{lj}^{-\theta}}{\tau_{ij}^{-\theta}} \\
&= \pi_{ij}^{kl}
\end{aligned}$$

Notice that this arises naturally due to the markovian property of the recursive routing choice. To characterize traffic between nodes  $k$  and  $l$  along any mode, we characterize the share of goods that are being sourced from any location  $i$  to any location  $j$  and use the link  $kl$  along the way, i.e.

$$\begin{aligned}
\Xi_{kl} &= \sum_{i \in \mathcal{N}} \sum_{j \in \mathcal{N}} \pi_{ij,kl} E_j \iff \\
\Xi_{kl} &= \sum_{i \in \mathcal{N}} \sum_{j \in \mathcal{N}} \pi_{ij}^{kl} X_{ij} \iff \\
\Xi_{kl} &= \sum_{i \in \mathcal{N}} \sum_{j \in \mathcal{N}} \frac{\tau_{ik}^{-\theta} t_{kl}^{-\theta} \tau_{lj}^{-\theta}}{\tau_{ij}^{-\theta}} \times \tau_{ij}^{-\theta} \frac{Y_i}{\Pi_i^{-\theta}} \frac{E_j}{P_j^{-\theta}} \iff \\
\Xi_{kl} &= t_{kl}^{-\theta} \sum_{i \in \mathcal{N}} \tau_{ik}^{-\theta} \frac{Y_i}{\Pi_i^{-\theta}} \sum_{j \in \mathcal{N}} \tau_{lj}^{-\theta} \frac{E_j}{P_j^{-\theta}}, \\
\Xi_{kl} &= t_{kl}^{-\theta} \times P_k^{-\theta} \times \Pi_l^{-\theta}
\end{aligned}$$

where in the last line we used the definition of the consumer and producer market access terms. Furthermore, replacing market access terms,

$$\begin{aligned}
P_i &= \frac{1}{\bar{W}} \bar{u}_i L_i^{\beta-1} Y_i \\
\Pi_i &= \bar{A}_i L_i^{1+\alpha} Y_i^{-\frac{\theta+1}{\theta}}
\end{aligned}$$

we obtain,

$$\begin{aligned}\Xi_{kl} &= t_{kl}^{-\theta} \times \left( \frac{1}{\bar{W}} \bar{u}_k L_k^{\beta-1} Y_k \right)^{-\theta} \times \left( \bar{A}_l L_l^{1+\alpha} Y_l^{-\frac{\theta+1}{\theta}} \right)^{-\theta} \\ &= t_{kl}^{-\theta} \left( \frac{\bar{L}^{-(\alpha+\beta)\theta}}{W^{-\theta}} \right) \bar{L} \bar{A}_l^{-\theta} \bar{u}_k^{-\theta} l_k^{-\theta(\beta-1)} l_l^{-\theta(1+\alpha)} y_k^{-\theta} y_l^{(1+\theta)} \\ &= t_{kl}^{-\theta} \chi \bar{L} \bar{A}_l^{-\theta} \bar{u}_k^{-\theta} l_k^{-\theta(\beta-1)} l_l^{-\theta(1+\alpha)} y_k^{-\theta} y_l^{(1+\theta)}\end{aligned}$$

where in the last line we use the definition  $\chi = \frac{\bar{L}^{(\alpha+\beta)\theta}}{W^\theta}$ . We have,

$$\Xi_{kl} = t_{kl}^{-\theta} \chi^{-1} \bar{L} \bar{A}_l^{-\theta} \bar{u}_k^{-\theta} l_k^{-\theta} l_l^{-\theta} y_k^{-\theta} y_l^{(1+\theta)}$$

which characterizes aggregate flows between neighboring nodes  $k$  and  $l$  in terms of the endogenous variables along the network.

#### B.4.2 Mode-specific traffic

In the next step we now turn towards characterizing the probability of sourcing from location  $j$  to location  $i$  choosing neighboring node  $k$  as the cost-minimizing routing choice and furthermore opting for mode  $m$  between node  $i$  and  $k$ . The nested choice implies that this choice probability is given by,

$$\pi_{ijk,m} = \frac{\tilde{t}_{ik,m}^{-\eta}}{t_{ik}^{-\eta}} \frac{(t_{ik} \tau_{kj})^{-\theta} p_i^{-\theta}}{\sum_{i \in \mathcal{N}} \tau_{ij}^{-\theta} p_i^{-\theta}}$$

which can be decomposed in the sourcing share, link choice probability conditional on sourcing choice, and the modal share conditional on both sourcing and link choice, i.e.

$$\begin{aligned}\pi_{ij,kl,m} &= \frac{\tilde{t}_{ik,m}^{-\eta}}{t_{ik}^{-\eta}} \frac{(t_{ik} \tau_{ki})^{-\theta}}{\sum_{k' \in \mathcal{F}(i)} (t_{ik'} \tau_{k'i})^{-\theta}} \frac{\tau_{ij}^{-\theta} p_i^{-\theta}}{\sum_{i \in \mathcal{N}} \tau_{ij}^{-\theta} p_i^{-\theta}} \\ &= \pi_{ik}^m \times \pi_{ij}^k \times \pi_{ij}\end{aligned}$$

We can apply similar calculations as above to extend this for any link  $kl$  when transporting goods from  $i$  to  $j$ , i.e.

$$\pi_{ij,kl,m} = \frac{\tilde{t}_{kl,m}^{-\eta}}{t_{kl}^{-\eta}} \frac{\tau_{ik}^{-\theta} t_{kl}^{-\theta} \tau_{lj}^{-\theta}}{\tau_{ij}^{-\theta}} \frac{\tau_{ij}^{-\theta} p_i^{-\theta}}{\sum_{i \in \mathcal{N}} \tau_{ij}^{-\theta} p_i^{-\theta}}$$

Given this choice probability we can characterize the mode-specific traffic between neighboring nodes

$k$  and  $l$ , i.e.

$$\begin{aligned}
\Xi_{kl,m} &= \sum_{i \in \mathcal{N}} \sum_{j \in \mathcal{N}} \pi_{ijk,m} E_j \iff \\
&= \sum_{i \in \mathcal{N}} \sum_{j \in \mathcal{N}} \pi_{ik}^m \times \pi_{ij}^k \times X_{ij} \\
&= \frac{\tilde{t}_{kl,m}^{-\eta}}{t_{kl}^{-\eta}} \sum_{i \in \mathcal{N}} \sum_{j \in \mathcal{N}} \frac{\tau_{ik}^{-\theta} t_{kl}^{-\theta} \tau_{lj}^{-\theta}}{\tau_{ij}^{-\theta}} \times \tau_{ij}^{-\theta} \frac{Y_i}{\Pi_i^{-\theta}} \frac{E_j}{P_j^{-\theta}} \iff \\
&= \frac{\tilde{t}_{kl,m}^{-\eta}}{t_{kl}^{-\eta}} \times t_{kl}^{-\theta} \sum_{i \in \mathcal{N}} \tau_{ik}^{-\theta} \frac{Y_i}{\Pi_i^{-\theta}} \sum_{j \in \mathcal{N}} \tau_{lj}^{-\theta} \frac{E_j}{P_j^{-\theta}}, \\
&= \frac{\tilde{t}_{kl,m}^{-\eta}}{t_{kl}^{-\eta}} \times t_{kl}^{-\theta} \times P_k^{-\theta} \times \Pi_l^{-\theta} \\
&= \tilde{t}_{kl,m}^{-\eta} \times t_{kl}^{\eta-\theta} \times P_k^{-\theta} \times \Pi_l^{-\theta}
\end{aligned}$$

which gives us an expression for mode-specific traffic in terms of market access measures and the aggregate and mode specific iceberg transport cost along the edge. Note, that the nested formulation implies that mode-specific traffic is the conditional mode specific share of aggregate traffic, i.e.  $\Xi_{kl,m} = \pi_{ik}^m \times \Xi_{kl}$ .

#### B.4.3 Traffic at Terminals

In the final step we characterize the traffic at mode-specific terminals that allow multimodal movements between nodes  $kl$ . To do so we start by characterizing the probability of sourcing from location  $j$  to location  $i$  choosing any neighboring node  $k' \in \mathcal{F}(i)$ , but crucially choosing an alternative non-primary mode of transport and therefore traversing through a terminal while routing. This choice probability can be characterized in the following way,

$$\begin{aligned}
\pi_{ij,kk,m} &= \sum_{k \in \mathcal{F}(i)} \frac{\tilde{t}_{ik,m}^{-\eta}}{t_{ik}^{-\eta}} \frac{t_{ik}^{-\theta} \tau_{kj}^{-\theta} p_j^{-\theta}}{\sum_{j \in 0} \sum_{k'} t_{ik} \tau_{kj} p_j^{-\theta}} \\
&= s_{ii}^{-\eta} \sum_{k \in \mathcal{F}(i)} \frac{(\tau_{ik} s_{kk,m})^{-\eta}}{t_{ik}^{-\eta}} \frac{t_{ik}^{-\theta} \tau_{kj}^{-\theta} p_j^{-\theta}}{\sum_{j \in 0} \sum_{k'} t_{ik} \tau_{kj} p_j^{-\theta}}
\end{aligned}$$

which can be decomposed into which can again be decomposed into sourcing shares, link choice shares conditional on sourcing choice, and mode choice conditional on link choice, i.e.

$$\begin{aligned}
\pi_{ij,kk,m} &= \sum_{k \in \mathcal{F}(i)} \frac{s_{ii}^{-\eta} (\tau_{ik} s_{kk,m})^{-\eta}}{t_{ik}^{-\eta}} \frac{(t_{ik} \tau_{ki})^{-\theta}}{\sum_{k' \in \mathcal{F}(i)} (t_{ik'} \tau_{k'i})^{-\theta}} \frac{\tau_{ij}^{-\theta} p_i^{-\theta}}{\sum_{i \in \mathcal{N}} \tau_{ij}^{-\theta} p_i^{-\theta}} \\
&= \pi_{ij} \sum_{k \in \mathcal{F}(i)} \pi_{ik}^m \times \pi_{ij}^k
\end{aligned}$$

We can apply similar calculations as above to extend this for any link  $kl$  when transporting goods

from  $i$  to  $j$ , i.e.

$$\begin{aligned}\pi_{ij,kk,m} &= \sum_{l \in \mathcal{F}(k)} \frac{s_{kk}^{-\eta} (\tau_{kl} s_{ll,m})^{-\eta}}{t_{kl}^{-\eta}} \frac{\tau_{ik}^{-\theta} t_{kl}^{-\theta} \tau_{lj}^{-\theta}}{\tau_{ij}^{-\theta}} \frac{\tau_{ij}^{-\theta} p_i^{-\theta}}{\sum_{i \in \mathcal{N}} \tau_{ij}^{-\theta} p_i^{-\theta}} \\ &= \pi_{ij} \sum_{l \in \mathcal{F}(k)} \pi_{kl}^m \times \pi_{ij}^{kl}\end{aligned}$$

Given this choice probability we can characterize the mode-specific traffic between neighboring nodes  $k$  and  $l$ , i.e.

$$\begin{aligned}\Xi_{kk,m} &= \sum_{i \in \mathcal{N}} \sum_{j \in \mathcal{N}} \pi_{ij,kk,m} E_j \iff \\ &= \sum_{i \in \mathcal{N}} \sum_{j \in \mathcal{N}} \left( \sum_{l \in \mathcal{F}(k)} \pi_{kl}^m \times \pi_{ij}^{kl} \right) \times X_{ij} \\ &= \sum_{l \in \mathcal{F}(k)} \frac{s_{kk}^{-\eta} (\tau_{kl} s_{ll,m})^{-\eta}}{t_{kl}^{-\eta}} \sum_{i \in \mathcal{N}} \sum_{j \in \mathcal{N}} \frac{\tau_{ik}^{-\theta} t_{kl}^{-\theta} \tau_{lj}^{-\theta}}{\tau_{ij}^{-\theta}} \times \tau_{ij}^{-\theta} \frac{Y_i}{\Pi_i^{-\theta}} \frac{E_j}{P_j^{-\theta}} \iff \\ &= \sum_{l \in \mathcal{F}(k)} \frac{s_{kk}^{-\eta} (\tau_{kl} s_{ll,m})^{-\eta}}{t_{kl}^{-\eta}} \times t_{kl}^{-\theta} \sum_{i \in \mathcal{N}} \tau_{ik}^{-\theta} \frac{Y_i}{\Pi_i^{-\theta}} \sum_{j \in \mathcal{N}} \tau_{lj}^{-\theta} \frac{E_j}{P_j^{-\theta}}, \\ &= \sum_{l \in \mathcal{F}(k)} \frac{s_{kk}^{-\eta} (\tau_{kl} s_{ll,m})^{-\eta}}{t_{kl}^{-\eta}} \times t_{kl}^{-\theta} \times P_k^{-\theta} \times \Pi_l^{-\theta} \\ &= s_{kk}^{-\eta} \times P_k^{-\theta} \times \sum_{l \in \mathcal{F}(k)} (\tau_{kl} s_{ll,m})^{-\eta} \times t_{kl}^{\eta-\theta} \times \Pi_l^{-\theta}\end{aligned}$$

#### B.4.4 Traffic with congestion

Incorporating congestion, for the primary mode of transport ( $m = 0$ ), we have the following relationship,

$$\begin{aligned}\tilde{t}_{kl,m} &= \bar{\tilde{t}}_{kl,m} [\Xi_{ij,m}]^{\lambda_m} \iff \\ \tilde{t}_{kl,m} &= \bar{\tilde{t}}_{kl,m} \left[ \tilde{t}_{kl,m}^{-\eta} \times t_{kl}^{\eta-\theta} \times P_k^{-\theta} \times \Pi_l^{-\theta} \right]^{\lambda_m} \iff \\ \tilde{t}_{kl,m} &= \bar{\tilde{t}}_{kl,m} \times \tilde{t}_{kl,m}^{-\eta\lambda_m} \times t_{kl}^{\lambda_m(\eta-\theta)} \times P_k^{-\theta\lambda_m} \times \Pi_l^{-\theta\lambda_m} \iff \\ \tilde{t}_{kl,m}^{1+\eta\lambda_m} &= \bar{\tilde{t}}_{kl,m} \times t_{kl}^{\lambda_m(\eta-\theta)} \times P_k^{-\theta\lambda_m} \times \Pi_l^{-\theta\lambda_m} \iff \\ \tilde{t}_{kl,m} &= \bar{\tilde{t}}_{kl,m}^{\frac{1}{1+\eta\lambda_m}} \times t_{kl}^{\frac{\lambda_m(\eta-\theta)}{1+\eta\lambda_m}} \times P_k^{\frac{-\theta\lambda_m}{1+\eta\lambda_m}} \times \Pi_l^{\frac{-\theta\lambda_m}{1+\eta\lambda_m}}\end{aligned}$$

For any secondary mode of transportation, we have instead congestion at terminal stations. Let us

characterize the transport cost net of congestion at any terminal, i.e.

$$\begin{aligned}
s_{kk,m} &= \bar{s}_{kk,m} [\Xi_{kk,m}]^{\lambda_m} \\
s_{kk,m} &= \bar{s}_{kk,m} \left[ s_{kk,m}^{-\eta} \times P_k^{-\theta} \times \sum_{l \in \mathcal{F}(k)} (\tau_{kl} s_{ll,m})^{-\eta} \times t_{kl}^{\eta-\theta} \times \Pi_l^{-\theta} \right]^{\lambda_m} \\
s_{kk,m} &= \bar{s}_{kk,m} \times s_{kk,m}^{-\eta \lambda_m} \times P_k^{-\theta \lambda_m} \times \left( \sum_{l \in \mathcal{F}(k)} (\tau_{kl} s_{ll,m})^{-\eta} \times t_{kl}^{\eta-\theta} \times \Pi_l^{-\theta} \right)^{\lambda_m} \\
s_{kk,m}^{1+\eta \lambda_m} &= \bar{s}_{kk,m} \times P_k^{-\theta \lambda_m} \times \left( \sum_{l \in \mathcal{F}(k)} (\tau_{kl} s_{ll,m})^{-\eta} \times t_{kl}^{\eta-\theta} \times \Pi_l^{-\theta} \right)^{\lambda_m} \\
s_{kk,m} &= \bar{s}_{kk,m}^{\frac{1}{1+\eta \lambda_m}} \times P_k^{\frac{-\theta \lambda_m}{1+\eta \lambda_m}} \times \left( \sum_{l \in \mathcal{F}(k)} (\tau_{kl} s_{ll,m})^{-\eta} \times t_{kl}^{\eta-\theta} \times \Pi_l^{-\theta} \right)^{\frac{\lambda_m}{1+\eta \lambda_m}}
\end{aligned}$$

## C Data and Additional Results

### C.1 Data Appendix

#### C.1.1 AIS Vessel Traffic Data

USACE only captures draft if it's for ships carrying foreign cargo since they have to report with customs. Our AIS data captures all ships big and small maybe going empty so have more ships but no draft measure.

#### C.1.2 Ports

While we include the top 30 container ports in the US in our analysis, we merge some of these ports into the one polygon due to the USACE-provided polygons either overlapping or being very close to each other. Specifically, Tacoma + Seattle are merged into a single polygon due to their port alliance (NWSA). Additionally, Tacoma and Seattle share a port alliance. Tampa + Manatee were merged do to overlap issues between the rather large Tampa region and the manually applied Manatee port statistical area. Lastly, we include Chester in the Philadelphia PSA because the USACE-provided polygon area includes Chester. All in all, we have 27 unique ports.

#### C.1.3 Rail Traffic Data

#### C.1.4 Rail Dwell Times Data

#### C.1.5 Matching Rail Traffic Data to MSAs

Using 1999 MSA polygons from the Census Bureau, we match the rail stations from the Waybill data to the 228 MSAs in [Duranton and Turner \(2011\)](#). By rail destination, we observe 224 MSAs and by origin we observe 223 MSAs. Since some of these unobserved MSAs overlap, we have 7 MSAs. We conduct our analysis on the remaining 221 MSAs, so that both the origin and destination results are comparable. The 7 MSAs that we do not have rail traffic for Daytona Beach FL, Fort Myers-Cape Coral FL, Fort Walton Beach FL, New Haven-Bridgeport-Stamford-Waterbury-Danbury CT, Providence-Warwick-Pawtucket RI, Punta Gorda FL, and Santa Fe NM.

To match the MSA-level truck vehicle-kilometers traveled (VKT) measure in [Duranton and Turner \(2011\)](#), we calculate the rail equivalent in two ways. First, we utilize the number of rail carloads, transported in and out of MSAs, multiplied by the weighted average of their distance traveled. We call this railcar-kilometers-traveled (rail VKT) and distinguish by destination for rail shipments transported into these MSAs, and by origin for shipments transported out of these MSAs. We also observe the weight of these rail shipments and can calculate rail weight VKT using the same method outlined previously.

## C.2 Modal Diversion: Additional Results

Since we have a slightly smaller set of MSAs due to the matching process between MSAs and our rail traffic data (see Section C.1.5 for more information), we first show that we are able to replicate the [Duranton and Turner \(2011\)](#) results in Table 5. We find that our fixed effects and IV estimates have the same sign and are within one standard deviation of the results from [Duranton and Turner \(2011\)](#) (Columns (6) to (10), Table 9, [Duranton and Turner \(2011\)](#)).<sup>1</sup>

---

<sup>1</sup>First stage results are in Table A.2.

**Table. A.2.** Elasticity of Truck VKT with respect to Interstate Highway Lane Kilometers: First Stage

	(1)	(2)	(3)
1898 Railroads	0.0879* (0.0460)	0.0939* (0.0499)	0.119** (0.0474)
1947 Planned Interstates	0.156*** (0.0332)	0.127*** (0.0322)	0.114*** (0.0284)
1835 Exploration Routes	0.0249** (0.0117)	0.0268** (0.0124)	0.0222* (0.0122)
Population	0.516*** (0.0393)	0.599*** (0.0481)	0.545*** (0.0597)
Geography		✓	✓
Census Divisions		✓	✓
Socioeconomic Characteristics			✓
Year FE	✓	✓	✓
Observations	663	663	663
KP F-stat	13.48	10.08	10.02

**Notes:** Robust standard errors clustered by MSAs in parentheses. All variables are in logs. Instruments are 1835 exploration routes, 1898 railroad route kilometers, and 1947 planned interstate highways. 663 observations corresponding to 221 MSAs for each regression.

**Table. A.3.** Elasticity of Rail Traffic Use (in Railcar-Kilometers) with respect to Road Infrastructure Improvements: First Stage

	(1)	(2)	(3)
1898 Railroads	0.0879* (0.0460)	0.0939* (0.0499)	0.119** (0.0474)
1947 Planned Interstates	0.156*** (0.0332)	0.127*** (0.0322)	0.114*** (0.0284)
1835 Exploration Routes	0.0249** (0.0117)	0.0268** (0.0124)	0.0222* (0.0122)
Population	0.516*** (0.0393)	0.599*** (0.0481)	0.545*** (0.0597)
Geography		✓	✓
Census Divisions		✓	✓
Socioeconomic Characteristics			✓
Year FE	✓	✓	✓
Observations	663	663	663
KP F-stat	13.48	10.08	10.02

**Notes:** Robust standard errors clustered by MSAs in parentheses. All variables are in logs. Instruments are ln 1835 exploration routes, ln 1898 railroads, and ln 1947 planned interstates; 684 observations corresponding to 228 MSAs for each regression.

**Table. A.4.** Elasticity of Rail to Truck Traffic Use by Destination with respect to Road Infrastructure Improvements

	(1)	(2)	(3)	(4)	(5)
Rail to Truck Traffic Use by Destination	OLS	OLS	IV	IV	IV
Interstate Highway Lane (km)	-1.060*** (0.185)	-1.061*** (0.185)	-1.101*** (0.405)	-1.210*** (0.426)	-0.999** (0.405)
Population		0.0605 (0.337)	1.132*** (0.298)	1.303*** (0.351)	1.145*** (0.336)
Geography				✓	✓
Census Divisions				✓	✓
Socioeconomic Characteristics		✓			✓
MSA FE	✓	✓			
Year FE	✓	✓	✓	✓	✓
Observations	658	658	658	658	658
R-squared	0.89	0.89	-	-	-
KP F-stat			14.48	10.76	10.04

*Notes:* \*  $p < 0.1$ , \*\*  $p < 0.05$ , \*\*\*  $p < 0.01$ . Robust standard errors clustered by MSAs in parentheses. All variables are in logs. Rail traffic use, measured in railcar-kilometers, is constructed using confidential rail waybill data. Truck traffic use (in vehicle-kilometers) and other variables are from Duranton and Turner (2011). Instruments are 1835 exploration routes, 1898 railroad route kilometers, and 1947 planned interstate highways. 663 observations corresponding to 221 MSAs for each regression. See Table A.17 for first stage regressions.

**Table. A.5.** Elasticity of Rail Car Traffic-Kilometers by Destination with respect to Interstate Highway Lane Kilometers

	(1)	(2)	(3)	(4)	(5)
Rail Traffic Use by Destination (railcar-km)	OLS	OLS	IV	IV	IV
Interstate Highway Lane (km)	0.181 (0.113)	0.187 (0.114)	0.225 (0.417)	0.295 (0.466)	0.525 (0.465)
Population		0.548** (0.247)	1.110*** (0.307)	1.086*** (0.380)	0.986** (0.380)
Geography				✓	✓
Census Divisions				✓	✓
Socioeconomic Characteristics		✓			✓
MSA FE	✓	✓			
Year FE	✓	✓	✓	✓	✓
Observations	663	663	663	663	663
R-squared	0.95	0.95	-	-	-
KP F-stat			13.48	10.08	10.02

*Notes:* \*  $p < 0.1$ , \*\*  $p < 0.05$ , \*\*\*  $p < 0.01$ . Robust standard errors clustered by MSAs in parentheses. All variables are in logs. Instruments are 1835 exploration routes, 1898 railroad route kilometers, and 1947 planned interstate highways. 663 observations corresponding to 221 MSAs for each regression. See Table A.6 for first stage regressions.

### C.3 Railroad Infrastructure Improvement: Heartland Corridor

In order to illustrate the main channel of our model, i.e. modal diversion, we present preliminary empirical evidence on the impact of a large infrastructure improvement that is mode-specific on US regional rail traffic flows. The Heartland Corridor is a \$150 million infrastructure plan to increase capacity of rail lines by increasing height clearance in tunnels/bridges to allow for double-stack intermodal trains.

**Table. A.6.** Elasticity of Rail Traffic Use (in Railcar-Kilometers) by Destination with respect to Road Infrastructure Improvements: First Stage

	(1)	(2)	(3)
1898 Railroads	0.0879*	0.0939*	0.119**
	(0.0460)	(0.0499)	(0.0474)
1947 Planned Interstates	0.156***	0.127***	0.114***
	(0.0332)	(0.0322)	(0.0284)
1835 Exploration Routes	0.0249**	0.0268**	0.0222*
	(0.0117)	(0.0124)	(0.0122)
Population	0.516***	0.599***	0.545***
	(0.0393)	(0.0481)	(0.0597)
Geography		✓	✓
Census Divisions		✓	✓
Socioeconomic Characteristics			✓
Year FE	✓	✓	✓
Observations	663	663	663
KP F-stat	13.48	10.08	10.02

**Notes:** Robust standard errors clustered by MSAs in parentheses. All variables are in logs. Instruments are ln 1835 exploration routes, ln 1898 railroads, and ln 1947 planned interstates; 684 observations corresponding to 228 MSAs for each regression.

**Table. A.7.** Elasticity of Rail Traffic Use (in railcar-km) by Origin with respect to Road Infrastructure Improvements

	(1)	(2)	(3)	(4)	(5)
Rail Traffic Use by Origin (railcar-km)	OLS	OLS	IV	IV	IV
Interstate Highway Lane (km)	0.197	0.200	0.630*	0.230	0.231
	(0.122)	(0.123)	(0.380)	(0.347)	(0.332)
Population		0.266	0.474	0.923***	0.905***
		(0.374)	(0.296)	(0.302)	(0.295)
Geography			✓	✓	
Census Divisions			✓	✓	
Socioeconomic Characteristics		✓		✓	
MSA FE	✓	✓			
Year FE	✓	✓	✓	✓	✓
Observations	663	663	663	663	663
R-squared	0.94	0.94	-	-	-
KP F-stat			13.48	10.08	10.02

**Notes:** \*  $p < 0.1$ , \*\*  $p < 0.05$ , \*\*\*  $p < 0.01$ . Robust standard errors clustered by MSAs in parentheses. All variables are in logs. Rail traffic use is constructed using the confidential rail waybill data. All other variables are from Duranton and Turner (2011). Instruments are 1835 exploration routes, 1898 railroad route kilometers, and 1947 planned interstate highways. 663 observations corresponding to 221 MSAs for each regression. See Table A.14 for first stage regressions.

This new route saves double-stack trains 230 miles (up to 2 days) between Norfolk & Chicago (Board, National Academies of Sciences and Medicine, 2017).

**Table. A.8.** Elasticity of Rail Traffic Use (in Railcar-Kilometers) by Origin with respect to Road Infrastructure Improvements: First Stage

	(1)	(2)	(3)
1898 Railroads	0.0879*	0.0939*	0.119**
	(0.0460)	(0.0499)	(0.0474)
1947 Planned Interstates	0.156***	0.127***	0.114***
	(0.0332)	(0.0322)	(0.0284)
1835 Exploration Routes	0.0249**	0.0268**	0.0222*
	(0.0117)	(0.0124)	(0.0122)
Population	0.516***	0.599***	0.545***
	(0.0393)	(0.0481)	(0.0597)
Geography		✓	✓
Census Divisions		✓	✓
Socioeconomic Characteristics			✓
Year FE	✓	✓	✓
Observations	663	663	663
KP F-stat	13.48	10.08	10.02

**Notes:** Robust standard errors clustered by MSAs in parentheses. All variables are in logs. Instruments are ln 1835 exploration routes, ln 1898 railroads, and ln 1947 planned interstates; 684 observations corresponding to 228 MSAs for each regression.

**Table. A.9.** Elasticity of Rail Traffic Use (in Weight-Kilometers) with respect to Road Infrastructure Improvements

	(1) OLS	(2) OLS	(3) IV	(4) IV	(5) IV
Interstate Highway Lane KM	-0.135 (0.161)	-0.131 (0.163)	0.367 (0.320)	0.131 (0.335)	0.292 (0.314)
Population		0.393 (0.251)	0.524** (0.248)	0.798*** (0.282)	0.647** (0.269)
Geography				✓	✓
Census Divisions				✓	✓
Socioeconomic Characteristics		✓			✓
MSA FE	✓	✓			
Year FE	✓	✓	✓	✓	✓
Observations	663	663	663	663	663
R-squared	0.94	0.94	0.29	0.49	0.52
KP F-stat			13.48	10.08	10.02

**Notes:** \*  $p < 0.1$ , \*\*  $p < 0.05$ , \*\*\*  $p < 0.01$ . Robust standard errors clustered by MSAs in parentheses. All variables are in logs. Instruments are 1835 exploration routes, 1898 railroad route kilometers, and 1947 planned interstate highways. 663 observations corresponding to 221 MSAs for each regression. See Table A.2 for first stage regressions.

Using waybill rail data, we estimate the evolution of rail shipment flows as a result of Heartland

**Table. A.10.** Elasticity of Rail Traffic Use (in Weight-Kilometers) with respect to Road Infrastructure Improvements: First Stage

	(1)	(2)	(3)
1898 Railroads	0.0879*	0.0939*	0.119**
	(0.0460)	(0.0499)	(0.0474)
1947 Planned Interstates	0.156***	0.127***	0.114***
	(0.0332)	(0.0322)	(0.0284)
1835 Exploration Routes	0.0249**	0.0268**	0.0222*
	(0.0117)	(0.0124)	(0.0122)
Population	0.516***	0.599***	0.545***
	(0.0393)	(0.0481)	(0.0597)
Geography		✓	✓
Census Divisions		✓	✓
Socioeconomic Characteristics			✓
Year FE	✓	✓	✓
Observations	663	663	663
KP F-stat	13.48	10.08	10.02

**Notes:** Robust standard errors clustered by MSAs in parentheses. All variables are in logs. Instruments are ln 1835 exploration routes, ln 1898 railroads, and ln 1947 planned interstates; 684 observations corresponding to 228 MSAs for each regression.

**Table. A.11.** Elasticity of Rail Traffic Use (in Weight-Kilometers) by Destination with respect to Road Infrastructure Improvements

Rail Traffic Use by Destination (weight-km)	(1) OLS	(2) OLS	(3) IV	(4) IV	(5) IV
Interstate Highway Lane (km)	0.151 (0.0972)	0.156 (0.0989)	0.184 (0.426)	0.225 (0.470)	0.494 (0.469)
Population		0.562** (0.236)	0.939*** (0.312)	0.975** (0.382)	0.824** (0.383)
Geography			✓	✓	✓
Census Divisions				✓	✓
Socioeconomic Characteristics		✓			✓
MSA FE	✓	✓			
Year FE	✓	✓	✓	✓	✓
Observations	663	663	663	663	663
R-squared	0.95	0.95	-	-	-
KP F-stat			13.48	10.08	10.02

**Notes:** \*  $p < 0.1$ , \*\*  $p < 0.05$ , \*\*\*  $p < 0.01$ . Robust standard errors clustered by MSAs in parentheses. All variables are in logs. Instruments are 1835 exploration routes, 1898 railroad route kilometers, and 1947 planned interstate highways. 663 observations corresponding to 221 MSAs for each regression. See Table A.2 for first stage regressions.

Corridor:

$$Y_{odt} = \sum_{t'=2001 \setminus 2007}^{2014} \beta_{t'} \Delta \text{Rail Distance}_{od} \mathbf{1}_{t'} + \lambda_{ot} + \theta_{dt} + \text{Distance}_{od} + \varepsilon_{odt}$$

where  $Y_{odt}$  is the trade flows from origin  $o$  to destination  $d$  at year  $t$ ,  $\Delta \text{Rail Distance}_{od}$  is change in log

**Table. A.12.** Elasticity of Rail Traffic Use (in Weight-Kilometers) by Destination with respect to Road Infrastructure Improvements: First Stage

	(1)	(2)	(3)
1898 Railroads	0.0879*	0.0939*	0.119**
	(0.0460)	(0.0499)	(0.0474)
1947 Planned Interstates	0.156***	0.127***	0.114***
	(0.0332)	(0.0322)	(0.0284)
1835 Exploration Routes	0.0249**	0.0268**	0.0222*
	(0.0117)	(0.0124)	(0.0122)
Population	0.516***	0.599***	0.545***
	(0.0393)	(0.0481)	(0.0597)
Geography		✓	✓
Census Divisions		✓	✓
Socioeconomic Characteristics			✓
Year FE	✓	✓	✓
Observations	663	663	663
KP F-stat	13.48	10.08	10.02

**Notes:** Robust standard errors clustered by MSAs in parentheses. All variables are in logs. Instruments are ln 1835 exploration routes, ln 1898 railroads, and ln 1947 planned interstates; 684 observations corresponding to 228 MSAs for each regression.

**Table. A.13.** Elasticity of Rail Traffic Use (in Weight-Kilometers) by Origin with respect to Road Infrastructure Improvements

	(1)	(2)	(3)	(4)	(5)
Rail Traffic Use by Origin (weight-km)	OLS	OLS	IV	IV	IV
Interstate Highway Lane (km)	0.167	0.169	0.621	0.150	0.155
	(0.117)	(0.117)	(0.401)	(0.355)	(0.347)
Population		0.209	0.206	0.757**	0.707**
		(0.300)	(0.310)	(0.307)	(0.303)
Geography			✓	✓	
Census Divisions			✓	✓	
Socioeconomic Characteristics		✓		✓	
MSA FE	✓	✓			
Year FE	✓	✓	✓	✓	✓
Observations	663	663	663	663	663
R-squared	0.94	0.94	-	-	-
KP F-stat			13.48	10.08	10.02

**Notes:** \*  $p < 0.1$ , \*\*  $p < 0.05$ , \*\*\*  $p < 0.01$ . Robust standard errors clustered by MSAs in parentheses. All variables are in logs. Instruments are 1835 exploration routes, 1898 railroad route kilometers, and 1947 planned interstate highways. 663 observations corresponding to 221 MSAs for each regression. See Table A.2 for first stage regressions.

shortest rail distance between  $o$  and  $d$  before and after the Corridor, indicator  $\mathbf{1}_{t'}$  equals one for year  $t'$ ,  $\lambda_{ot}$  is origin-year-level fixed effects,  $\theta_{dt}$  is destination-year fixed effects, and  $\text{Distance}_{od}$  is the direct distance between origin and destination. The key parameter of interest,  $\beta_{t'}$ , is the cumulative Heartland

**Table. A.14.** Elasticity of Rail Traffic Use (in Weight-Kilometers) by Origin with respect to Road Infrastructure Improvements: First Stage

	(1)	(2)	(3)
1898 Railroads	0.0879*	0.0939*	0.119**
	(0.0460)	(0.0499)	(0.0474)
1947 Planned Interstates	0.156***	0.127***	0.114***
	(0.0332)	(0.0322)	(0.0284)
1835 Exploration Routes	0.0249**	0.0268**	0.0222*
	(0.0117)	(0.0124)	(0.0122)
Population	0.516***	0.599***	0.545***
	(0.0393)	(0.0481)	(0.0597)
Geography		✓	✓
Census Divisions		✓	✓
Socioeconomic Characteristics			✓
Year FE	✓	✓	✓
Observations	663	663	663
KP F-stat	13.48	10.08	10.02

**Notes:** Robust standard errors clustered by MSAs in parentheses. All variables are in logs. Instruments are ln 1835 exploration routes, ln 1898 railroads, and ln 1947 planned interstates; 684 observations corresponding to 228 MSAs for each regression.

Corridor impact on the trade flows outcome by each year. Corridor construction started in 2007 and is the base year for outcome changes. Preliminary results show that the Heartland Corridor has resulted in an increase of rail traffic immediately in origin-destination pairs that have been impacted more after its implementation, after which they accumulate more slowly but continue to rise (Panel (B), Figure A.3).

This large improvement on rail network can potentially have spillover effects onto other modes of transportation. Utilizing the Commodity Flow Surveys (CFS, Bureau of Transportation Statistics), we present suggestive evidence on the modal diversion effects of the Heartland Corridor on road traffic. The CFS is published every 5 years and so we utilize the 2002, 2007, 2012, and 2017 volumes. Due to data limitations on earlier CFS volumes, we present goods movement between US states via road transport.<sup>2</sup> For each state pair, we calculate their shortest rail distance before and after the Corridor. Figure A.4 compares the road shipments between pairs that have a decrease in rail distance due to the Corridor to pairs that do not. Only state pairs that report non-missing road shipment observations for all 4 CFS volumes are included. Panel (A) presents the road shipments measured in value while Panel (B) is measured in tons with both normalized to their 2002 values. We find that for pairs that would potentially benefit from the Heartland Corridor, the amount of shipments transported by road increased about 40% from 2002 (3.1 billion dollars in 2002 to 4.4 billion dollars in 2012, dashed blue line in Panel (A) Figure A.4). Comparatively, pairs that do not have a decrease in their rail distance due to the Corridor see their road shipments almost double over this period (4 billion dollars in 2002 to 7.8 billion dollars in 2012, solid blue line in Panel (A) Figure A.4). We see similar patterns using the weight measure—almost no increase in weight shipments for pairs that are impacted between 2002 and 2017 compared to an increase of about 25% for pairs that are not (Panel (B) Figure A.4).<sup>3</sup>

<sup>2</sup>The 2002 CFS does not publish goods movement data at the CFS area by transport mode level. Instead this information is only available at the state level.

<sup>3</sup>3.1 million tons in 2002 to 3.2 million tons in 2017 for impacted pairs, 8 million tons in 2002 to 10 million tons in 2017 for the unimpacted pairs.

**Table. A.15.** Elasticity of Rail to Truck Traffic Use with respect to Road Infrastructure Improvements: First Stage

	(1)	(2)	(3)
1898 Railroads	0.102** (0.0445)	0.107** (0.0481)	0.129*** (0.0478)
1947 Planned Interstates	0.148*** (0.0317)	0.117*** (0.0298)	0.108*** (0.0274)
1835 Exploration Routes	0.0244** (0.0117)	0.0257** (0.0124)	0.0220* (0.0122)
Population	0.511*** (0.0386)	0.597*** (0.0474)	0.535*** (0.0600)
Geography		✓	✓
Census Divisions		✓	✓
Socioeconomic Characteristics			✓
Year FE	✓	✓	✓
Observations	658	658	658
KP F-stat	14.48	10.76	10.04

**Notes:** Robust standard errors clustered by MSAs in parentheses. All variables are in logs. Rail traffic use, measured in railcar-kilometers, is constructed using confidential rail waybill data. Instruments are ln 1835 exploration routes, ln 1898 railroads, and ln 1947 planned interstates; 684 observations corresponding to 228 MSAs for each regression.

While the CFS also report shipments by multiple modes, this variable has many missing observations particularly in the earlier volumes.<sup>4</sup> We focus on one state pair where we have consistent data for these road and multiple transport shipments—Illinois and Virginia. As mentioned earlier, the Corridor saves double-stack trains 230 miles between Norfolk & Chicago (Board, National Academies of Sciences and Medicine, 2017). This translates into time savings of up to 2 days. Figure A.5 plots the share of shipment between road and multiple modes for Illinois and Virginia. For both value and weight, we see an increase in shipment via multiple modes over this time period coupled with a corresponding decrease in road shipment share. These figures present suggestive evidence on the modal diversion effects of a large-scale infrastructure improvement on one transport mode.

<sup>4</sup>The CFS defines multiple mode shipments as shipments which uses two or more of the following modes of transportation in addition to parcel delivery/courier/US parcel post shipments: truck, railroad, water, pipeline, and air. We acknowledge that this is a noisy measure of multiple-mode shipment since we are unable to disaggregate this measure further due to lack of observation.

**Table. A.16.** Elasticity of Rail to Truck Traffic Use by Destination with respect to Road Infrastructure Improvements

	(1)	(2)	(3)	(4)	(5)
Rail to Truck Traffic Use by Destination	OLS	OLS	IV	IV	IV
Interstate Highway Lane (km)	-1.060*** (0.185)	-1.061*** (0.185)	-1.101*** (0.405)	-1.210*** (0.426)	-0.999** (0.405)
Population		0.0605 (0.337)	1.132*** (0.298)	1.303*** (0.351)	1.145*** (0.336)
Geography				✓	✓
Census Divisions				✓	✓
Socioeconomic Characteristics		✓			✓
MSA FE	✓	✓			
Year FE	✓	✓	✓	✓	✓
Observations	658	658	658	658	658
R-squared	0.89	0.89	-	-	-
KP F-stat			14.48	10.76	10.04

*Notes:* \*  $p < 0.1$ , \*\*  $p < 0.05$ , \*\*\*  $p < 0.01$ . Robust standard errors clustered by MSAs in parentheses. All variables are in logs. Rail traffic use, measured in railcar-kilometers, is constructed using confidential rail waybill data. Truck traffic use (in vehicle-kilometers) and other variables are from Duranton and Turner (2011). Instruments are 1835 exploration routes, 1898 railroad route kilometers, and 1947 planned interstate highways. 663 observations corresponding to 221 MSAs for each regression. See Table A.17 for first stage regressions.

## D Additional Derivations

This section provides additional derivations for the equilibrium equations in Section 3.3, the derivations for the regression design as well as a comparison with Fan and Luo (2020).

### D.1 Section 3.3: Equilibrium for Economic Geography Model with Multimodal Routing

Start with equilibrium equation,

$$\bar{A}_i^{-\theta} y_i^{1+\theta} l_i^{-\theta(1+\alpha)} = \chi \sum_{j=1}^N \tau_{ij}^{-\theta} \bar{u}_j^\theta y_j^{1+\theta} l_j^{\theta(\beta-1)}$$

Re-arranging,

$$\bar{A}_i^{-\theta} y_i^{1+\theta} l_i^{-\theta(1+\alpha)} = \chi \tau_{ii}^{-\theta} \bar{u}_i^\theta y_i^{1+\theta} l_i^{\theta(\beta-1)} + \chi \sum_{j \neq i} \tau_{ij}^{-\theta} \bar{u}_j^\theta y_j^{1+\theta} l_j^{\theta(\beta-1)}$$

Substitute the definition of the recursive transport cost,

$$\tau_{ij}^{-\theta} = \sum_{k \in \mathcal{F}(i)} t_{ik}^{-\theta} \tau_{kj}^{-\theta}$$

and we obtain,

**Table. A.17.** Elasticity of Rail to Truck Traffic Use by Destination with respect to Road Infrastructure Improvements: First Stage

	(1)	(2)	(3)
1898 Railroads	0.102** (0.0445)	0.107** (0.0481)	0.129*** (0.0478)
1947 Planned Interstates	0.148*** (0.0317)	0.117*** (0.0298)	0.108*** (0.0274)
1835 Exploration Routes	0.0244** (0.0117)	0.0257** (0.0124)	0.0220* (0.0122)
Population	0.511*** (0.0386)	0.597*** (0.0474)	0.535*** (0.0600)
Geography		✓	✓
Census Divisions		✓	✓
Socioeconomic Characteristics			✓
Year FE	✓	✓	✓
Observations	658	658	658
KP F-stat	14.48	10.76	10.04

**Notes:** Robust standard errors clustered by MSAs in parentheses. All variables are in logs. Rail traffic use, measured in railcar-kilometers, is constructed using confidential rail waybill data. Instruments are ln 1835 exploration routes, ln 1898 railroads, and ln 1947 planned interstates; 684 observations corresponding to 228 MSAs for each regression.

$$\bar{A}_i^{-\theta} y_i^{1+\theta} l_i^{-\theta(1+\alpha)} = \chi \tau_{ii}^{-\theta} \bar{u}_j^\theta y_j^{1+\theta} l_j^{\theta(\beta-1)} + \chi \sum_{j \neq i}^N \left( \sum_{k \in \mathcal{F}(i)} t_{ik}^{-\theta} \tau_{kj}^{-\theta} \right) \bar{u}_j^\theta y_j^{1+\theta} l_j^{\theta(\beta-1)}$$

Re-arranging,

$$\begin{aligned} \bar{A}_i^{-\theta} y_i^{1+\theta} l_i^{-\theta(1+\alpha)} &= \chi \tau_{ii}^{-\theta} \bar{u}_j^\theta y_j^{1+\theta} l_j^{\theta(\beta-1)} + \chi \sum_{k \in \mathcal{F}(i)} t_{ik}^{-\theta} \left( -\tau_{ki}^{-\theta} \bar{u}_i^\theta y_i^{1+\theta} l_i^{\theta(\beta-1)} + \sum_{j=1}^N \tau_{kj}^{-\theta} \bar{u}_j^\theta y_j^{1+\theta} l_j^{\theta(\beta-1)} \right) \\ \bar{A}_i^{-\theta} y_i^{1+\theta} l_i^{-\theta(1+\alpha)} &= \chi t_{ii}^{-\theta} \bar{u}_j^\theta y_j^{1+\theta} l_j^{\theta(\beta-1)} + \chi \sum_{k \in \mathcal{F}(i)} t_{ik}^{-\theta} \left( \sum_{j=1}^N \tau_{kj}^{-\theta} \bar{u}_j^\theta y_j^{1+\theta} l_j^{\theta(\beta-1)} \right) \\ \bar{A}_i^{-\theta} y_i^{1+\theta} l_i^{-\theta(1+\alpha)} &= \chi t_{ii}^{-\theta} \bar{u}_j^\theta y_j^{1+\theta} l_j^{\theta(\beta-1)} + \sum_{k \in \mathcal{F}(i)} t_{ik}^{-\theta} \bar{A}_k^{-\theta} y_k^{1+\theta} l_k^{-\theta(1+\alpha)} \end{aligned}$$

substitute the expected link transport cost from the nested multi-modal choice, i.e.

**Table. A.18.** Elasticity of Rail to Truck Traffic Use by Origin with respect to Road Infrastructure Improvements

Rail to Truck Traffic Use by Origin	(1) OLS	(2) OLS	(3) IV	(4) IV	(5) IV
Interstate Highway Lane (km)	-1.075*** (0.207)	-1.075*** (0.207)	-0.635 (0.468)	-1.235*** (0.451)	-1.220*** (0.444)
Population		-0.255 (0.378)	0.452 (0.352)	1.107*** (0.379)	1.000*** (0.367)
Geography				✓	✓
Census Divisions				✓	✓
Socioeconomic Characteristics		✓			✓
MSA FE	✓	✓			
Year FE	✓	✓	✓	✓	✓
Observations	658	658	658	658	658
R-squared	0.90	0.90	-	-	-
KP F-stat			14.48	10.76	10.04

*Notes:* \*  $p < 0.1$ , \*\*  $p < 0.05$ , \*\*\*  $p < 0.01$ . Robust standard errors clustered by MSAs in parentheses. All variables are in logs. Rail traffic use, measured in railcar-kilometers, is constructed using the confidential rail waybill data. Truck traffic use (in vehicle-kilometers) and other variables are from Duranton and Turner (2011). Instruments are 1835 exploration routes, 1898 railroad route kilometers, and 1947 planned interstate highways. 663 observations corresponding to 221 MSAs for each regression. See Table A.19 for first stage regressions.

**Table. A.19.** Elasticity of Rail to Truck Traffic Use by Origin with respect to Road Infrastructure Improvements: First Stage

	(1)	(2)	(3)
1898 Railroads	0.102** (0.0445)	0.107** (0.0481)	0.129*** (0.0478)
1947 Planned Interstates	0.148*** (0.0317)	0.117*** (0.0298)	0.108*** (0.0274)
1835 Exploration Routes	0.0244** (0.0117)	0.0257** (0.0124)	0.0220* (0.0122)
Population	0.511*** (0.0386)	0.597*** (0.0474)	0.535*** (0.0600)
Geography		✓	✓
Census Divisions		✓	✓
Socioeconomic Characteristics			✓
Year FE	✓	✓	✓
Observations	658	658	658
KP F-stat	14.48	10.76	10.04

*Notes:* Robust standard errors clustered by MSAs in parentheses. All variables are in logs. Rail traffic use, measured in railcar-kilometers, is constructed using confidential rail waybill data. Instruments are ln 1835 exploration routes, ln 1898 railroads, and ln 1947 planned interstates; 684 observations corresponding to 228 MSAs for each regression.

$$t_{ik}^{-\theta} = \left( \sum_{m \in A_{27}^{(i,k)}} \tilde{t}_{ik,m}^{-\eta} \right)^{\frac{\theta}{\eta}}$$

**Table. A.20.** Elasticity of Rail to Truck Traffic Use with respect to Road Infrastructure Improvements, by Rail Weight

	(1)	(2)	(3)	(4)	(5)
	OLS	OLS	IV	IV	IV
Interstate Highway Lane KM	-1.473*** (0.171)	-1.472*** (0.172)	-0.930** (0.392)	-1.373*** (0.403)	-1.203*** (0.382)
Population		-0.101 (0.308)	0.524* (0.297)	1.012*** (0.338)	0.774** (0.316)
Geography				✓	✓
Census Divisions				✓	✓
Socioeconomic Characteristics		✓			✓
MSA FE	✓	✓			
Year FE	✓	✓	✓	✓	✓
Observations	658	658	658	658	658
R-squared	0.89	0.89	-0.03	0.23	0.28
KP F-stat			14.48	10.76	10.04

**Notes:** \*  $p < 0.1$ , \*\*  $p < 0.05$ , \*\*\*  $p < 0.01$ . Robust standard errors clustered by MSAs in parentheses. All variables are in logs. Rail traffic use, measured in rail weight-kilometers, is constructed using confidential rail waybill data. All other variables are from Duranton and Turner (2011). Instruments are 1835 exploration routes, 1898 railroad route kilometers, and 1947 planned interstate highways. 663 observations corresponding to 221 MSAs for each regression. See Table A.2 for first stage regressions.

**Table. A.21.** Elasticity of Rail to Truck Traffic Use with respect to Road Infrastructure Improvements, by Rail Weight: First Stage

	(1)	(2)	(3)
1898 Railroads	0.102** (0.0445)	0.107** (0.0481)	0.129*** (0.0478)
1947 Planned Interstates	0.148*** (0.0317)	0.117*** (0.0298)	0.108*** (0.0274)
1835 Exploration Routes	0.0244** (0.0117)	0.0257** (0.0124)	0.0220* (0.0122)
Population	0.511*** (0.0386)	0.597*** (0.0474)	0.535*** (0.0600)
Geography		✓	✓
Census Divisions		✓	✓
Socioeconomic Characteristics			✓
Year FE	✓	✓	✓
Observations	658	658	658
KP F-stat	14.48	10.76	10.04

**Notes:** Robust standard errors clustered by MSAs in parentheses. All variables are in logs. Rail traffic use, measured in rail weight-kilometers, is constructed using confidential rail waybill data. Instruments are ln 1835 exploration routes, ln 1898 railroads, and ln 1947 planned interstates; 684 observations corresponding to 228 MSAs for each regression.

**Table. A.22.** Elasticity of Rail to Truck Traffic Use by Destination with respect to Road Infrastructure Improvements, by Rail Weight

Rail Weight to Truck Traffic Use by Destination	(1) OLS	(2) OLS	(3) IV	(4) IV	(5) IV
Interstate Highway Lane (km)	-1.104*** (0.167)	-1.104*** (0.167)	-1.133*** (0.421)	-1.273*** (0.447)	-1.019** (0.430)
Population		0.0823 (0.331)	0.953*** (0.306)	1.185*** (0.366)	0.973*** (0.352)
Geography				✓	✓
Census Divisions				✓	✓
Socioeconomic Characteristics			✓		✓
MSA FE	✓	✓			
Year FE	✓	✓	✓	✓	✓
Observations	658	658	658	658	658
R-squared	0.89	0.89	-	-	-
KP F-stat			14.48	10.76	10.04

**Notes:** \*  $p < 0.1$ , \*\*  $p < 0.05$ , \*\*\*  $p < 0.01$ . Robust standard errors clustered by MSAs in parentheses. All variables are in logs. Rail traffic use, measured in rail weight-kilometers, is constructed using confidential rail waybill data. All other variables are from Duranton and Turner (2011). Instruments are 1835 exploration routes, 1898 railroad route kilometers, and 1947 planned interstate highways. 663 observations corresponding to 221 MSAs for each regression. See Table A.2 for first stage regressions.

**Table. A.23.** Elasticity of Rail to Truck Traffic Use by Destination with respect to Road Infrastructure Improvements, by Rail Weight: First Stage

	(1)	(2)	(3)
1898 Railroads	0.102** (0.0445)	0.107** (0.0481)	0.129*** (0.0478)
1947 Planned Interstates	0.148*** (0.0317)	0.117*** (0.0298)	0.108*** (0.0274)
1835 Exploration Routes	0.0244** (0.0117)	0.0257** (0.0124)	0.0220* (0.0122)
Population	0.511*** (0.0386)	0.597*** (0.0474)	0.535*** (0.0600)
Geography		✓	✓
Census Divisions		✓	✓
Socioeconomic Characteristics			✓
Year FE	✓	✓	✓
Observations	658	658	658
KP F-stat	14.48	10.76	10.04

**Notes:** Robust standard errors clustered by MSAs in parentheses. All variables are in logs. Rail traffic use, measured in rail weight-kilometers, is constructed using confidential rail waybill data. Instruments are ln 1835 exploration routes, ln 1898 railroads, and ln 1947 planned interstates; 684 observations corresponding to 228 MSAs for each regression.

we obtain,

$$\bar{A}_i^{-\theta} y_i^{1+\theta} l_i^{-\theta(1+\alpha)} = \chi t_{ii}^{-\theta} \bar{u}_j^\theta y_j^{1+\theta} l_j^{\theta(\beta-1)} + \sum_{k \in \mathcal{F}(i)} \left( \sum_{m \in \mathcal{M}(i,k)} \tilde{t}_{ik,m}^{-\eta} \right)^{\frac{\theta}{\eta}} | \bar{A}_k^{-\theta} y_k^{1+\theta} l_k^{-\theta(1+\alpha)} |$$

A29

**Table. A.24.** Elasticity of Rail to Truck Traffic Use by Origin with respect to Road Infrastructure Improvements, by Rail Weight

	(1)	(2)	(3)	(4)	(5)
Rail Weight to Truck Traffic Use by Origin	OLS	OLS	IV	IV	IV
Interstate Highway Lane (km)	-1.106*** (0.200)	-1.105*** (0.200)	-0.630 (0.496)	-1.308*** (0.465)	-1.283*** (0.462)
Population		-0.314 (0.326)	0.176 (0.370)	0.936** (0.388)	0.789** (0.376)
Geography				✓	✓
Census Divisions				✓	✓
Socioeconomic Characteristics			✓		✓
MSA FE	✓	✓			
Year FE	✓	✓	✓	✓	✓
Observations	658	658	658	658	658
R-squared	0.91	0.91	-	-	-
KP F-stat		14.48	10.76	10.04	

**Notes:** \*  $p < 0.1$ , \*\*  $p < 0.05$ , \*\*\*  $p < 0.01$ . Robust standard errors clustered by MSAs in parentheses. All variables are in logs. Rail traffic use, measured in rail weight-kilometers, is constructed using confidential rail waybill data. All other variables are from Duranton and Turner (2011). Instruments are 1835 exploration routes, 1898 railroad route kilometers, and 1947 planned interstate highways. 663 observations corresponding to 221 MSAs for each regression. See Table A.2 for first stage regressions.

**Table. A.25.** Elasticity of Rail to Truck Traffic Use by Origin with respect to Road Infrastructure Improvements, by Rail Weight: First Stage

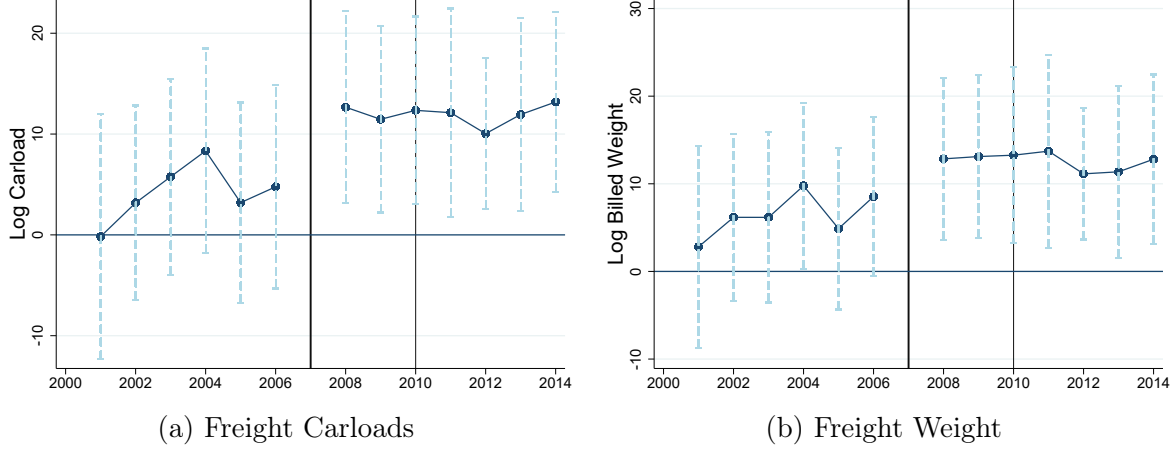
	(1)	(2)	(3)
1898 Railroads	0.102** (0.0445)	0.107** (0.0481)	0.129*** (0.0478)
1947 Planned Interstates	0.148*** (0.0317)	0.117*** (0.0298)	0.108*** (0.0274)
1835 Exploration Routes	0.0244** (0.0117)	0.0257** (0.0124)	0.0220* (0.0122)
Population	0.511*** (0.0386)	0.597*** (0.0474)	0.535*** (0.0600)
Geography		✓	✓
Census Divisions		✓	✓
Socioeconomic Characteristics			✓
Year FE	✓	✓	✓
Observations	658	658	658
KP F-stat	14.48	10.76	10.04

**Notes:** Robust standard errors clustered by MSAs in parentheses. All variables are in logs. Rail traffic use, measured in rail weight-kilometers, is constructed using confidential rail waybill data. Instruments are ln 1835 exploration routes, ln 1898 railroads, and ln 1947 planned interstates; 684 observations corresponding to 228 MSAs for each regression.

For the second equilibrium condition, we have,

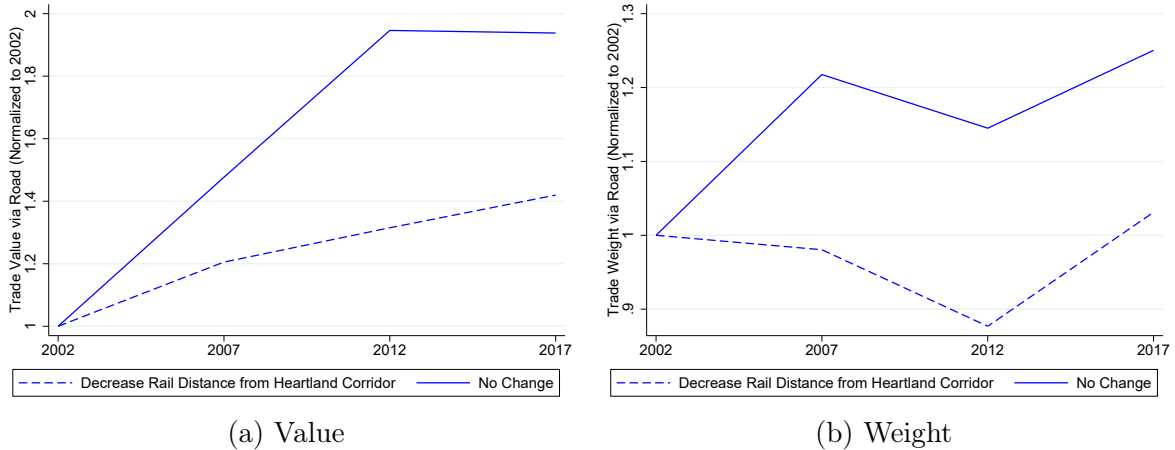
$$u_i^{-\theta} y_i^{-\theta} l_i^{\theta(1-\beta)} = \frac{\bar{L}^{(\alpha+\beta)\theta}}{W^\theta} \sum_{j=1}^N \tau_{ji}^{-\theta} \bar{A}_j^\theta y_j^{-\theta} l_j^{\theta(\alpha+1)}$$

**Figure A.3.** Impact of Double-Stack Infrastructure Improvement



**Notes:** The Heartland Corridor started in 2007 and was completed in 2010. Robust standard errors both Panels are clustered by origin and destination. Source: Authors' calculations using confidential rail data from the Surface Transportation Board.

**Figure A.4.** Comparison of Road Shipments for Locations Impacted by Double-Stack Rail Improvement



**Notes:** The Heartland Corridor started in 2007 and was completed in 2010. Source: Authors' calculations using Commodity Flow Survey (Bureau of Transportation Statistics).

Re-arranging,

$$u_i^{-\theta} y_i^{-\theta} l_i^{\theta(1-\beta)} = \chi \tau_{ii}^{-\theta} \bar{A}_j^\theta y_j^{-\theta} l_j^{\theta(\alpha+1)} + \chi \sum_{j \neq i}^N \tau_{ji}^{-\theta} \bar{A}_j^\theta y_j^{-\theta} l_j^{\theta(\alpha+1)}$$

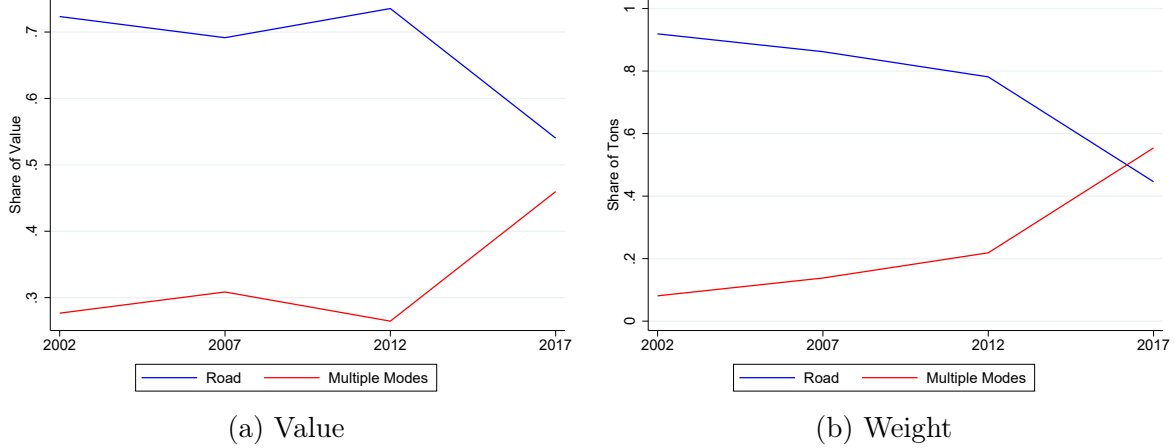
Substitute the definition of the recursive transport cost,

$$\tau_{ji}^{-\theta} = \sum_{k \in \mathcal{F}(i)} t_{jk}^{-\theta} \tau_{ki}^{-\theta}$$

and we obtain,

$$u_i^{-\theta} y_i^{-\theta} l_i^{\theta(1-\beta)} = \chi \tau_{ii}^{-\theta} \bar{A}_j^\theta y_j^{-\theta} l_j^{\theta(\alpha+1)} + \chi \sum_{j \neq i}^N \left( \sum_{k \in \mathcal{F}(i)} t_{jk}^{-\theta} \tau_{ki}^{-\theta} \right) \bar{A}_j^\theta y_j^{-\theta} l_j^{\theta(\alpha+1)}$$

**Figure A.5.** Road and Multiple-Mode Shipments between Illinois and Virginia



**Notes:** The Heartland Corridor started in 2007 and was completed in 2010. Source: Authors' calculations using Commodity Flow Survey (Bureau of Transportation Statistics).

Re-arranging,

$$\begin{aligned}
 u_i^{-\theta} y_i^{-\theta} l_i^{\theta(1-\beta)} &= \chi \tau_{ii}^{-\theta} \bar{A}_i^\theta y_i^{-\theta} l_i^{\theta(\alpha+1)} + \chi \sum_{k \in \mathcal{F}(i)} t_{ik}^{-\theta} \left( -\tau_{ki}^{-\theta} \bar{A}_i^\theta y_i^{-\theta} l_i^{\theta(\alpha+1)} + \sum_{j=1}^N \tau_{kj}^{-\theta} \bar{A}_j^\theta y_j^{-\theta} l_j^{\theta(\alpha+1)} \right) \\
 u_i^{-\theta} y_i^{-\theta} l_i^{\theta(1-\beta)} &= \chi t_{ii}^{-\theta} \bar{A}_i^\theta y_i^{-\theta} l_i^{\theta(\alpha+1)} + \chi \sum_{k \in \mathcal{F}(i)} t_{ik}^{-\theta} \left( \sum_{j=1}^N \tau_{kj}^{-\theta} \bar{A}_j^\theta y_j^{-\theta} l_j^{\theta(\alpha+1)} \right) \\
 u_i^{-\theta} y_i^{-\theta} l_i^{\theta(1-\beta)} &= \chi t_{ii}^{-\theta} \bar{A}_i^\theta y_i^{-\theta} l_i^{\theta(\alpha+1)} + \sum_{k \in \mathcal{F}(i)} t_{ki}^{-\theta} u_k^{-\theta} y_k^{-\theta} l_k^{\theta(1-\beta)}
 \end{aligned}$$

substitute the expected link transport cost from the nested multi-modal choice, i.e.

$$t_{ik}^{-\theta} = \left( \sum_{m \in \mathcal{M}(i,k)} \tilde{t}_{ik,m}^{-\eta} \right)^{\frac{\theta}{\eta}}$$

we obtain,

$$u_i^{-\theta} y_i^{-\theta} l_i^{\theta(1-\beta)} = \chi t_{ii}^{-\theta} \bar{A}_i^\theta y_i^{-\theta} l_i^{\theta(\alpha+1)} + \sum_{k \in \mathcal{F}(i)} \left( \sum_{m \in \mathcal{M}(k,i)} \tilde{t}_{ki,m}^{-\eta} \right)^{\frac{\theta}{\eta}} u_k^{-\theta} y_k^{-\theta} l_k^{\theta(1-\beta)}$$

## D.2 Regression design for modal diversion

We are interested in deriving a regression that studies the impact of secondary network traffic in a specific MSA with regard to plausibly exogenous changes in the primary network (road) transportation cost in the same location. Consider an MSA located at node  $k$ . We will make an additional assumption that there exists some localized primary network fully contained within the MSA that any unimodal route originating or terminating in  $k$  needs to transition through before accessing the national primary road network. Let this localized network be represented by the transportation cost  $\bar{t}_k$ . We are therefore

interested in running the following regression,

$$d \ln \Xi_{kk'} = \alpha + \beta_k \times d \ln \bar{t}_k + \epsilon_{kk'}$$

where  $\Xi_{kk'}$  refers to the amount of traffic at the intermodal station in  $k$  and represents traffic from the primary to the secondary network in that location and  $d \ln \bar{t}_k$  refers to changes in transportation cost of the localized primary network.

Given the assumption above we can simplify the expression for the unimodal transportation cost (Equation XZ), i.e.

$$\begin{aligned} (\tau_{kj}^1)^{-\theta} &= \left( \sum_{r \in \mathcal{R}_{ij}^1} \left( \prod_{l=1}^K t_{r_{l-1}, r_l}^{-\theta} \right) \right) \\ &= t_k^{-\theta} \left( \sum_{r \in \mathcal{R}_{ij}^1} \left( \prod_{l=2}^K t_{r_{l-1}, r_l}^{-\theta} \right) \right) \end{aligned}$$

which factorizes out the transportation cost associated with the localized network,  $t_k^{-\theta}$ , since it is assumed to be used on all routes.

In order to derive the regression we start from equilibrium traffic at terminal stations (Equation XZ), i.e.

$$\Xi_{kk'}^2 = \bar{s}_{kk'}^{-\frac{\theta}{1+\theta\lambda_2}} \times P_k^{-\frac{\theta}{1+\theta\lambda_2}} \times \left( \sum_l \tau_{k'l'}^{-\theta} s_{l'l}^{-\theta} \Pi_l^{-\theta} \right)^{\frac{1}{1+\theta\lambda_2}}$$

and we examine the responsiveness of traffic flows with regard to changes in the price index,  $d \ln P_k$ , which implies,

$$d \ln \Xi_{kk'} = d \ln P_k^{-\frac{\theta}{1+\theta\lambda_2}}$$

we then differentiate the price index and examine the responsiveness of the price index with regard to changes in the transportation cost,

$$\begin{aligned} P_k^{-\frac{\theta}{1+\theta\lambda_2}} &= \left( \sum_{i=1}^N \tau_{ik}^{-\theta} Y_i \Pi_i^\theta \right)^{\frac{1}{1+\theta\lambda_2}} \\ dP_k^{-\frac{\theta}{1+\theta\lambda_2}} &= \frac{1}{1+\theta\lambda_2} \times \left( \sum_{i=1}^N Y_i \Pi_i^\theta \tau_{ik}^{-\theta} \right)^{\frac{1}{1+\theta\lambda_2}-1} \times \sum_i Y_i \Pi_i^\theta d\tau_{ik}^{-\theta} \\ d \ln P_k^{-\frac{\theta}{1+\theta\lambda_2}} &= \frac{1}{1+\theta\lambda_2} \sum_{i=1}^N \frac{\tau_{ik}^{-\theta} Y_i \Pi_i^\theta}{\sum_{i=1}^N \tau_{ik}^{-\theta} Y_i \Pi_i^\theta} d \ln \tau_{ik}^{-\theta} \end{aligned}$$

Instead of considering arbitrary changes to the primary road transportation network instead focus on changes in the transportation cost at node  $k$  only. Totally differentiating the expression for unimodal transportation costs (Equation XZ), we obtain,

$$d \ln (\tau_{kj}^1)^{-\theta} = -\theta d \ln t_k \forall j$$

Combining we obtain,

$$\begin{aligned} d \ln P_k^{-\frac{\theta}{1+\theta\lambda_2}} &= -\frac{\theta}{1+\theta\lambda_2} d \ln t_k \sum_{i=1}^N \frac{\tau_{ik}^{-\theta} Y_i \Pi_i^\theta}{\sum_{i=1}^N \tau_{ik}^{-\theta} Y_i \Pi_i^\theta} d \ln \tau_{ik}^{-\theta} \\ &= -\frac{\theta}{1+\theta\lambda_2} d \ln t_k \end{aligned}$$

we have,

$$d \ln \Xi_{kk'} = d \ln P_k^{-\frac{\theta}{1+\theta\lambda_2}}$$

combining we have,

$$d \ln \Xi_{kk'} = -\frac{\theta}{1+\theta\lambda_2} d \ln t_{k,u}$$

Furthermore, we have,

$$t_{kl} = \bar{t}_{kl}^{\frac{1}{1+\theta\lambda_1}} \times P_k^{-\frac{\theta\lambda_1}{1+\theta\lambda_1}} \times \Pi_l^{-\frac{\theta\lambda_1}{1+\theta\lambda_1}}$$

which implies,

$$d \ln t_{kl} = \frac{1}{1+\theta\lambda_1} d \ln \bar{t}_{kl}$$

plugging in, we finally obtain,

$$d \ln \Xi_{kk'} = -\theta \frac{1}{1+\theta\lambda_2} \frac{1}{1+\theta\lambda_1} d \ln \bar{t}_{k,u}$$

which implies that the structural elasticity depends on the separate congestion forces on the primary and secondary network as well as the strength of substitution between routes and modes.

### D.3 Comparison with Fan and Luo (2020)

Our project studies multimodal transport networks and their impact on the returns to new technology and infrastructure investment. In particular, we focus on how these outcomes depend on the geography of the multimodal network as well as the intermodal terminals which allows for switches between transport modes. To this end, we develop a quantitative spatial equilibrium model by extending the routing-based formulation of transport cost in [Allen and Arkolakis \(2022\)](#) to incorporate transportation across multiple transport modes and possible mode switching conditional on the geography of the multimodal transport network, including the location of intermodal terminals, and incurred switching costs. Employing the properties of partitioned matrices, we derive closed-form expressions for the expected transport cost over the multimodal transport network despite the increased dimensionality and complexity of the underlying network. This tractable model of routing allows for counterfactual experiments which allows us to evaluate the welfare consequences to new technology and modal or terminal infrastructure improvements.

In what follows, we demonstrate that our results are consistent with the transportation cost derived in Proposition 1 in [Fan and Luo \(2020\)](#). [Fan and Luo \(2020\)](#) is a note which presents a model of transshipment building on [Allen and Arkolakis \(2022\)](#) and [Fan, Lu and Luo \(2019\)](#).

We first restate our expected transport cost from origin  $i$  to destination  $j$  over the multimodal transportation network below for convenience:

$$\tau_{ij} = e_{ij}^{-\frac{1}{\theta}}$$

where  $\mathbf{E} = [e_{ij}]$  refers to the inverse of the Schur complement of the Laplacian of the partitioned infrastructure matrix for the multimodal transport network and is defined as follows,

$$\mathbf{E} \equiv (\mathbf{B}^{-1} - \mathbf{D})^{-1} \equiv S(\Omega)^{-1}$$

where  $\mathbf{B} \equiv (\mathbf{I} - \mathbf{A}_1)^{-1}$  is the geometric sum of the primary transport network matrix  $\mathbf{A}_1$  and  $\mathbf{D} \equiv \mathbf{S} (\sum_{K=0}^{\infty} \mathbf{A}_2^K) \mathbf{S}'$  is the geometric sum of the secondary transport matrix  $\mathbf{A}_2$  that is inclusive of inter-modal switching linkages between the primary and secondary transport network  $\mathbf{S}$ .

To do so, instead of deriving the matrix representation from the explicit numeration and recursive formula as in the main text, we instead employ the inverse of the Leontief matrix of the underlying infrastructure matrix

$$\begin{aligned} \tau_{ij} &\equiv \lim_{N \rightarrow \infty} \tau_{ij,N} \\ &= \lim_{N \rightarrow \infty} \Gamma \left( \frac{\theta - 1}{\theta} \right) \left( \sum_{K=1}^N \left[ \Omega_{(i,j)}^K \right] \right)^{-\frac{1}{\theta}} \\ &= \Gamma \left( \frac{\theta - 1}{\theta} \right) \left( \left[ (\mathbf{I} - \boldsymbol{\Omega}_{(i,j)}^{-1}) \right] \right)^{-\frac{1}{\theta}}, i \neq j \\ &= \Gamma \left( \frac{\theta - 1}{\theta} \right) \left( \left[ \begin{array}{cc} \mathbf{B} + \mathbf{B}\mathbf{S}(S(\Omega)^{-1})\mathbf{S}'\mathbf{B} & \mathbf{B}\mathbf{S}(S(\Omega)^{-1}) \\ (S(\Omega)^{-1})\mathbf{S}\mathbf{B} & (S(\Omega)^{-1}) \end{array} \right]_{(i,j)} \right)^{-\frac{1}{\theta}} \end{aligned}$$

where  $N$  is maximum number of edges each  $ij$  pair can have, and  $S(\Omega)$  defines the Schur complement of the Laplacian of the partitioned infrastructure matrix, as above.

If the freight shipment originates and terminates on the primary network, commonly known as the first and last mile in freight transportation, we can then express bilateral transportation costs more succinctly below as a decomposition of the transport costs that arise from (A) the universe of unimodal transportation over the primary network, and (B) the additional multimodal transportation over the primary network that traverses through the secondary network taking into account the possible linkages

between the two networks:

$$\tau_{ij}^{-\theta} = \left[ \underbrace{\mathbf{B}}_{\substack{\text{Unimodal costs over} \\ \text{primary network}}} + \underbrace{\mathbf{BS}(S(\Omega)^{-1})\mathbf{S}'\mathbf{B}}_{\substack{\text{Multimodal costs over} \\ \text{primary \& secondary networks}}} \right]_{ij} = (\tau_{ij}^1)^{-\theta} + (\tau_{ij}^{1,2})^{-\theta} \quad (21)$$

which corresponds to equation (??) in our draft and is an alternative expression that is equivalent to equation (??). The first and second terms in the equation above corresponds to items (A) and (B) respectively.

If we abstract from this first and last mile assumption—that freight shipments originate and terminate on the primary network—then we can trace out the sum of paths that might either originate or terminate on either network. In matrix notation this corresponds to the following:

$$\begin{aligned} \tau_{ij} &= \Gamma\left(\frac{\theta-1}{\theta}\right) \cdot \left( \left[ [\mathbf{A}_1 \mathbf{A}_2] \begin{bmatrix} \mathbf{B} + \mathbf{BS}(S(\Omega)^{-1})\mathbf{S}'\mathbf{B} & \mathbf{BS}(S(\Omega)^{-1}) \\ (S(\Omega)^{-1})\mathbf{S}\mathbf{B} & (S(\Omega)^{-1}) \end{bmatrix} \begin{bmatrix} \mathbf{I} \\ \mathbf{I} \end{bmatrix} \right]_{ij} \right)^{-\frac{1}{\theta}} \\ &= \Gamma\left(\frac{\theta-1}{\theta}\right) \cdot \left( \left[ [\mathbf{A}_1 \mathbf{A}_2] (\mathbf{I} - \boldsymbol{\Omega})^{-1} \begin{bmatrix} \mathbf{I} \\ \mathbf{I} \end{bmatrix} \right]_{ij} \right)^{-\frac{1}{\theta}} \end{aligned} \quad (22)$$

where the second line above corresponds to the expression for transportation costs in Proposition 1 Part (a) of [Fan and Luo \(2020\)](#), but where the first line utilizes the block matrix structure to make explicit the underlying decomposition that we are introducing in our framework.

## E Proofs

This section presents the proof for Proposition 1.

### E.1 Proof of Proposition 1: Counterfactual Equilibrium

We proceed in two steps. In a first step we derive the change in the equilibrium conditions in terms of market access terms before then substitution the model specific elements.

#### E.1.1 Preliminaries

We can write equilibrium trade flows as,

$$X_{ij} = \tau_{ij}^{-\theta} \times \frac{\gamma_i}{\Pi_i^{-\theta}} \times \frac{\delta_j}{P_j^{-\theta}}$$

where  $\gamma_i$  and  $\delta_j$  are cumulative flows out of and origin and into a destination, respectively, and  $\Pi_i$  and  $P_j$  are origin and destination market access terms. Given the recursive routing formulation, trade costs can be represented as:

$$\tau_{ij} = \left( \sum_{k \in \mathcal{F}(i)} (t_{ik} \tau_{kj})^{-\theta} \right)^{-\frac{1}{\theta}}$$

And furthermore from the nested choice along the multi-layered graph, we have,

$$t_{ik}^{-\theta} = \left( \sum_{m \in \mathcal{M}(i,k)} \tilde{t}_{ik,m}^{-\eta} \right)^{\frac{\theta}{\eta}}$$

In terms of market clearing and trade balance we have the following equilibrium conditions,

$$\begin{aligned} \gamma_i &= \sum_j X_{ij} \\ \delta_i &= \sum_j X_{ji} \end{aligned}$$

### E.1.2 Deriving the equilibrium equation

Starting with the first equilibrium condition we have:

$$\begin{aligned}
\gamma_i &= \sum_j X_{ij} \iff \\
\gamma_i &= \sum_j \tau_{ij}^{-\theta} \times \frac{\gamma_i}{\Pi_i^{-\theta}} \times \frac{\delta_j}{P_j^{-\theta}} \iff \\
\Pi_i^{-\theta} &= \sum_j \tau_{ij}^{-\theta} \times \frac{\delta_j}{P_j^{-\theta}} \iff \\
\Pi_i^{-\theta} &= \tau_{ii}^{-\theta} \frac{\delta_i}{P_i^{-\theta}} + \sum_{j \neq i} \tau_{ij}^{-\theta} \frac{\delta_j}{P_j^{-\theta}} \iff \\
\Pi_i^{-\theta} &= \tau_{ii}^{-\theta} \frac{\delta_i}{P_i^{-\theta}} + \sum_{j \neq i} \left( \sum_{k \in \mathcal{F}(i)} t_{ik}^{-\theta} \tau_{kj}^{-\theta} \right) \frac{\delta_j}{P_j^{-\theta}} \iff \\
\Pi_i^{-\theta} &= \tau_{ii}^{-\theta} \frac{\delta_i}{P_i^{-\theta}} + \sum_{k \in \mathcal{F}(i)} t_{ik}^{-\theta} \left( -\tau_{ki}^{-\theta} \frac{\delta_i}{P_i^{-\theta}} + \sum_j \tau_{kj}^{-\theta} \frac{\delta_j}{P_j^{-\theta}} \right) \iff \\
\Pi_i^{-\theta} &= t_{ii}^{-\theta} \frac{\delta_i}{P_i^{-\theta}} + \sum_{k \in \mathcal{F}(i)} t_{ik}^{-\theta} \Pi_k^{-\theta}
\end{aligned}$$

where in the last line we used the definition of the recursive transport cost,  $\tau_{ii}^{-\theta} = \left( t_{ii}^{-\theta} + \sum_{k \in \mathcal{F}(i)} (t_{ik} \tau_{kj})^{-\theta} \right)$ . Substituting the definition of the edge-specific transport cost in terms of the multi-layered mode specific transport cost,

$$\begin{aligned}
\Pi_i^{-\theta} &= t_{ii}^{-\theta} \frac{\delta_i}{P_i^{-\theta}} + \sum_{k \in \mathcal{F}(i)} \left( \sum_{m \in \mathcal{M}(i,k)} \tilde{t}_{ik,m}^{-\eta} \right)^{\frac{\theta}{\eta}} \Pi_k^{-\theta} \\
&= t_{ii}^{-\theta} \frac{\delta_i}{P_i^{-\theta}} + \sum_{k \in \mathcal{F}(i)} \left( \sum_{m \in \mathcal{M}(i,k)} \tilde{t}_{ik,m}^{-\eta} \Pi_k^{-\eta} \right)^{\frac{\theta}{\eta}}
\end{aligned}$$

Continuing with the second equilibrium condition,

$$\begin{aligned}
\delta_i &= \sum_j X_{ji} \iff \\
\delta_i &= \sum_j \tau_{ji}^{-\theta} \times \frac{\gamma_j}{\Pi_j^{-\theta}} \times \frac{\delta_i}{P_i^{-\theta}} \iff \\
P_i^{-\theta} &= \sum_j \tau_{ji}^{-\theta} \times \frac{\gamma_j}{\Pi_j^{-\theta}} \iff \\
P_i^{-\theta} &= \tau_{ii}^{-\theta} \frac{\gamma_i}{\Pi_i^{-\theta}} + \sum_{j \neq i} \tau_{ji}^{-\theta} \frac{\gamma_j}{\Pi_j^{-\theta}} \iff \\
P_i^{-\theta} &= \tau_{ii}^{-\theta} \frac{\gamma_i}{\Pi_i^{-\theta}} + \sum_{j \neq i} \left( \sum_{k \in \mathcal{B}(i)} t_{ki}^{-\theta} \tau_{kj}^{-\theta} \right) \frac{\gamma_j}{\Pi_j^{-\theta}} \iff \\
P_i^{-\theta} &= \tau_{ii}^{-\theta} \frac{\gamma_i}{\Pi_i^{-\theta}} + \sum_{k \in \mathcal{F}(j)} t_{ki}^{-\theta} \left( -\tau_{ki}^{-\theta} \frac{\gamma_i}{\Pi_i^{-\theta}} + \sum_j \tau_{kj}^{-\theta} \frac{\gamma_j}{\Pi_j^{-\theta}} \right) \iff \\
P_i^{-\theta} &= t_{ii}^{-\theta} \frac{\gamma_i}{\Pi_i^{-\theta}} + \sum_{k \in \mathcal{F}(j)} t_{ki}^{-\theta} P_k^{-\theta}
\end{aligned}$$

where in the last line we used the definition of the recursive transport cost,  $\tau_{ii}^{-\theta} = \left( t_{ii}^{-\theta} + \sum_{k \in \mathcal{F}(i)} (t_{ik} \tau_{kj})^{-\theta} \right)$ . Substituting the definition of the edge-specific transport cost in terms of the multi-layered mode specific transport cost,

$$\begin{aligned}
P_i^{-\theta} &= t_{ii}^{-\theta} \frac{\gamma_i}{\Pi_i^{-\theta}} + \sum_{k \in \mathcal{F}(j)} \left( \sum_{m \in \mathcal{M}(k,i)} \tilde{t}_{ki,m}^{-\eta} \right)^{\frac{\theta}{\eta}} P_k^{-\theta} \\
&= t_{ii}^{-\theta} \frac{\gamma_i}{\Pi_i^{-\theta}} + \sum_{k \in \mathcal{F}(j)} \left( \sum_{m \in \mathcal{M}(k,i)} \tilde{t}_{ki,m}^{-\eta} P_k^{-\eta} \right)^{\frac{\theta}{\eta}}
\end{aligned}$$

### E.1.3 Deriving the equilibrium system in changes